



The Potential Effects Of Global Climate Change On The United States

Appendix I Variability



**THE POTENTIAL EFFECTS OF GLOBAL CLIMATE CHANGE
ON THE UNITED STATES:**

APPENDIX I - VARIABILITY

Editors: Joel B. Smith and Dennis A. Tirpak

**OFFICE OF POLICY, PLANNING AND EVALUATION
U.S. ENVIRONMENTAL PROTECTION AGENCY
WASHINGTON, DC 20460**

MAY 1989

TABLE OF CONTENTS

	<u>Page</u>
APPENDIX I: VARIABILITY	
PREFACE	iii
ANALYSIS OF CLIMATE VARIABILITY IN GENERAL CIRCULATION MODELS: COMPARISON WITH OBSERVATIONS AND CHANGES IN VARIABILITY IN 2xCO₂ EXPERIMENTS	1-1
L.O. Mearns, S.H. Schneider, S.L. Thompson, and L.R. McDaniel	
CHANGE IN CLIMATE VARIABILITY IN THE 21st CENTURY	2-1
D. Rind, R. Goldberg, and R. Ruedy	

PREFACE

The ecological and economic implications of the greenhouse effect have been the subject of discussion within the scientific community for the past three decades. In recent years, members of Congress have held hearings on the greenhouse effect and have begun to examine its implications for public policy. This interest was accentuated during a series of hearings held in June 1986 by the Subcommittee on Pollution of the Senate Environment and Public Works Committee. Following the hearings, committee members sent a formal request to the EPA Administrator, asking the Agency to undertake two studies on climate change due to the greenhouse effect.

One of the studies we are requesting should examine the potential health and environmental effects of climate change. This study should include, but not be limited to, the potential impacts on agriculture, forests, wetlands, human health, rivers, lakes, and estuaries, as well as other ecosystems and societal impacts. This study should be designed to include original analyses, to identify and fill in where important research gaps exist, and to solicit the opinions of knowledgeable people throughout the country through a process of public hearings and meetings.

To meet this request, EPA produced the report entitled *The Potential Effects of Global Climate Change on the United States*. For that report, EPA commissioned fifty-five studies by academic and government scientists on the potential effects of global climate change. Each study was reviewed by at least two peer reviewers. The Effects Report summarizes the results of all of those studies. The complete results of each study are contained in Appendices A through J.

Appendix	Subject
A	Water Resources
B	Sea Level Rise
C	Agriculture
D	Forests
E	Aquatic Resources
F	Air Quality
G	Health
H	Infrastructure
I	Variability
J	Policy

GOAL

The goal of the Effects Report was to try to give a sense of the possible direction of changes from a global warming as well as a sense of the magnitude. Specifically, we examined the following issues:

- o sensitivities of systems to changes in climate (since we cannot predict regional climate change, we can only identify sensitivities to changes in climate factors)
- o the range of effects under different warming scenarios
- o regional differences among effects
- o interactions among effects on a regional level

- o national effects
- o uncertainties
- o policy implications
- o research needs

The four regions chosen for the studies were California, the Great Lakes, the Southeast, and the Great Plains. Many studies focused on impacts in a single region, while others examined potential impacts on a national scale.

SCENARIOS USED FOR THE EFFECTS REPORT STUDIES

The Effects Report studies used several scenarios to examine the sensitivities of various systems to changes in climate. The scenarios used are plausible sets of circumstances although none of them should be considered to be predictions of regional climate change. The most common scenario used was the doubled CO₂ scenario (2XCO₂), which examined the effects of climate under a doubling of atmospheric carbon dioxide concentrations. This doubling is estimated to raise average global temperatures by 1.5 to 4.5°C by the latter half of the 21st century. Transient scenarios, which estimate how climate may change over time in response to a steady increase in greenhouse gases, were also used. In addition, analog scenarios of past warm periods, such as the 1930s, were used.

The scenarios combined average monthly climate change estimates for regional grid boxes from General Circulation Models (GCMs) with 1951-80 climate observations from sites in the respective grid boxes. GCMs are dynamic models that simulate the physical processes of the atmosphere and oceans to estimate global climate under different conditions, such as increasing concentrations of greenhouse gases (e.g., 2XCO₂).

The scenarios and GCMs used in the studies have certain limitations. The scenarios used for the studies assume that temporal and spatial variability do not change from current conditions. The first of two major limitations related to the GCMs is their low spatial resolution. GCMs use rather large grid boxes where climate is averaged for the whole grid box, while in fact climate may be quite variable within a grid box. The second limitation is the simplified way that GCMs treat physical factors such as clouds, oceans, albedo, and land surface hydrology. Because of these limitations, GCMs often disagree with each other on estimates of regional climate change (as well as the magnitude of global changes) and should not be considered to be predictions.

To obtain a range of scenarios, EPA asked the researchers to use output from the following GCMs:

- o Goddard Institute for Space Studies (GISS)
- o Geophysical Fluid Dynamics Laboratory (GFDL)
- o Oregon State University (OSU)

Figure 1 shows the temperature change from current climate to a climate with a doubling of CO₂ levels, as modeled by the three GCMs. The figure includes the GCM estimates for the four regions. Precipitation changes are shown in Figure 2. Note the disagreement in the GCM estimates concerning the direction of change of regional and seasonal precipitation and the agreement concerning increasing temperatures.

Two transient scenarios from the GISS model were also used, and the average decadal temperature changes are shown in Figure 3.

FIGURE 1. TEMPERATURE SCENARIOS

2xCO₂ LESS 1xCO₂

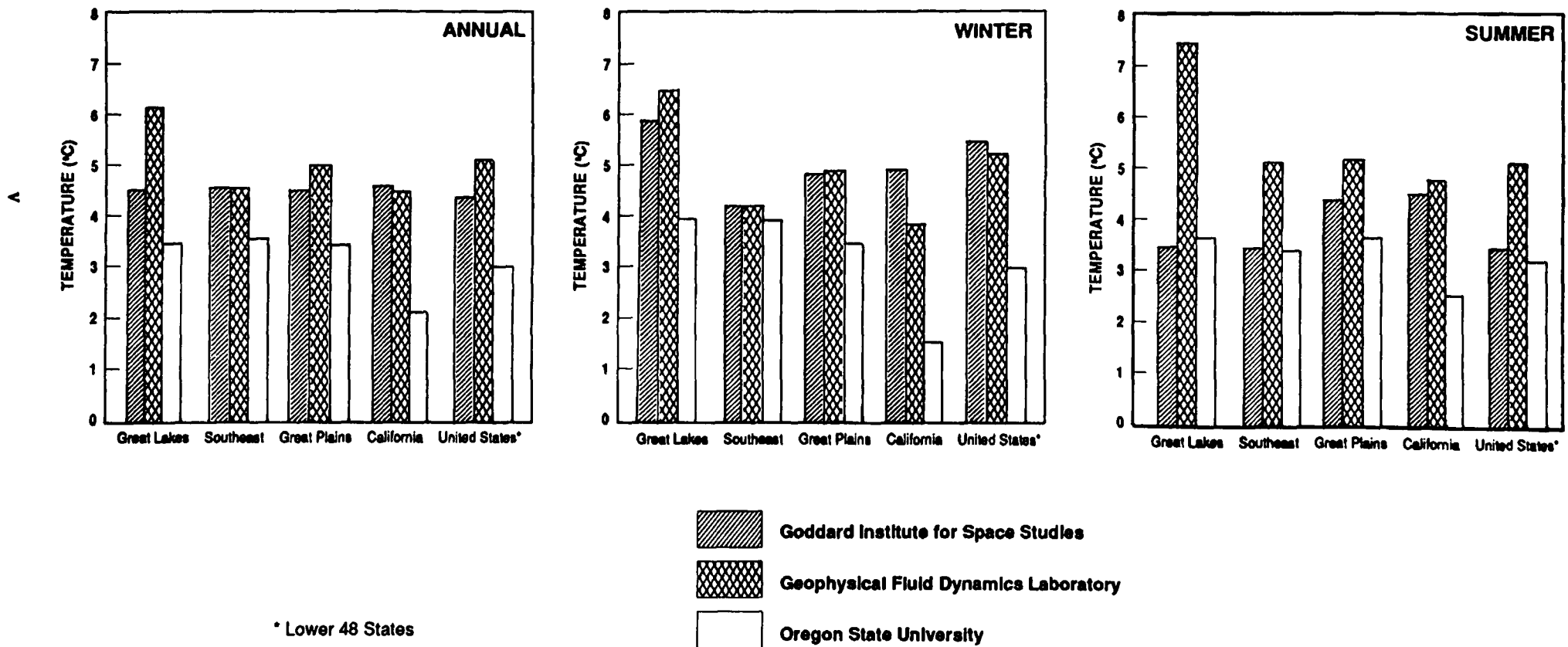
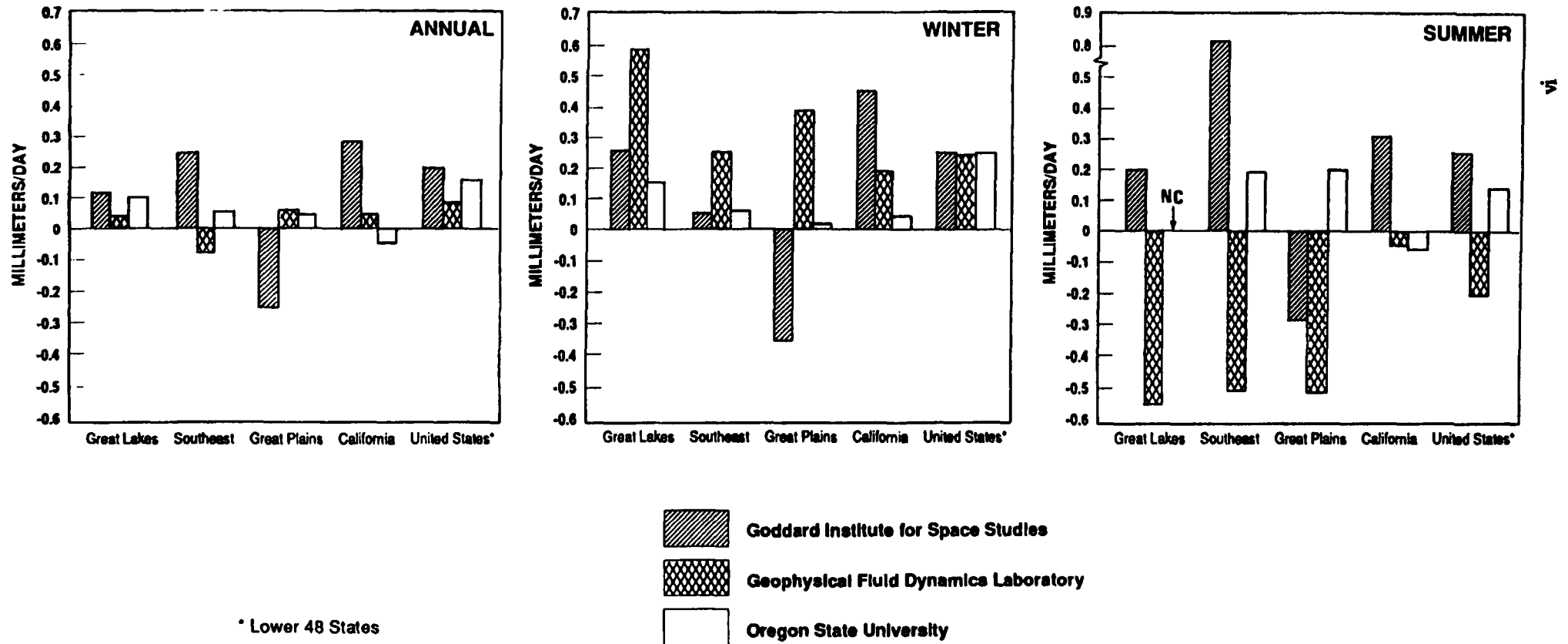
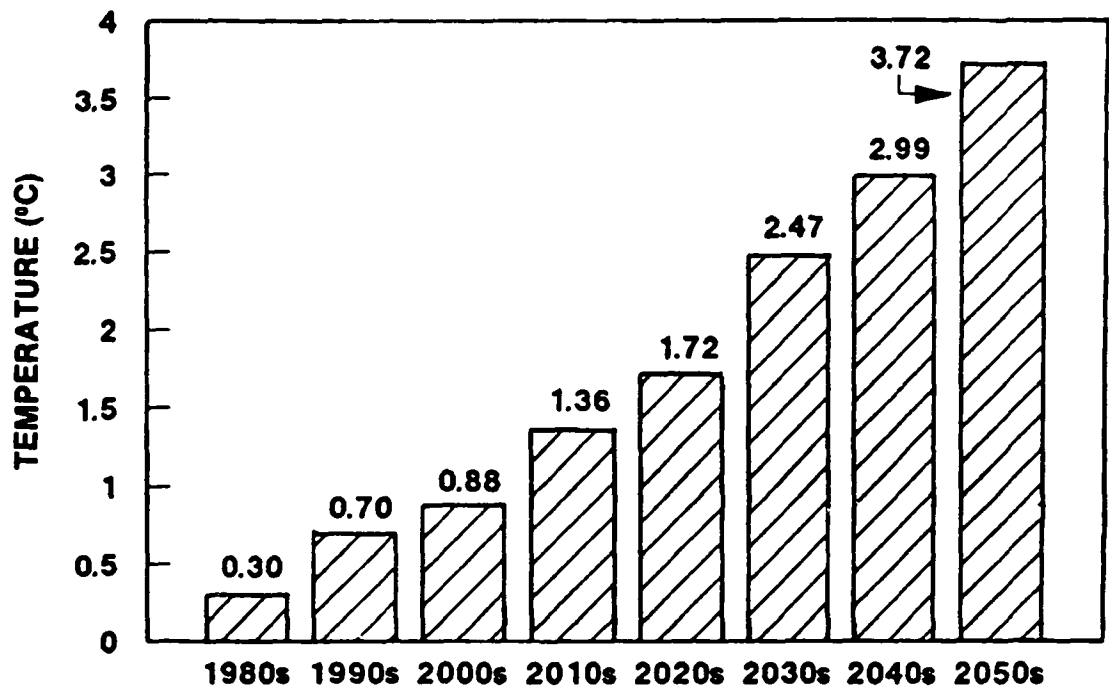


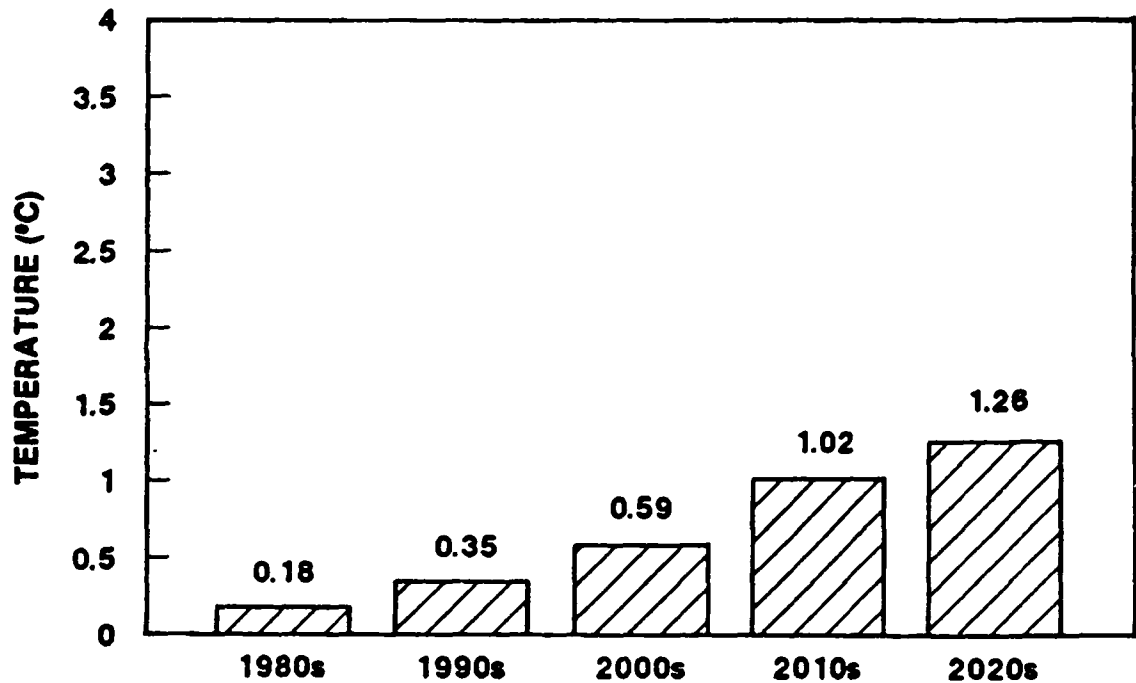
FIGURE 2. PRECIPITATION SCENARIOS

$2\times\text{CO}_2$ LESS $1\times\text{CO}_2$





TRANSIENT SCENARIO A



TRANSIENT SCENARIO B

FIGURE 3. GISS TRANSIENTS "A" AND "B" AVERAGE TEMPERATURE CHANGE FOR LOWER 48 STATES GRID POINTS.

EPA specified that researchers were to use three doubled CO₂ scenarios, two transient scenarios, and an analog scenario in their studies. Many researchers, however, did not have sufficient time or resources to use all of the scenarios. EPA asked the researchers to run the scenarios in the following order, going as far through the list as time and resources allowed:

1. GISS doubled CO₂
2. GFDL doubled CO₂
3. GISS transient A
4. OSU doubled CO₂
5. Analog (1930 to 1939)
6. GISS transient B

ABOUT THESE APPENDICES

The studies contained in these appendices appear in the form that the researchers submitted them to EPA. These reports do not necessarily reflect the official position of the U.S. Environmental Protection Agency. Mention of trade names does not constitute an endorsement.

**ANALYSIS OF CLIMATE VARIABILITY IN GENERAL CIRCULATION MODELS:
COMPARISON WITH OBSERVATIONS AND CHANGES IN
VARIABILITY IN $2\times\text{CO}_2$ EXPERIMENTS**

by

**L. O. Mearns
S. H. Schneider
S. L. Thompson
and
L. R. McDaniel
National Center for Atmospheric Research
Boulder, CO 80397-3000**

Grant No. DW49932663-01-0

CONTENTS

	<u>Page</u>
FINDINGS	1-1
CHAPTER 1: INTRODUCTION	1-2
PURPOSE OF THE STUDY	1-2
REVIEW OF PRIOR WORK	1-2
CHAPTER 2: METHODS	1-5
DESCRIPTION OF THREE NCAR CCM VERSIONS	1-5
STUDY AREA AND OBSERVATIONAL DATA	1-6
VARIABLES ANALYZED AND COMPUTATIONAL METHODS	1-6
CHAPTER 3: COMPARISON OF OBSERVED VS. CHERVIN CONTROL RUN DATA	1-8
SOLAR RADIATION	1-14
PRECIPITATION	1-14
INTERANNUAL VARIABILITY STATISTICS OF TEMPERATURE AND PRECIPITATION	1-18
CHAPTER 4: INTERCOMPARISONS OF THREE CCM VERSIONS AND OBSERVED DATA ..	1-29
COMPARISONS OF MEAN CONDITIONS: TEMPERATURE AND PRECIPITATION ..	1-29
RELATIVE HUMIDITY	1-29
DAILY VARIABILITY OF TEMPERATURE	1-35
DAILY PRECIPITATION VARIABILITY	1-39
CHAPTER 5: PILOT STUDY OF CONTROL VS. CO₂ PERTURBED RUNS	1-48
CHAPTER 6: SUMMARY AND CONCLUSIONS	1-54
APPENDIX 1: STATISTICAL TESTS OF DIFFERENCES IN VARIANCE OF SURFACE TEMPERATURE	1-56
APPENDIX 2: STATISTICAL TESTS OF DIFFERENCES BETWEEN INTERQUARTILE RANGES	1-57
REFERENCES	1-58

FINDINGS¹

This study concerns analysis of climatic variability in general circulation models first to determine how faithfully the models reproduce measures of the present variability and then to examine how variability changes in CO₂ perturbed cases. The control run output of three different versions of the NCAR Community Climate Model (CCM) is examined for selected regions of the United States including the Great Plains, the Southeast, the Great Lakes region, and the upper West Coast. Mainly temperature and precipitation are analyzed, but some preliminary analysis of relative humidity and solar radiation is also included. Interannual variability is analyzed in one version (the Chervin version) for only the present day climate. Results indicate that this version underestimates the interannual variability of temperature, but generally successfully reproduces the relative variability of precipitation. Two versions of the CCM tend to overestimate daily temperature variability while the third (Dickinson version) accurately reproduces it or slightly underestimates it. Reasons for these differences are discussed. Daily precipitation variability is overestimated by two model versions (Chervin and Dickinson) but fairly well reproduced by the Washington version. The CO₂ perturbed run of one version (Washington) produces mixed results for changes in daily temperature variability and tends to produce increased variability for precipitation.

¹The authors thank Rick Katz for providing statistical assistance and for comments on an earlier draft of this paper. This research was partially supported by the U.S. Environmental Protection Agency under Grant No. DW49932663-01-0.

CHAPTER 1

INTRODUCTION

PURPOSE OF THE STUDY

In considering the impacts of climatic change on society it is recognized that impacts accrue not only from the relatively slow trend in the mean of a climate variable, but also from the attending shifts in the frequency of extreme events. This issue has already received some attention in the literature (e.g., Schwarz, 1977; Parry, 1978; Mearns et al., 1984) where the non-linear relationship between changes in the mean and extreme events has been underlined.

Given the importance of extreme events to climate impact analysis, it is most appropriate to analyze changes in statistical moments which affect changes in the frequencies of extreme events. All moments could be important in this regard, but as a starting point (or minimally) the mean and variance of time series of climate variables should be considered.

In this study we analyze the first and second moments of climate variable time series from selected observational stations and those produced by general circulation model (GCM) control and perturbed runs. Our goal is first to determine how faithfully different GCMs reproduce these measures of the present variability and then to present a pilot study illustrating a method of investigation of variability changes in CO₂ perturbed cases. We believe that this type of research should become an essential part of standard GCM diagnostic analyses. This is because the variability performance of a GCM is relevant not only to the credibility of its control climate statistics, but also because it serves as a diagnostic of the validity of model physics, since it is often internal physical processes that give rise to climate variability. By comparing the relative performance (i.e., model vs. observations) of various versions of the NCAR CCM (i.e., versions with different physical parameterizations or formulations), we can both help to determine what formulations may be needed for forecasting certain measures of variability and how much credibility to assign to those forecasts.

REVIEW OF PRIOR WORK

Studies comparing variability statistics of GCM generated time series of climate variables relevant to climate impacts to observed time series are not numerous in the atmospheric sciences literature, although studies first appeared in the early 1980s (e.g., Manabe and Hahn, 1981; Chervin, 1981). Here we review five of the more recent and relevant works which address comparison of variability. Very often these studies also involve a study of the change in variability under doubled CO₂ conditions.

Of particular interest to the focus of the present study is Chervin's (1986) investigation of interannual variability and climate prediction, since we use the 20-year history tapes from Chervin's study as one of the GCM data sets in our present study. He designed a special version of the NCAR CCM0(A) (CCM = Community Climate Model) with seasonal variations of sea surface temperatures (SSTs). No other measures of SST variability were included in order to eliminate external (i.e., SST) variability of interannual time series of climate variables in the hope that discrepancies between modeled and observed variability would reflect the external component of variability present in the observed data. The additional variability attributed to external (SST) boundary conditions is considered the "potential predictability" of the climate. The model was modified such that external boundary conditions remained the same each date of each year of the 20-year model run. This entailed the prescription of monthly sea surface temperatures and sea ice distributions. The variability of mean sea level pressure and 700-mb geopotential height were analyzed in the Northern Hemisphere, with particular focus on the United States. Comparisons were made using the F-test. Results indicated that there were no significant differences between modeled and observed variabilities of mean sea level pressure over the United States and only limited areas of differences in the variability of 700-mb geopotential height. It should be noted, however,

that Chervin's assignment of potential predictability regions depends on the assumption that processes responsible for the internal variation of the atmosphere are correctly simulated by the model.

Bates and Meehl (1986) also used the CCM to investigate changes in the frequency of blocking events on a global scale under doubled CO₂ conditions. Their version of the CCM0(A) included a seasonal cycle, computed hydrology, and a simple mixed layer ocean. The dynamical equations were solved, as by Chervin (1986), with a 15-wave resolution with model physics computed on a 4.5° latitude and a 7.5° longitude grid size. The statistics of the 500 mb height field are examined as well as blocking events defined as persistent positive height anomalies. Blocking events are strongly related to persistent surface temperature anomalies, such as heat waves in the summer. Hence, changes in the frequencies of blocking events have significant implications for changes in the frequencies of extreme temperature events. In comparing 10 years of modeled data with observed data, they found that the model does a "reasonable" job of simulating 500-mb height standard deviations, particularly in winter in both hemispheres. The model, however, produces too few extreme blocking events. Under doubled CO₂ conditions, standard deviations of 500-mb height and blocking activity were found to decrease in all seasons.

Two studies have recently been conducted on local or regional scales using the U.K. Meteorological Office 5-layer GCM. The treatment of radiation and land surface processes has been modified, including a full diurnal cycle. The model has a quasi-uniform grid of 330 km resolution (i.e., the number of latitudinal grid boxes decreases with increasing latitude). Reed (1986) analyzed observed vs. model control run results for one grid point in Eastern England, and addressed the problem of creating the appropriate correspondence between the model grid square and the spatial average of several observation points. He analyzed the mean and variance of surface air temperature for a 3-year integration of model runs. Compared to observations, the model tended to produce too cool temperatures and too high variability as measured by the standard deviation. For precipitation the model produced too many rain days but underpredicted extreme rain events of greater than 20 mm/day.

More recently Wilson and Mitchell (1987) examined the modeled distribution of extreme daily climate events over Western Europe using the same model. Comparisons were made of minimum surface temperatures and precipitation. Again the model produced temperatures that were too cold, and hence, extreme minimum temperatures were overestimated. This problem was most pronounced in grid boxes away from the coasts. The model also produces too much precipitation in Western Europe, but does not successfully reproduce observed highest daily totals. The number of rain days is also overestimated. They go on to examine changes under quadrupled CO₂ conditions and find that variability of temperature generally decreases, which, given the general warming, means that there is a marked reduction in the occurrence of freezing temperatures. The authors compare the changes in intra-annual temperature variability using the more rigorous procedures of Katz (1984) as well as using the more conventional F-test. Both tests indicate a significant decrease in winter temperature variability. The authors emphasize the need to examine variables of importance to climate impact analysis and also the importance of using a model that faithfully reproduces the present day climate in terms of means and extremes.

Hansen et al. (1988) used the GISS model II general circulation model to simulate the global climate effects of time-dependent variations of atmospheric trace gases and aerosols. Several different scenarios of trace gas increase from 1958 to the present were used. A 100-year control run was also produced. From this run it was determined that globally the model only slightly underestimates the observed interannual temperature variability. However, the model's variability tends to be larger than observed over land. Among the calculations made with output from the transient (i.e., progressive climate change from scenarios of increasing CO₂) run were changes in the frequencies of extreme temperature events. This was accomplished by adding the change in temperature with climate warming predicted by the model to observed local daily temperatures. Hence the authors assumed no change in variability in making these calculations. Results indicate that predicted changes in the frequency of extremes beyond the 1990s at such locations as New York, Washington, and Memphis, become quite large and would have serious impacts.

Mearns

The studies reviewed above indicate some important shortcomings of GCMs with regard to their ability to faithfully reproduce observed variability statistics. Clearly more research is needed to further determine the sensitivity of the models to changes in the physics, resolution, etc., with regard to the determination of variability. Moreover, only one of these studies is explicitly concerned with variables of importance to climate impact analysis. We propose here to respond to Wilson and Mitchell's comments (as well as those of Mearns et al., 1984) regarding the importance of studying the higher moments of climate variable statistics, and of carefully verifying the models' ability to reproduce observed variability on regional scales, as the necessary prerequisites to rigorously analyzing possible changes in these statistics under doubled CO₂ conditions.

CHAPTER 2

METHODS

DESCRIPTION OF THREE NCAR CCM VERSIONS

Given that all GCMs differ in their ability to accurately reproduce the many measures of observed climate, it is useful to compare the simulation skill of different model versions against the present climate in order to document the possible ranges of errors and to evaluate more fully the effects of model structure differences.

This study uses the output from control runs of three different versions of the NCAR Community Climate Model (CCM). However, the version of Chervin (1986) is the primary one used for comparison of observed and model control output (i.e., model runs to simulate the actual present day climate), since it has the longest time integration (20 years) and thus carries less sampling error than shorter runs. Model versions of Chervin (1986), Washington (Washington and Meehl, 1984) and Dickinson (Dickinson et al., 1986) are described below.

The "Chervin" version of the CCM0(A) model used is documented in Chervin (1986). The CCM0 is a spectral general circulation model originally developed by Bourke and collaborators (Bourke, 1974; Bourke et al., 1977), which has been modified by the incorporation of radiation and cloud parameterization schemes. The model has a resolution for physical processes of approximately 4.5° in latitude and 7.5° in longitude, and there are nine levels in the vertical. The major modification of the model made by Chervin was the inclusion of an annual solar cycle featuring identical, seasonally varying forcing each year. Identical forcing each year was accomplished by prescribing for each month ocean surface temperatures and sea ice distributions. The soil moisture in CCM0(A) is fixed at 25% of field capacity (which supplies evapotranspiration at only 25% of potential), and cloudiness is predicted interactively as a function of internally generated moisture fields. Hence we compare here, the present day control climate runs of models incorporating physics different from those of the CCM0(A) version of Chervin (1986) investigated in Chapter III.

Two other versions of the CCM are used; what we will call the "Washington" version of CCM0(A) (Washington and Meehl, 1984), which includes an interactive thermodynamic ocean and surface bucket hydrology, and the "Dickinson" version (Dickinson et al., 1986), a modification of CCM1(B) containing a diurnal cycle and the Biosphere-Atmosphere Transfer Scheme (BATS).

The Washington model closely resembles the Chervin version of CCM0(A), except for the treatment of the hydrologic cycle and the mixed layer ocean. The Washington CCM is coupled to a simple fixed depth (50 m) thermodynamic ocean model which accounts for seasonal heat storage in the upper layer of the ocean. Thus sea surface temperatures are predicted, not prescribed as in the Chervin version. The ocean model, however, does not account for vertical or horizontal heat transport by the ocean. A simple interactive bucket hydrology parameterization is implemented, wherein model-derived precipitation and evaporation rates are used to simulate changes in runoff, soil moisture and snow cover. The albedo scheme for land is identical to that used by Chervin.

The Dickinson model is the most advanced in terms of modeling surface-atmosphere interactions. As a version of CCM1 (Williamson et al., 1987), there are also fundamental differences in the vertical subgrid scale heat transport parameterization and the radiative scheme of Dickinson's model and those of Washington and Chervin. In the CCM1, there are substantial changes in the radiative scheme. The solar albedo parameterization is improved, absorption by H_2O and O_2 of solar radiation is improved, and the CO_2 and ozone absorptance models are changed. Condensation occurs at 100% relative humidity rather than at 80% relative humidity as in CCM0. In addition, the BATS model of surface-atmosphere interactions is included (Dickinson, 1986). This model calculates the transfers of momentum, heat, and moisture between the earth's surface and atmospheric layers. It also determines wind, moisture, and temperature in the atmosphere, within vegetative canopies, and at the level of surface observations. It includes a very detailed surface hydrologic scheme which accounts for vegetation type and amount, water use by the vegetation, etc. Dickinson's version also includes a diurnal radiation cycle, which requires accounting for soil heat capacity. The ocean-atmosphere interaction is handled

as in Chervin's version, with fixed seasonally varying sea surface temperatures. Both Washington and Dickinson runs available so far consist of 3-year integrations, which implies much greater sampling uncertainty than for Chervin's 20-year run.

STUDY AREA AND OBSERVATIONAL DATA

The primary study area encompasses the area covered by three grid boxes located in the Great Plains (GP) region of the United States (see Figure 1). Three grid boxes are used instead of one so that the sensitivity of the spatial aggregation of the model, in terms of relative accuracy compared to observed data, could be examined. Because the only variability in the sea surface temperatures (SSTs) of two of the three versions of the CCM are seasonal changes, this reduces the total natural variability of atmospheric climate. These particular grid boxes (I, II and III on Figure 1) were selected because they are located well inland and in fairly homogeneous terrain east of the "Rocky Mountains" in the model. Therefore, we anticipated this location to be less affected by oceanic influences or regional topography than most other U.S. locations; the grid boxes also correspond to the major wheat growing areas of the United States.

Three other grid boxes are also included in the analysis to represent other regions of the United States: one in the southeastern U.S. (SE), one in the Great Lakes region (GL), and one on the northern west coast (WC). These are also indicated on Figure 1.

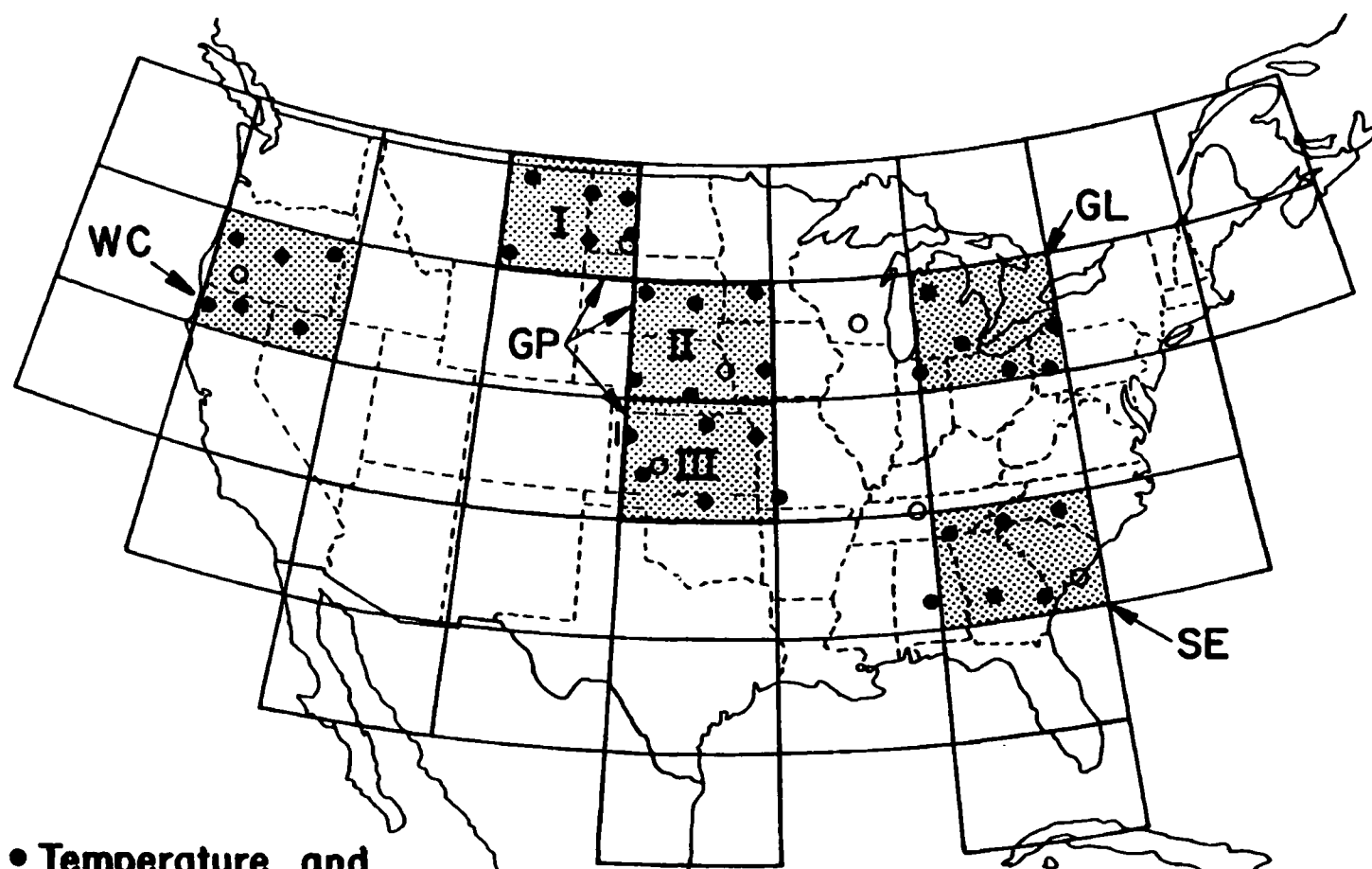
Real data corresponding to each grid box were generated from the average of six observation stations for time series of temperature and precipitation (NCAR, daily surface observations DS. 510). Solar radiation and relative humidity real data were taken from one SOLMET observation station (data available from the National Climate Data Center, Asheville) located in or near each grid box, except for the SE grid where two Solmet stations were used. Figure 1 shows the location of all observation stations and grid boxes.

VARIABLES ANALYZED AND COMPUTATIONAL METHODS

Four variables deemed particularly relevant to climate impact analysis were chosen for this analysis: daily mean surface air temperature, daily total precipitation, mean daily surface relative humidity, and daily mean absorbed solar radiation at the surface. The model time series consisted of 20 years of data generated from the Chervin GCM experiment, three years from the Washington experiment and three years from the Dickinson experiment. For the Chervin and Washington models daily mean temperature is calculated as the average of two 12-hour samples. For the Dickinson model, both maximum and minimum daily temperatures are available from model output, and these are averaged to produce daily average values.

The 20-year observational data set for temperature and precipitation included the years 1949-68. Observed mean daily temperatures were calculated as the average of daily maximum and minimum temperatures. The observational data set for solar radiation and relative humidity covered 18 years (1958-1976), except at the WC grid where only 10 years of observational data were available. Only absorbed, not incident surface radiation is available from the models' output, so observed incident solar radiation was converted to absorbed by multiplying by $1.0 - \alpha$, where α is the appropriate surface albedo value prescribed for land surfaces in the Chervin model. Only solar radiation results from the Chervin model are discussed in this paper. Observed relative humidity was calculated from surface dew point and air temperature data using polynomial algorithms to determine actual and saturation vapor pressure (Lowe, 1976).

For the Great Plains region, the analysis of time series is conducted on two different spatial scales: analysis of each grid box individually, and analysis of the spatial mean derived from the average across the three grid boxes (the latter referred to as "grand spatial means"). Analysis of the other three regions is conducted only on the individual grid level.



- Temperature and Precipitation Stations
- Relative Humidity and Radiation Stations

Figure 1. Model grid cells and station locations.

CHAPTER 3

COMPARISON OF OBSERVED VS. CHERVIN CONTROL RUN DATA

Figure 2 displays the time series of daily average temperature for modeled (Chervin) and observed data for the four regions under investigation. The value plotted for each day for the modeled data consists of the average on that day (consists of the average of two 12-hour samples on the history tapes) over 20 years. For the GP region an average is taken over the three grids. Observed data consist of the same except that six observation stations make up the equivalent of each grid box. The daily observed temperature at each observation station is calculated as the average of the recorded maximum and minimum daily temperatures.

It is evident from Figure 2 that, overall, the model simulates the annual cycle for the four regions fairly well. There are regional differences, however. In the GP region the model annual range is slightly smaller than that of the observed time series (Figure 2a), whereas in the GL region (Figure 2b) the model annual range is greater. The least successful simulation is that for the SE grid (Figure 2c), where winter minima are too high by about 7°C. Note that in the GP region, the model falls slightly short of attaining the appropriate maximum temperatures in summer.

The most successful simulation is found at the WC grid (Figure 2d). This result is somewhat problematic, since, of the four grids, WC has the greatest topographic variation, which is only crudely represented in the CCM. It may be the case that the six particular observation stations chosen to represent the area luckily cancel out the effect of topographic irregularity in the data. Perhaps more likely, the specified observed, and seasonally varying sea surface temperatures (SSTs) impose a major oceanic effect on the climate of this ocean bordering grid point.

Figure 3 displays histograms for modeled vs. observed temperature data for four key months for the GP region (all three grids). The histograms are formed by including each day's observation at each grid point for each year as a data point. Hence for January, the histogram contains 1860 observation points for the modeled data (60x31). The histograms for January and April show generally good agreement between the modeled and observed data. The distributions are very similar (approximately normal), although the modeled data tend to be slightly too warm and have too wide a spread. In July the narrowing of distributions (both observed and modeled) becomes evident. This seasonal change in daily variance is well simulated by the model, a gratifying result. The transition month of October again shows good agreement between modeled and observed data as the distributions widen again. Agreement in November and December (not shown) is also good, although the modeled data again become slightly too warm, and the model distributions are also a little too wide.

Additional analyses were performed by comparing histograms from each of the three grids of the GP region (histograms not shown). Preliminary results suggest that for January through March Grid I model data compare well with observed data, but discrepancies are found at Grids II and III (model data are too warm). In November and December at Grids I and II, the model histograms have long left tails (i.e., too many cold extremes are produced). At Grid III, too wide a distribution and too many warm events are evident. This is all to say that the spatial aggregation over three grids mitigates discrepancies between model and observed results and that the nature of departures from the observed distributions are not consistent among the three grids making up the spatial average.

Figures 4 and 5 present selected temperature histograms (for 4 months) for the GL and SE grids respectively. At the GL grid, the model distributions are flatter and wider than those for observed data in the winter and fall months, which indicates that both warm and cool extremes are over-represented by the model. However, in the spring and summer, the distributions (observed vs. model) are quite similar. At the SE grid the observed and model distributions are similar in most months, except for winter months, when the model distribution departs from that of the observed. Yet the model distribution widths are not dissimilar from those of the observed in winter months. The good agreement of modeled and observed temperatures at the WC grid is seen in Figure 6. Note the lower variability (indicated by narrower histograms) at this location in modeled

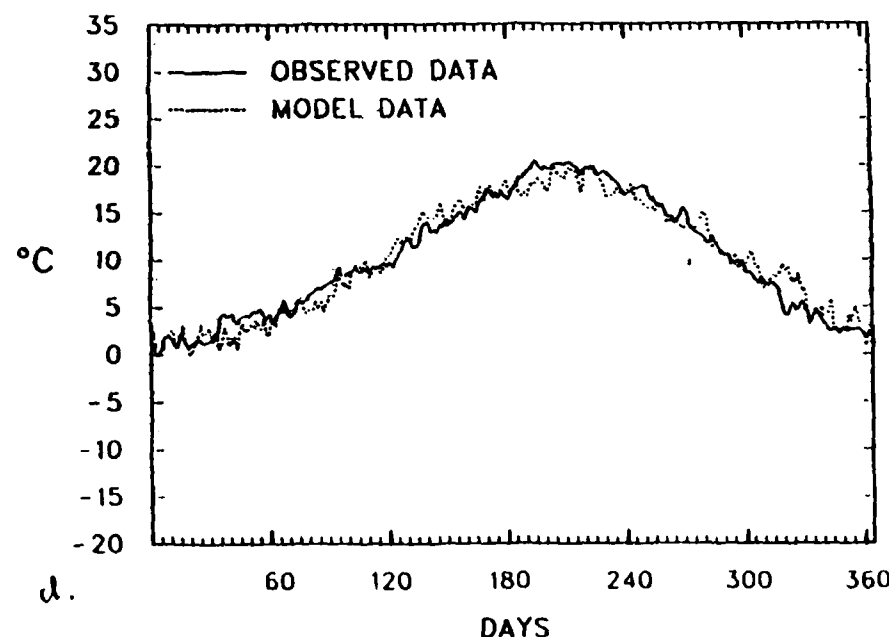
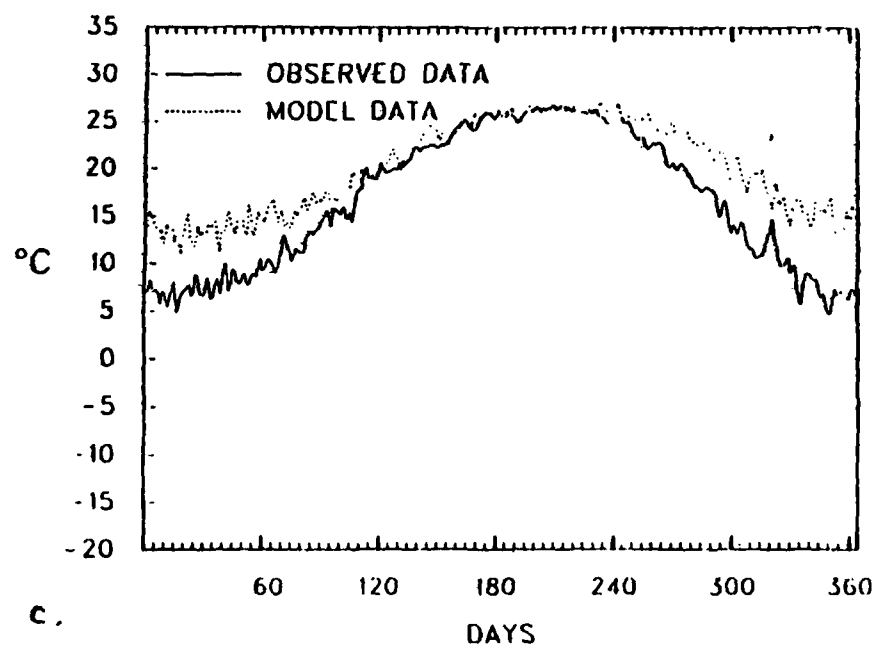
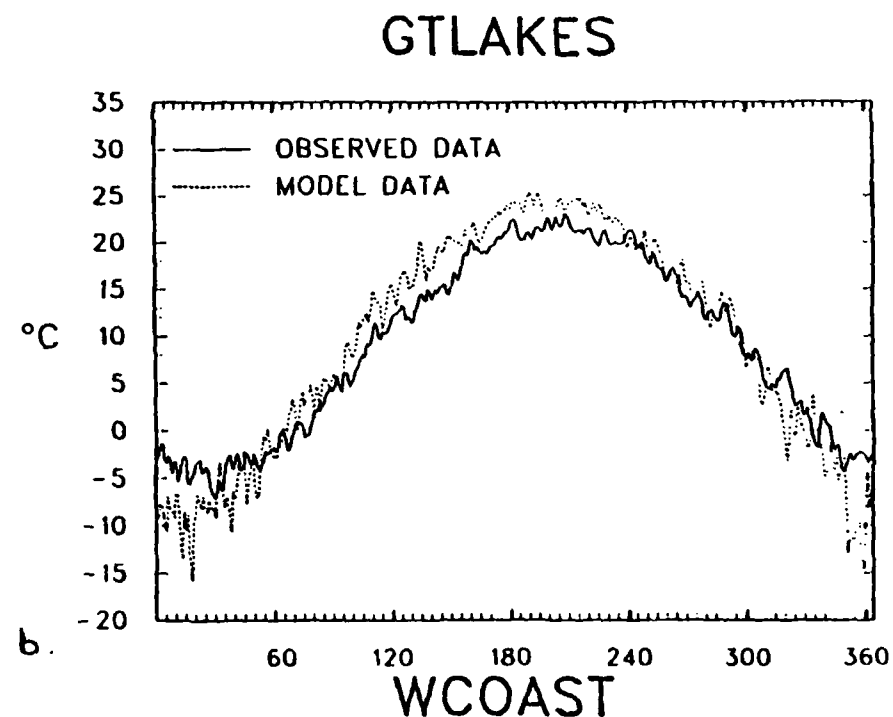
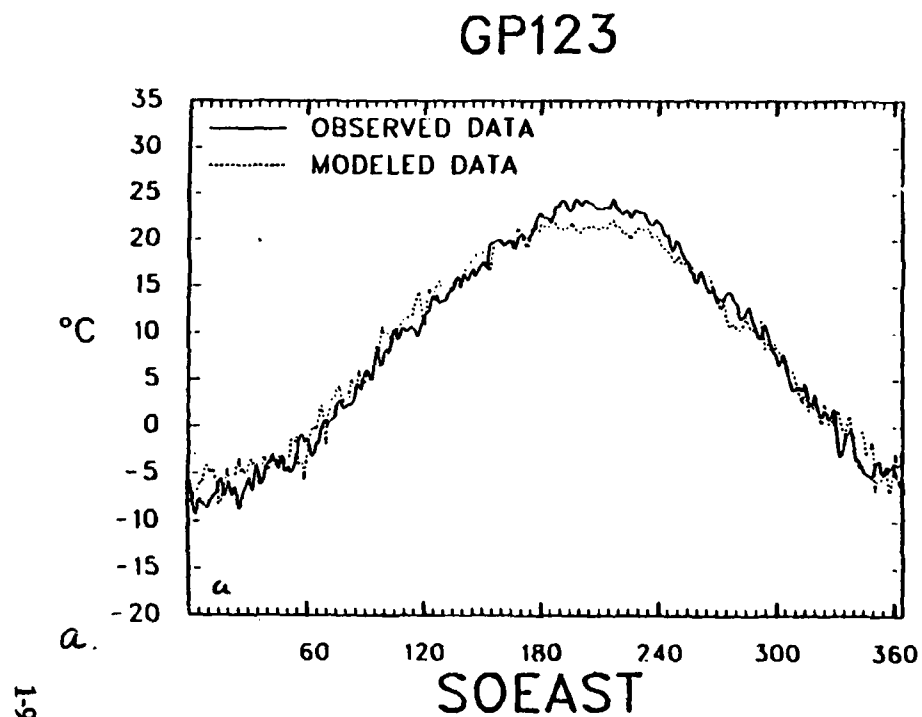


Figure 2. Average temperature for a 20-year average year, Chervin model vs. observed for the four regions.

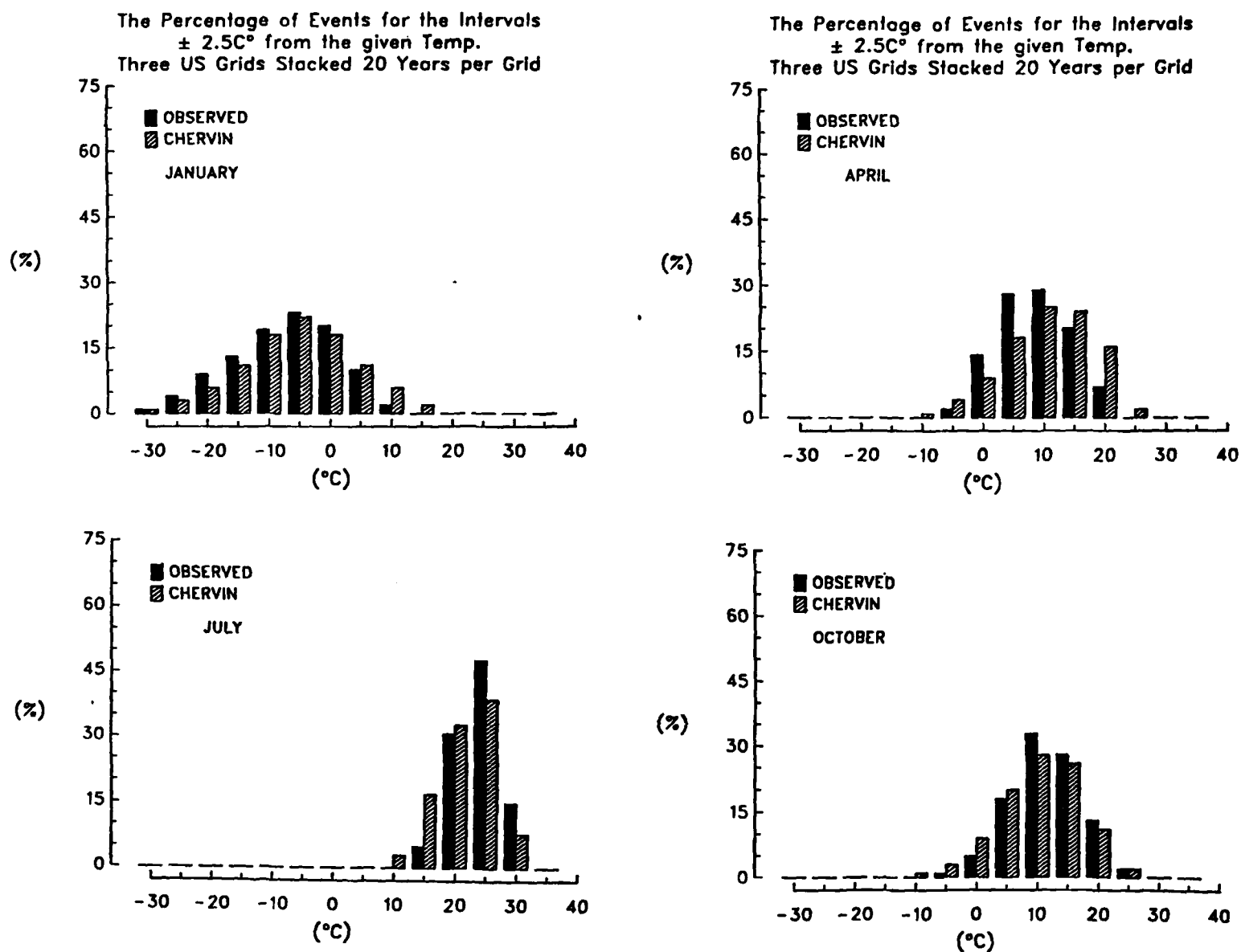


Figure 3. Histograms of daily temperature ($^\circ\text{C}$) (20 years) for the three GP grids, four selected months.

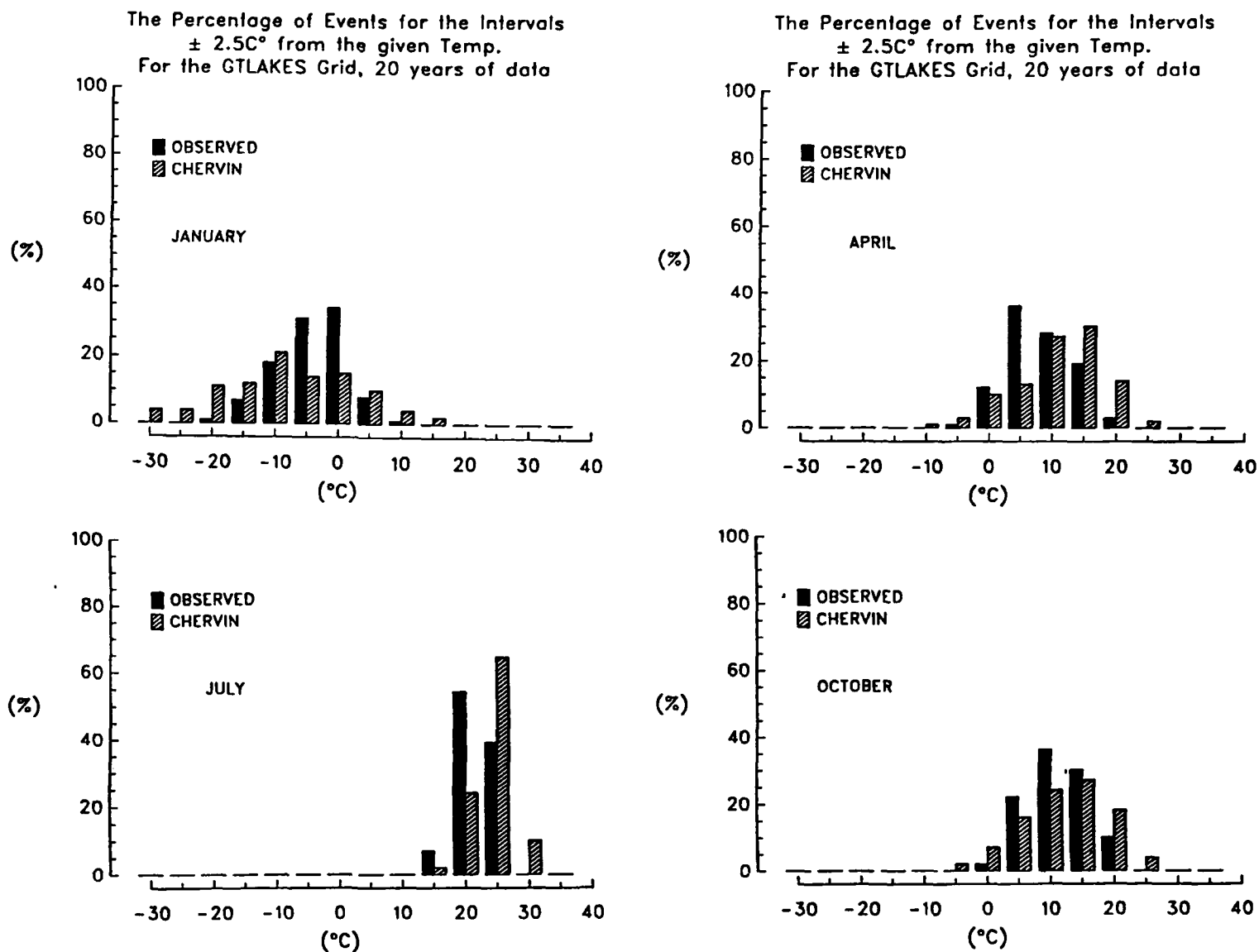


Figure 4. Histograms of daily temperature ($^\circ\text{C}$) (20 years) for the GL grid, 4 selected months.

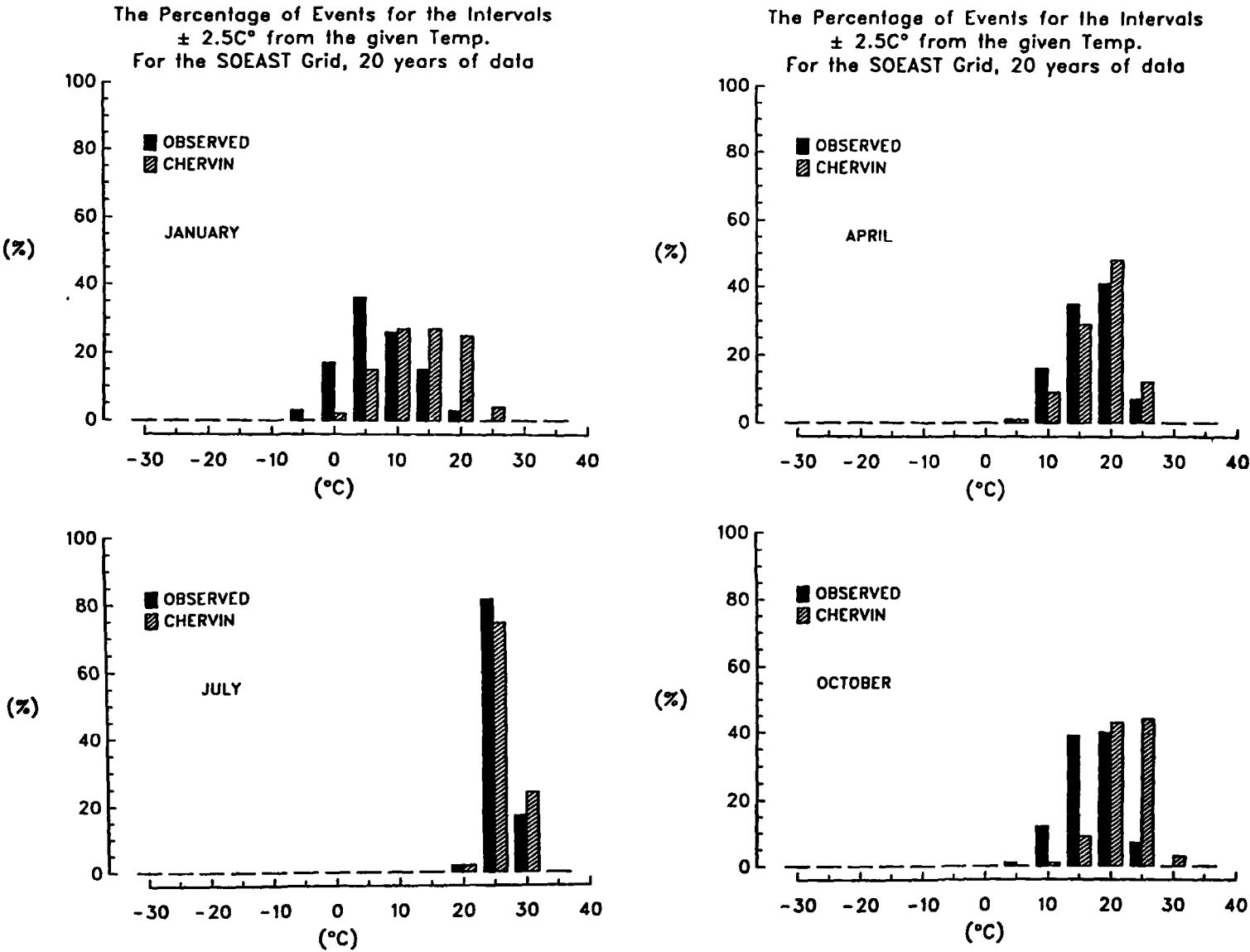


Figure 5. Histograms of daily temperature (°C) (20 years) for the SE grid, 4 selected months.

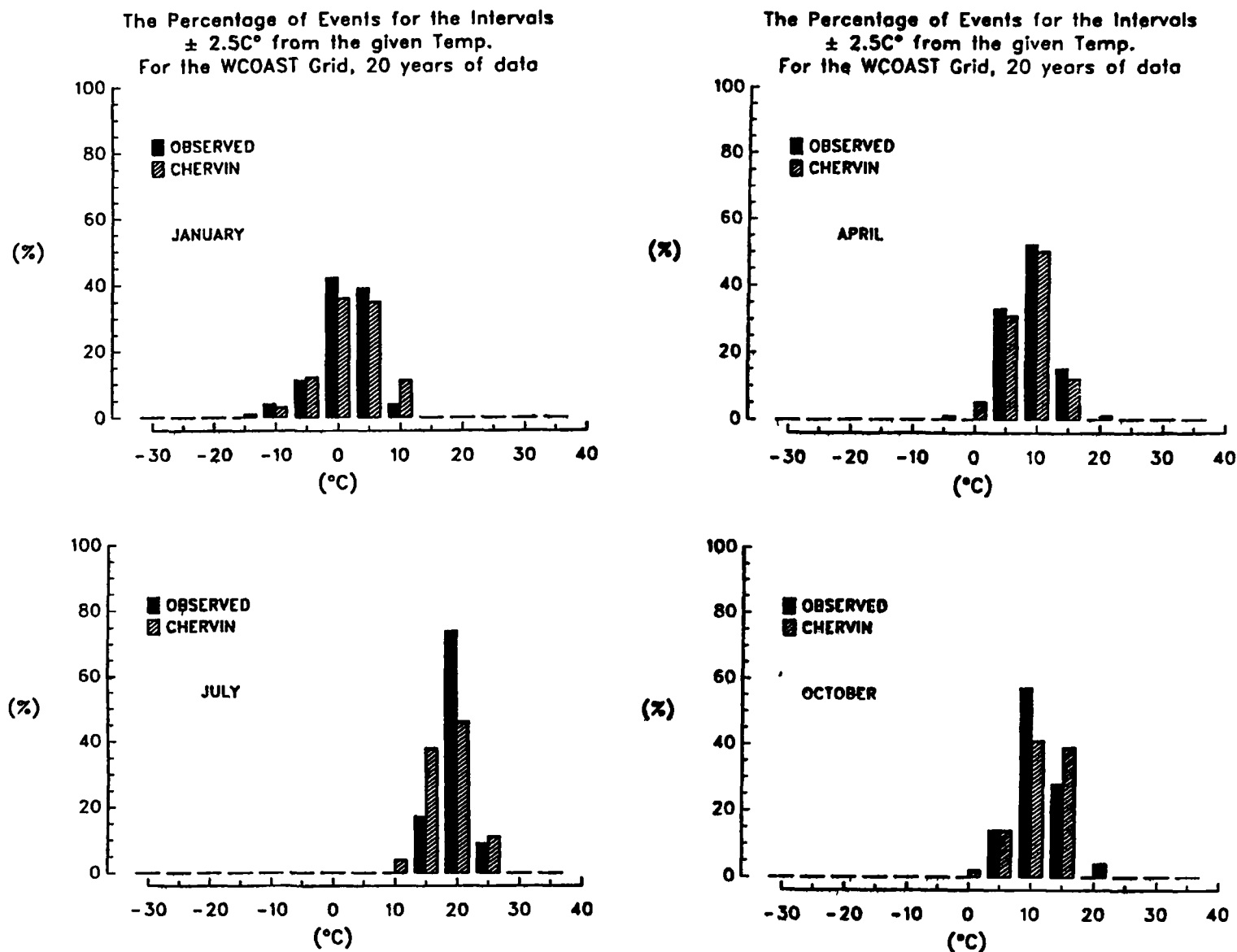


Figure 6. Histograms of daily temperature ($^\circ\text{C}$) (20 years) for the WC grid, 4 selected months.

Mearns

and observed values compared to those at the other three locations. This reflects the lower variability expected of a West Coast location resulting from the moderating oceanic influence and prevailing westerly wind. The seasonal decrease in variability from winter to summer is again well simulated. However, the model slightly overestimates the variability in the spring and fall as indicated by the wider model histograms for April and October.

Possible explanations about the discrepancies (e.g., why this version of the model is too warm in winter and too cold in summer in the GP region grids) will be offered later on.

SOLAR RADIATION

Solar radiation is relevant both for crop impact assessments and as a diagnostic of model-predicted cloudiness. The daily average time series for absorbed solar radiation (model and observed) for the four regions are presented in Figure 7. In the GP region the annual cycle is fairly well simulated but there are significant departures of the modeled values from observed for March-May (day 60-day 150) and September-November. In both periods model values are too high. Similarly, at the GL grid, the model values are too high during most months except for late summer. The poorest comparison is seen at the SE grid, where the model consistently overestimates absorbed solar radiation in all months, which is consistent with the excessively warm temperatures seen on Figure 2c. At the WC grid, the summer maximum is well simulated but winter minimum values are too high so that the annual cycle of solar radiation is underestimated.

The selected monthly histograms for the GP region reflect overestimation of the amount of surface solar radiation (Figure 8). In examining these histograms it should be recalled that comparison with observed values for solar radiation and relative humidity are more problematic than for temperature and precipitation, since only one observation station is used to represent each grid. Hence, the comparisons here should be made with some caution. In general for the GP region, the modeled solar radiation values in each month, in addition to being too high, have a narrower distribution than the observed values, and hence daily variability is underestimated. The overall distribution shapes (model vs. observations) are rather dissimilar for most months, the greatest discrepancy in distribution being seen in January although sampling considerations limit the confidence in quantitative inferences). The narrowing range of values from summer to winter seen in the observations is well reproduced by the model.

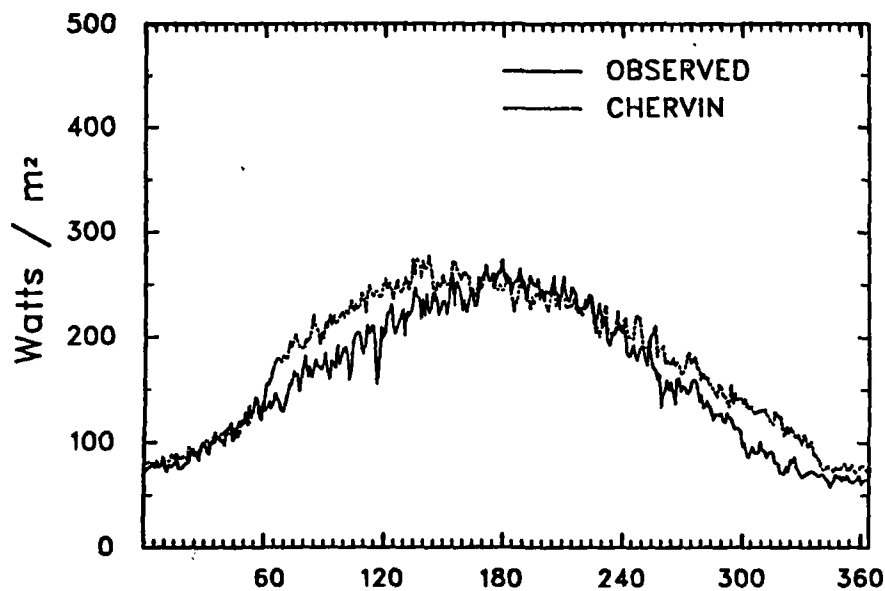
Of particular interest are conditions in spring (e.g., April on Figure 8) when modeled solar radiation is frequently too high compared with observations. This suggests that cloudiness is too low. A possible explanation for this arises from the fixed soil moisture in the model. In reality in spring the soil moisture content is usually high, whereas the model soil moisture content is fixed at 25% of field capacity. This too low soil moisture will limit evaporation and hence could result in an underestimation of cloud amount, which leads to an overestimation of surface absorbed solar radiation. Moreover, possible overestimation of evaporation in summer (when soil moisture can be less than 25% saturated) could also lower surface temperature by local cooling in the form of latent heat. Of course more fundamental problems with large scale cloud parameterization schemes undoubtedly also contribute to the errors. Further analysis will be necessary to confirm these speculations.

At the other three grids (histograms not shown) (aside from the overall direction of error, too high or too low) there are no striking contrasts in the distributions, which suggests that the seasonal cycle of daily variance of solar radiation is qualitatively well represented by the model at these locations, even though there are significant discrepancies in mean values.

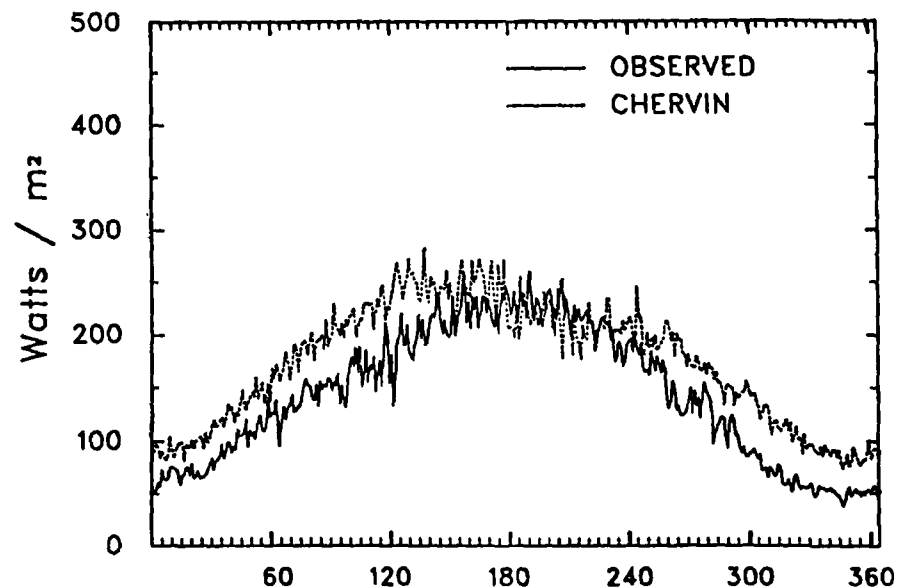
PRECIPITATION

The most perplexing direct comparison of Chervin model and observed values occurs with precipitation. The time series of average daily total precipitation for the four regions, displayed in Figure 9, clearly indicate a substantial discrepancy between model and observations. Daily model absolute values at the U.S. grid points

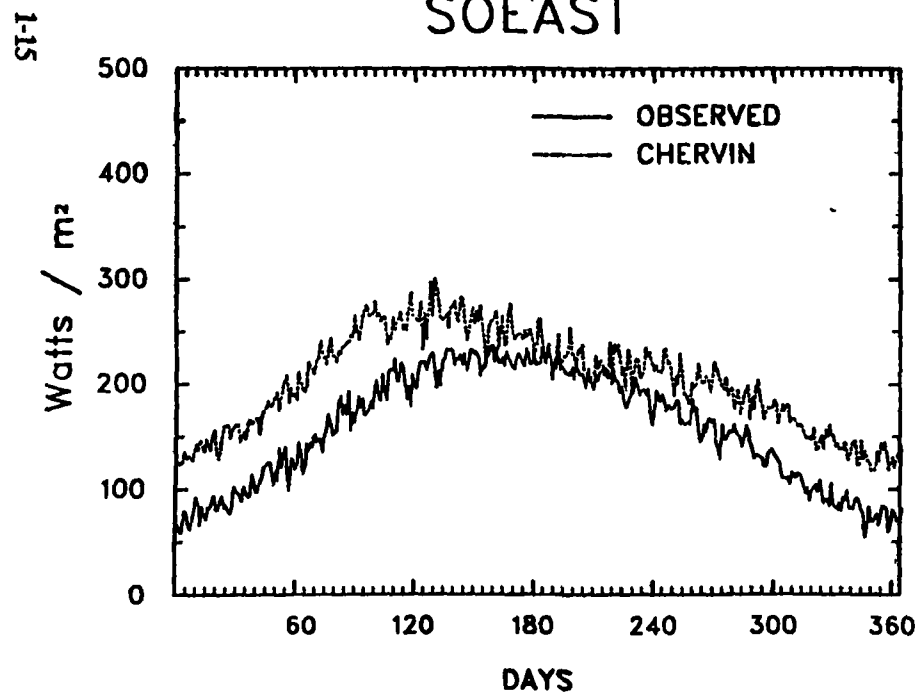
GP123



GTLAKES



SOEAST



WCOAST

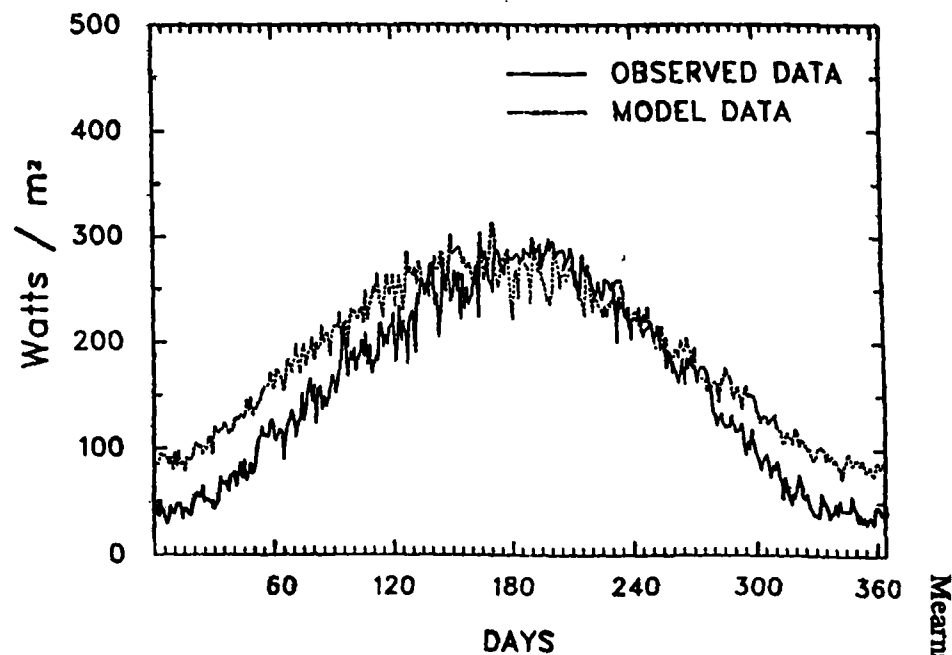


Figure 7. Average daily absorbed solar radiation (18-year average), Chervin model vs. observed for the four regions.

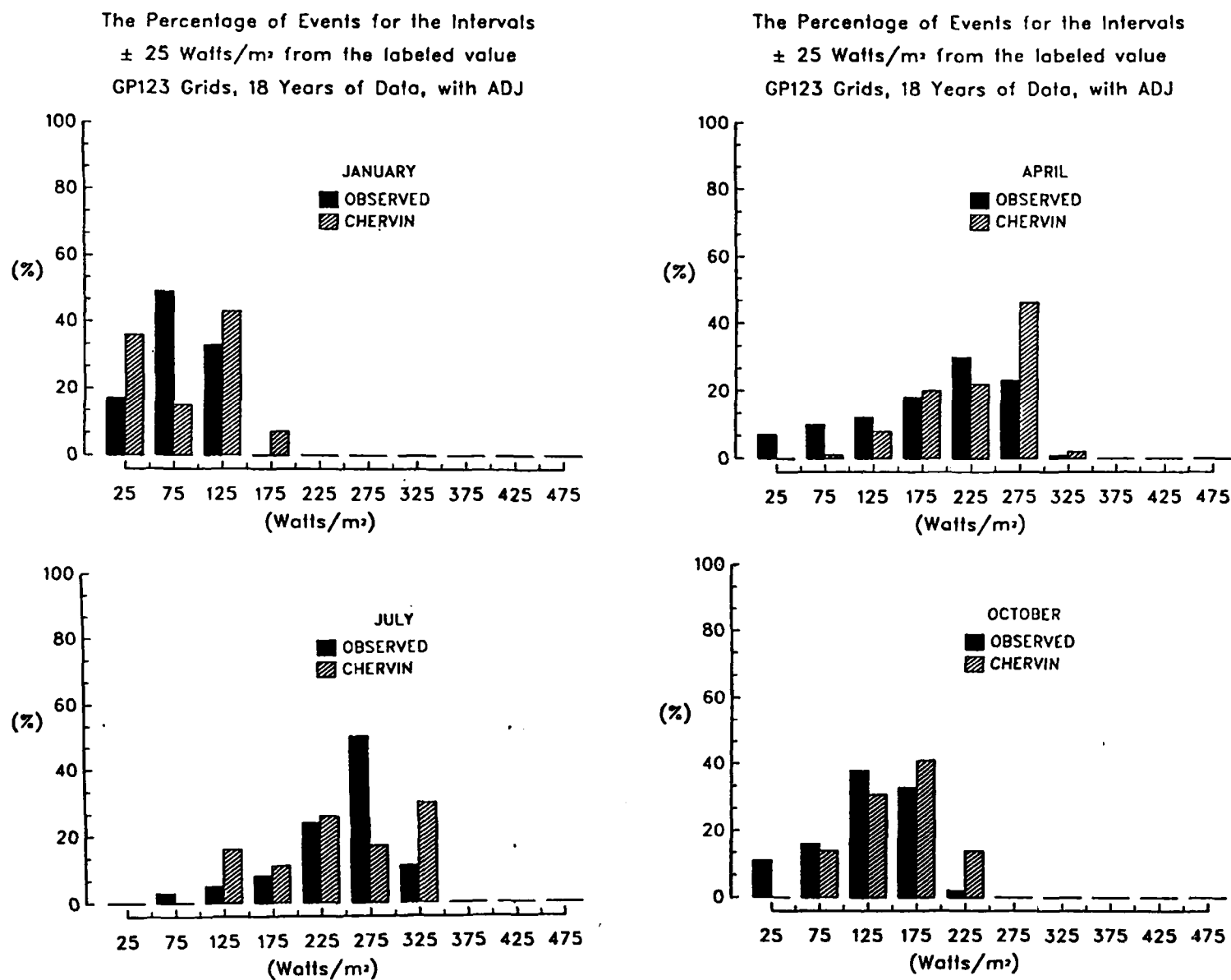


Figure 8. Histograms of daily absorbed surface solar radiation for the three GP grids, four selected months.

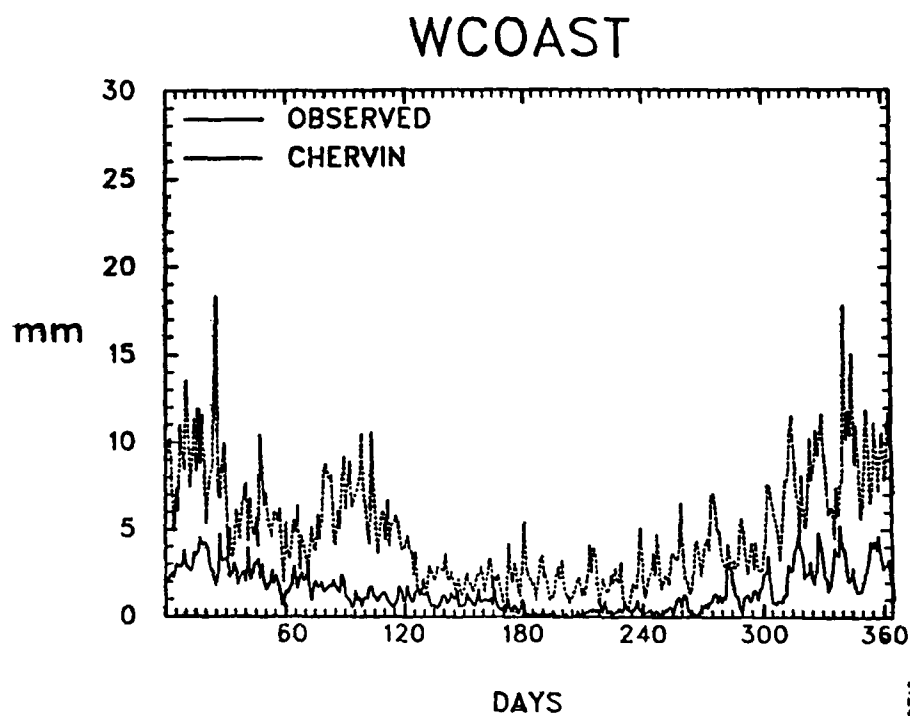
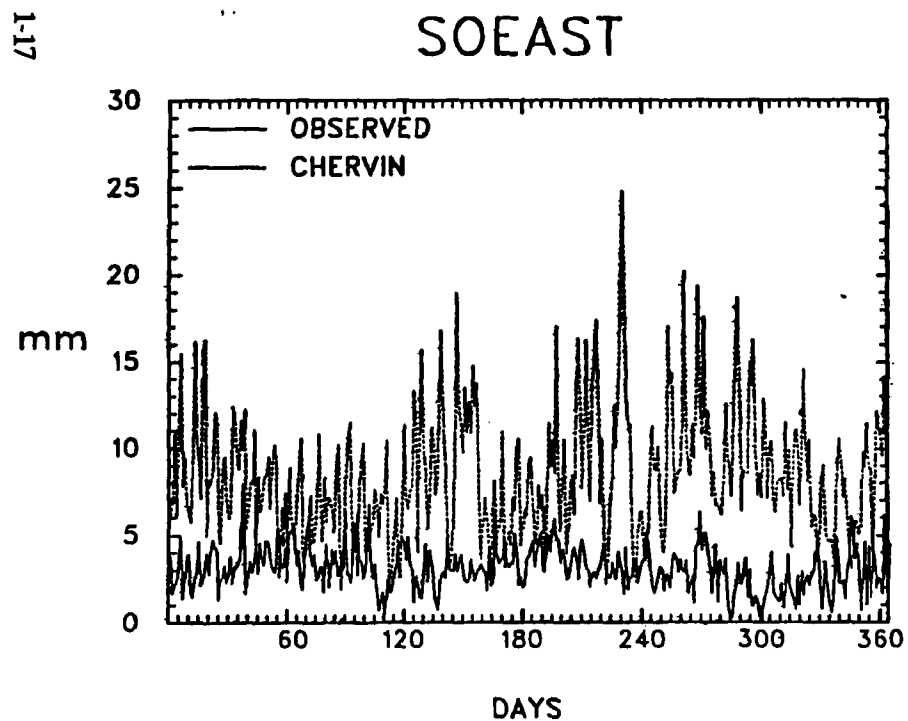
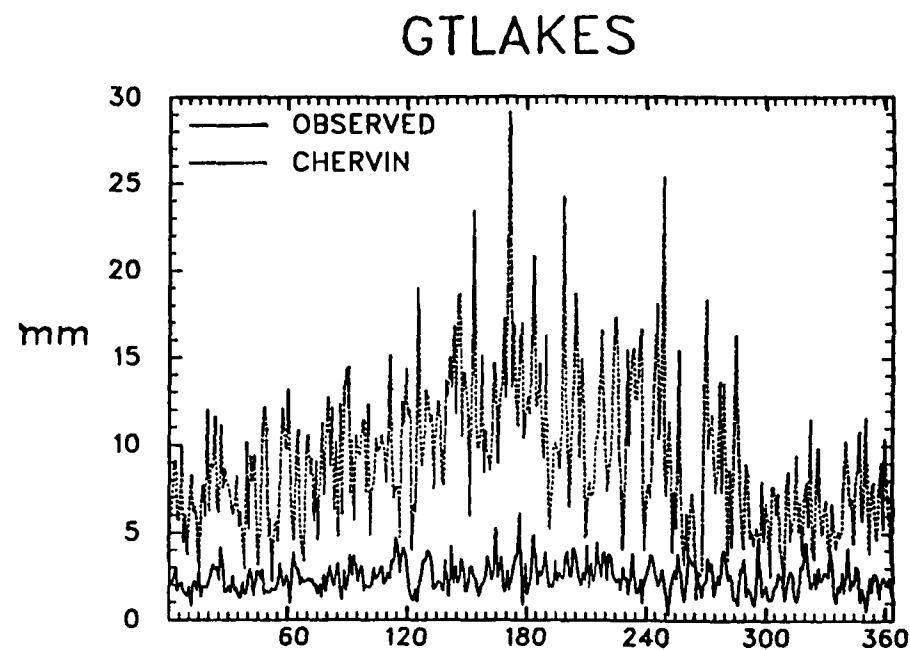
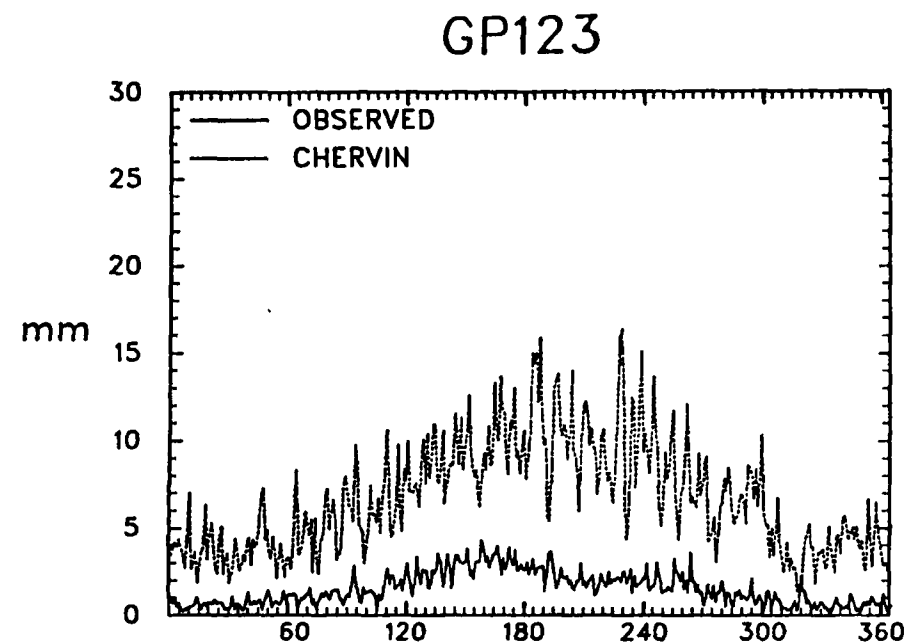


Figure 9. Average total daily precipitation for a 20-year average, Chervin model vs. observed, for the four regions.

are often three times greater than observed values, even though modeled global average precipitation amount is close to the observed value of 5 mm/day. At the GP (average) grid the discrepancies seem to be worst in late summer -- the time we have speculated that excess evaporation from fixed soil hydrology would be most serious. The annual cycle of precipitation is much better represented in that high precipitation values dominate in the summer in both the observed and simulated series. The observed series for the GL and SE grids exhibit no clear seasonal cycle, although there is a slight cycle similar to that of the GP region at the GL grid in the model time series. At the WC grid the observed seasonal cycle of high winter and low summer precipitation is well matched by a parallel (although greater in amount) simulated series.

Figures 10-13 present probability functions for total precipitation aggregated on a seasonal basis for the four regions. The graphs also include table inserts displaying the relative percentages of rain days and percentage of days with precipitation rates exceeding 20 mm/day. A rain day is defined as a day which receives greater than 0.1 mm of precipitation. At GP and SE the simulations consistently result in an over estimation of raindays, although the discrepancy is most severe in the fall (Figures 10d and 12d) and is relatively minor in the spring. At the GL grid, however, the model slightly underestimates raindays in the winter and fairly accurately represents raindays for the other seasons. These anomalous results could be due to a number of factors, including too much soil moisture in the fall in the Great Plains, or model structural factors such as the absence in the model of mesoscale features such as the Great Lakes or spectral truncation errors in the water vapor field. In regard to the GL grid, added moisture and precipitation events which result from atmospheric interaction with the lakes, cannot be modeled. Perhaps, the good results for three of the four seasons at GL are due to the cancelling of one type of model bias (too much local precipitation) with another (absence of lake influence). At the WC grid (Figure 13), although percentage of raindays is overestimated, the relative percentages across the four seasons are well reproduced.

The probability functions are truncated just below 20 mm/day on the figures, but the percentage of occurrences of extreme values (greater than 20 mm) is given by the table on the figure. In all seasons in all four regions the model produces large numbers of precipitation events exceeding 20 mm/day, (e.g., from 15% in the summer to 4% in winter at the GP region; observed percentages for the GP region range from 0.8 in summer to 0.0 in the winter).

The best agreement for overall shapes of the density functions occurs for the GP region, where the best matches are found in spring and summer. At the GL grid precipitation events up to five mm/day are underestimated in most seasons. At the SE grid the model curves do not fall off as quickly as do the observed curves, particularly in spring and fall. In most seasons at most locations, the model generates too few low precipitation events (the first interval, 0.1-1.0 mm). This is particularly true for winter at the GL grid (Figure 11a). However, at the WC grid in summer, the model overpredicts all precipitation amounts including the lowest amount category, as it does at the SE grid in all seasons but summer. Of course, this is consistent with the overall tendency to simulate too much absolute precipitation at these grid points.

We believe it is important to track down the reasons why the precipitation amounts are so high in the model in these four regions. Perhaps the precipitation parameterization criterion of 80% relative humidity in the model for precipitation is too low so that there is too much precipitation. Also, the fixed soil hydrology could well be responsible for overestimating evaporation and relative humidity, especially in late summer. This needs to be tested by analyzing other grid points, other variables and other versions of the CCM with different physical parameterizations. It may also be necessary to test other GCMs (especially those without spectral advection of water vapor) or CCM versions where water vapor is treated by non-spectral formulations since we suspect that spectral truncation of a heterogeneous field like water vapor could result in anomalously extreme precipitation events.

INTERANNUAL VARIABILITY STATISTICS OF TEMPERATURE AND PRECIPITATION

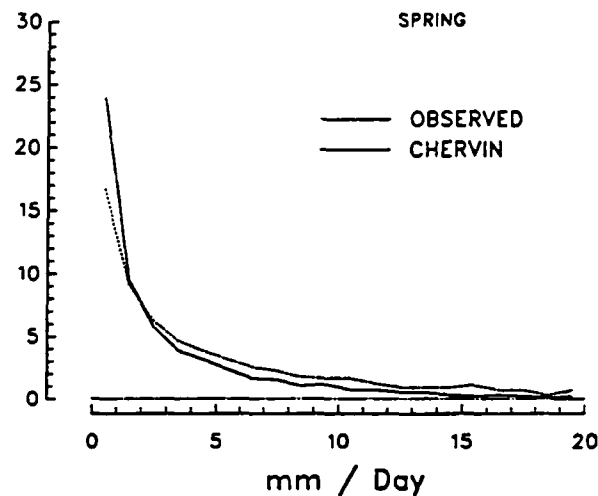
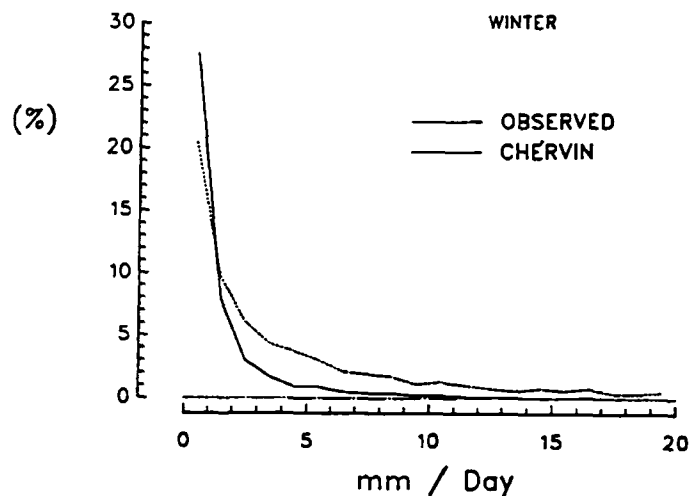
Tables 1-5 present statistics on interannual variability for temperature and precipitation for the four regions of analysis. Table 1 presents these for annual mean temperature and annual total precipitation for the

The % of Events Greater Than .1mm
 Bob Chervin History Tapes
 Three US Grids 20 Years Per Grid (STACKED)

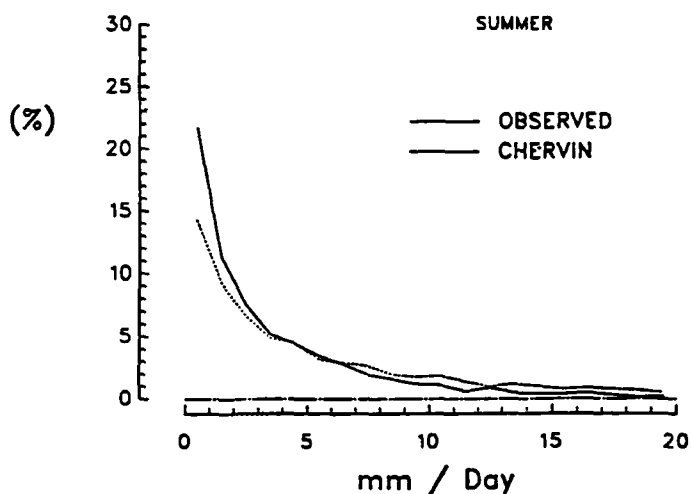
Parameter	OBSERVED	CHERVIN
% of Rain Days	44	66
Maximum Value (mm)	20.19	97.39
% GT 20mm	0.0	4.3

The % of Events Greater Than .1mm
 Bob Chervin History Tapes
 Three US Grids 20 Years Per Grid (STACKED)

Parameter	OBSERVED	CHERVIN
% of Rain Days	58	71
Maximum Value (mm)	32.64	128.94
% GT 20mm	0.3	10.1



Parameter	OBSERVED	CHERVIN
% of Rain Days	67	78
Maximum Value (mm)	37.55	167.59
% GT 20mm	0.8	15.1



Parameter	OBSERVED	CHERVIN
% of Rain Days	49	67
Maximum Value (mm)	45.13	151.47
% GT 20mm	0.3	8.4

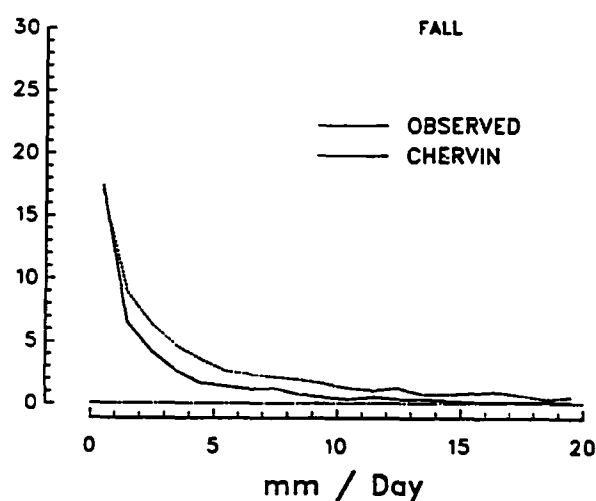
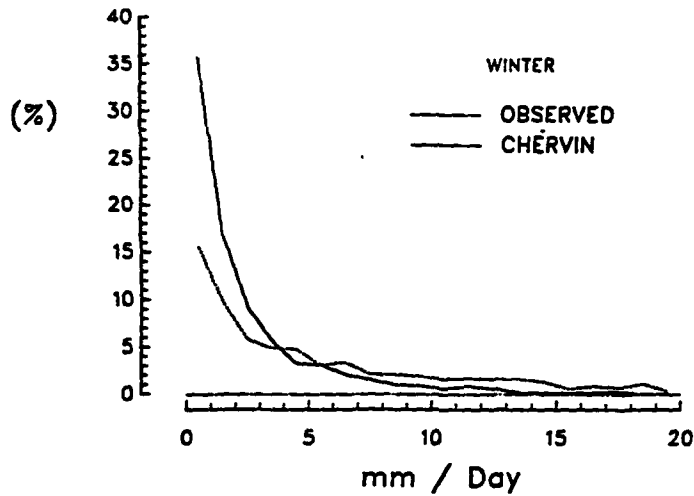


Figure 10. Probability functions of precipitation for the three GP grids, Chervin vs. observed for four seasons.

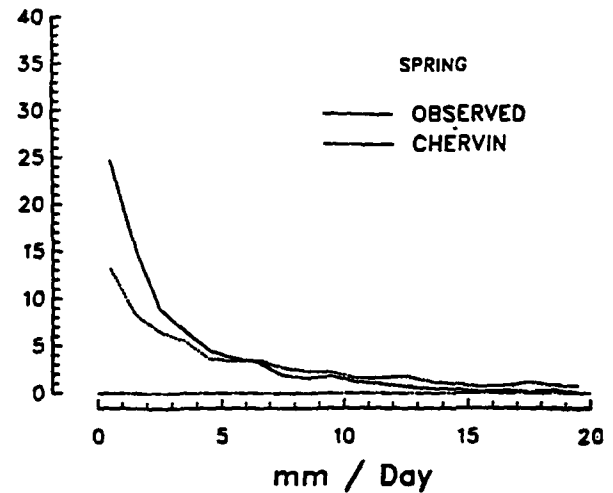
The % of Events Greater Than .1mm
Bob Chervin History Tapes
GTLAKES US Grid, 20 Years of data

Parameter	OBSERVED	CHERVIN
% of Rain Days	83	76
Maximum Value (mm)	30.44	86.40
% GT 20mm	0.2	11.4

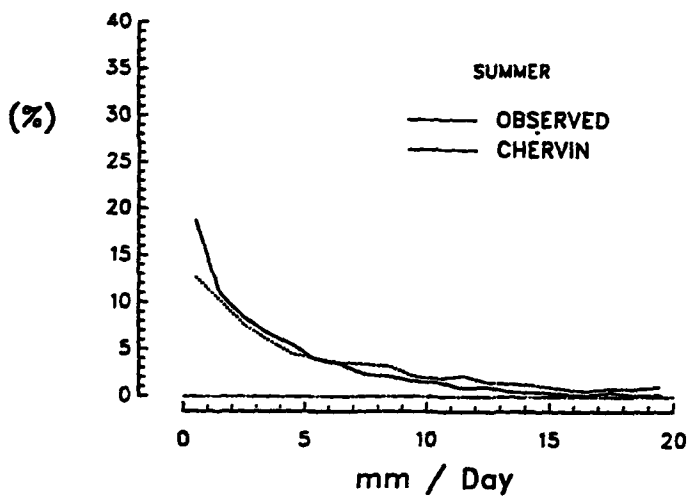


The % of Events Greater Than .1mm
Bob Chervin History Tapes
GTLAKES US Grid, 20 Years of data

Parameter	OBSERVED	CHERVIN
% of Rain Days	77	79
Maximum Value (mm)	22.31	137.42
% GT 20mm	0.3	16.1



Parameter	OBSERVED	CHERVIN
% of Rain Days	70	87
Maximum Value (mm)	41.99	132.06
% GT 20mm	0.5	17.1



Parameter	OBSERVED	CHERVIN
% of Rain Days	68	67
Maximum Value (mm)	26.52	126.22
% GT 20mm	0.6	10.7

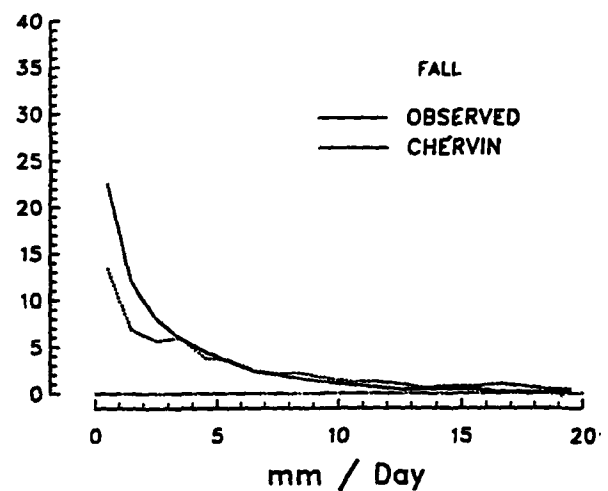
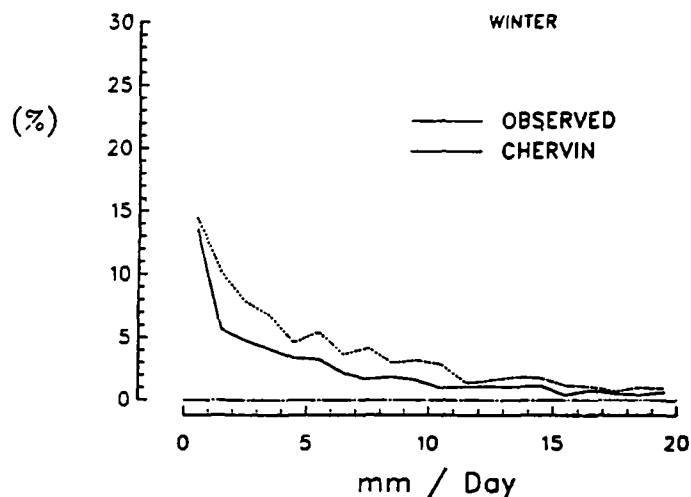


Figure 11. Probability functions of precipitation GL grid, Chervin vs. observed for four seasons.

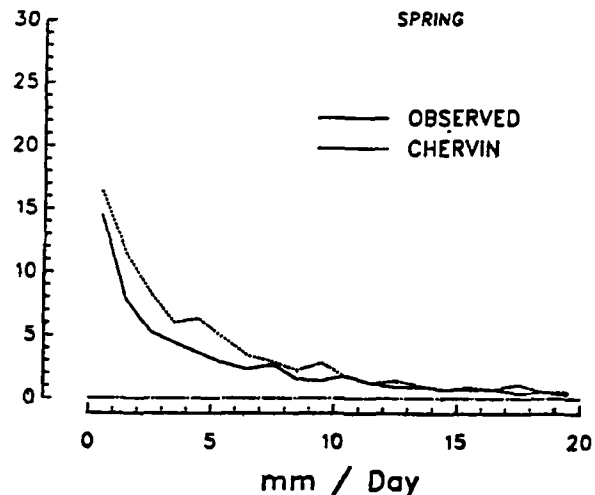
The % of Events Greater Than .1mm
Bob Chervin History Tapes
SOEAST US Grid, 20 Years of data

Parameter	OBSERVED	CHERVIN
% of Rain Days	53	88
Maximum Value (mm)	41.36	133.02
% GT 20mm	3.0	10.0

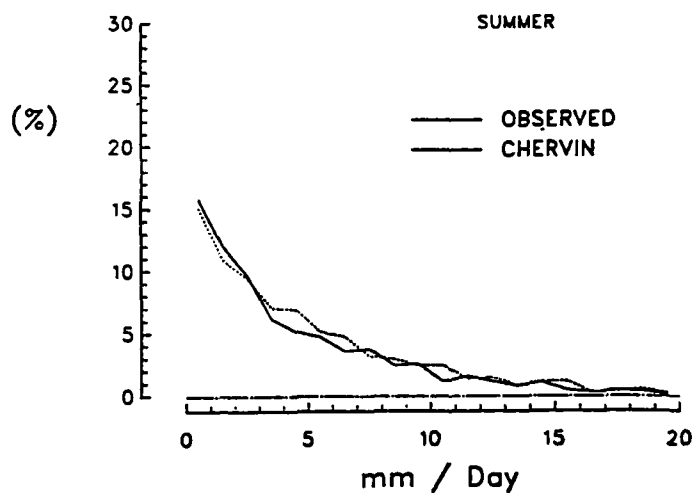


The % of Events Greater Than .1mm
Bob Chervin History Tapes
SOEAST US Grid, 20 Years of data

Parameter	OBSERVED	CHERVIN
% of Rain Days	57	85
Maximum Value (mm)	51.26	150.97
% GT 20mm	2.6	8.4



Parameter	OBSERVED	CHERVIN
% of Rain Days	75	87
Maximum Value (mm)	39.67	234.76
% GT 20mm	0.8	8.8



Parameter	OBSERVED	CHERVIN
% of Rain Days	47	89
Maximum Value (mm)	70.7	195.06
% GT 20mm	2.1	10.7

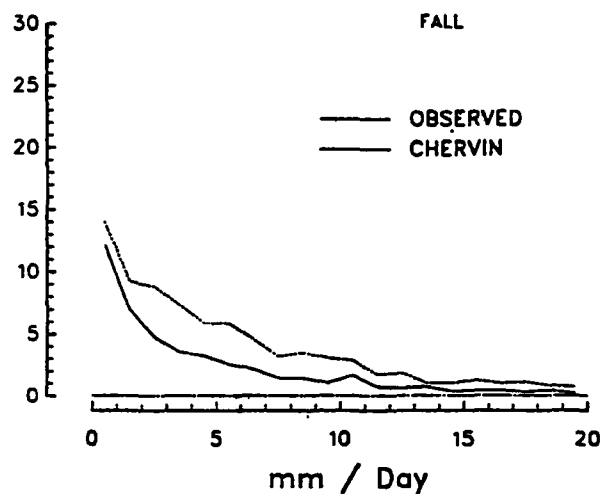


Figure 12. Probability functions of precipitation SE grid, Chervin vs. observed for four seasons.

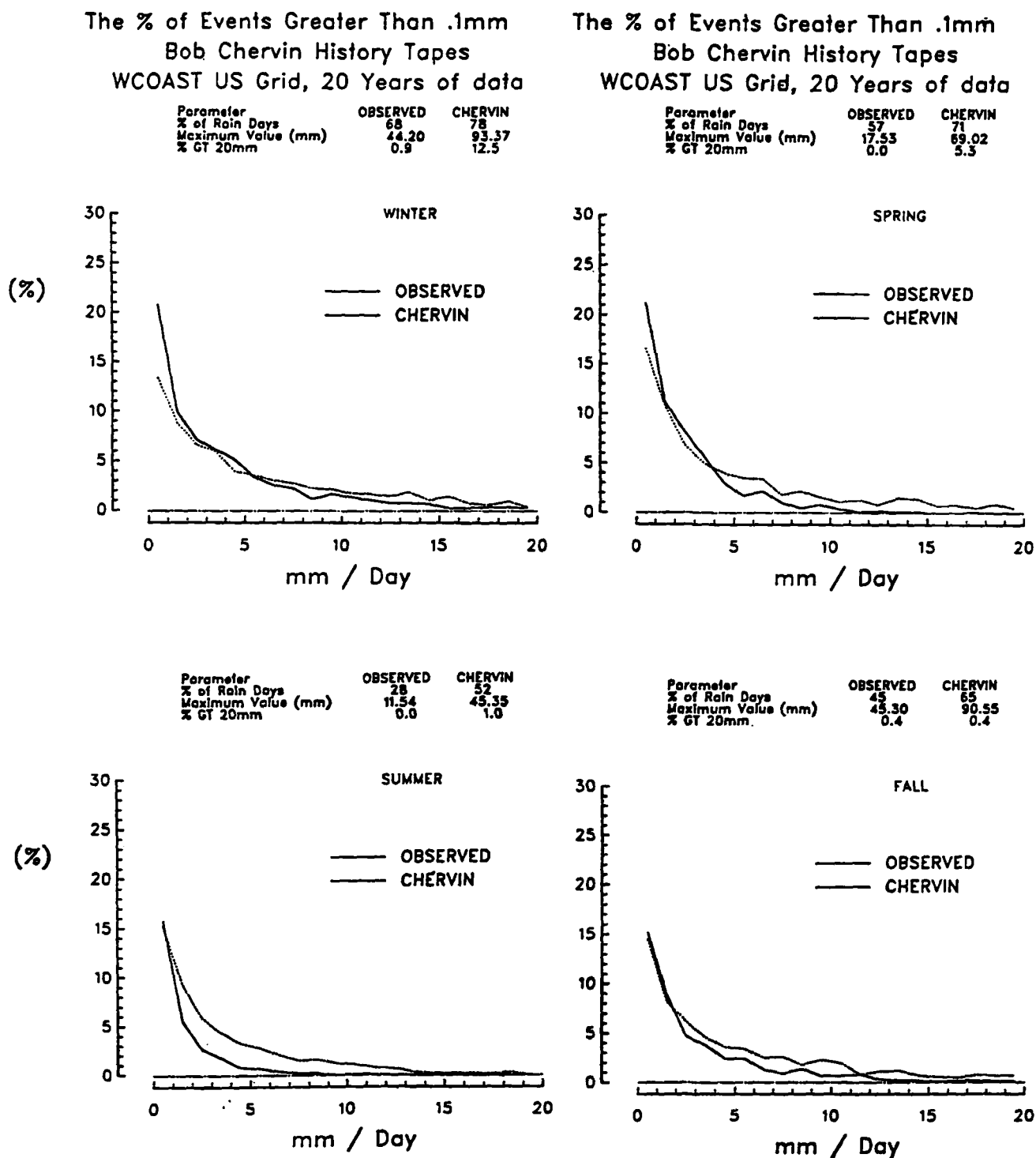


Figure 13. Probability functions of precipitation WC grid, Chervin vs. observed for four seasons.

Table 1. Great Plains (GP) Grids Average and Individual Grids -- Mean and Variance Statistics For Annual Mean Temperature and Annual Total Precipitation

	<u>Observations</u>			<u>Simulation</u>		
	<u>Mean</u>	<u>SD</u>	<u>CV</u>	<u>Mean</u>	<u>SD</u>	<u>CV</u>
A. GRAND SPATIAL MEANS						
T	8.89	0.72		8.93	0.39*	
P	558.9	80.6	14.4	2452.0	283.0	11.6
B. INDIVIDUAL GRIDS						
<u>Grid I</u>						
T	5.43	1.05		3.43	0.55*	
P	373.0	56.74	15.2	2619.1	343.1	13.1
<u>Grid II</u>						
T	8.46	0.70		9.99	0.41*	
P	577.9	90.40	15.6	2040.2	399.1	19.5
<u>Grid III</u>						
T	12.78	0.71		13.36	0.42*	
P	725.7	160.90	22.2	2690.8	447.8	16.6

T - mean temperature (°C)

P - total precipitation (mm)

SD - standard deviation (°C)

CV - coefficient of variation (%). (Calculated only for precipitation).

* - temperature variances of model and observed data are significantly (0.05 level) different on the F-test.

Mearns

Table 2. Great Plains (GP) Average Grids and Individual Grids -- Mean and Variance Statistics for Seasonal Mean Temperature and Seasonal Total Precipitation

	<u>Observations</u>			<u>Simulation</u>		
	<u>Mean</u>	<u>SD</u>	<u>CV</u>	<u>Mean</u>	<u>SD</u>	<u>CV</u>
A. GRAND SPATIAL MEANS						
1. Winter (D,J,F)						
T	-5.14	1.64		-4.2	1.2	
P	59.7	16.2	27.3	354.9	76.5	21.5
2. Summer (J,J,A)						
T	22.2	0.89		20.7	0.42*	
P	227.1	39.0	17.2	930.3	176.7	19.0
B. INDIVIDUAL GRIDS						
1. Winter (D,J,F)						
<u>Grid I</u>						
T	-9.5	2.8		-10.7	1.5*	
P	42.2	10.2	24.0	267.3	88.5	33.1
<u>Grid II</u>						
T	-6.2	1.6		-3.7	1.2	
P	55.8	20.1	35.8	255.4	74.7	29.3
<u>Grid III</u>						
T	0.35	1.1		1.7	1.3	
P	81.3	29.4	36.2	541.8	156.9	28.9
2. Summer (J,J,A)						
<u>Grid I</u>						
T	19.4	1.0		16.3	0.47*	
P	161.8	42.7	26.5	737.4	261.5	23.0
<u>Grid II</u>						
T	22.3	1.0		22.1	0.55	
P	243.0	37.0	15.2	775.0	184.4	23.8
<u>Grid III</u>						
T	24.9	1.2		23.8	0.14*	
P	276.9	79.6	28.7	877.7	318.5	36.3

T = mean temperature (°C)

P = total precipitation (mm)

SD = standard deviation (°C)

CV = coefficient of variation (%). (Calculated only for precipitation).

* = temperature variances of model and observed data are significantly (0.05 level) different on the F-test.

Table 3. Great Lakes (GL) Grid -- Mean and Interannual Variance Statistics For Annual and Seasonal Mean Temperature and Total Precipitation

<u>Observations</u>				<u>Simulation</u>		
	<u>Mean</u>	<u>SD</u>	<u>CV</u>	<u>Mean</u>	<u>SD</u>	<u>CV</u>
ANNUAL						
T	9.0	0.59		9.3	0.63	
P	887.4	101.1	11.4	3345.4	336.7	10.1
SEASONAL						
<u>Winter</u> (D,J,F)						
T	-3.1	1.6		-6.6	2.2	
P	187.2	46.1	24.6	640.0	127.0	19.8
<u>Summer</u> (J,J,A)						
T	20.5	0.88		22.8	0.71	
P	254.9	32.6	12.8	1105.4	269.7	24.4

T = mean temperature (°C)
P = total precipitation (mm)
SD = standard deviation (°C)
CV = coefficient of variation (%). (Calculated only for precipitation).

Table 4. Southeast (SE) Grid -- Mean and Interannual Variance Statistics For Annual and Seasonal Mean Temperature and Total Precipitation

<u>Observations</u>				<u>Simulation</u>		
	<u>Mean</u>	<u>SD</u>	<u>CV</u>	<u>Mean</u>	<u>SD</u>	<u>CV</u>
ANNUAL						
T	16.6	0.58		20.0	0.37	
P	1137.2	136.3	12.0	3085.5	305.7	9.9
SEASONAL						
<u>Winter</u> (D,J,F)						
T	7.4	1.8		14.1	1.0*	
P	293.2	59.2	20.2	739.8	130.1	17.6
<u>Summer</u> (J,J,A)						
T	25.5	0.73		25.9	0.38*	
P	317.0	54.2	17.1	786.4	203.9	25.9

T = mean temperature (°C)
P = total precipitation (mm)
SD = standard deviation (°C)
CV = coefficient of variation (%). (Calculated only for precipitation).
* = temperature variances of model and observed data are significantly (0.05 level) different on the F-test.

Mearns

Table 5. West Coast (WC) Grid -- Mean and Interannual Variance Statistics For Annual and Seasonal Mean Temperature and Total Precipitation

	<u>Observations</u>			<u>Simulation</u>		
	<u>Mean</u>	<u>SD</u>	<u>CV</u>	<u>Mean</u>	<u>SD</u>	<u>CV</u>
ANNUAL						
T	10.1	0.49		10.1	0.46	
P	553.2	93.43	16.9	1792.8	296.1	16.5
SEASONAL						
<u>Winter</u> (D,J,F)						
T	2.6	1.6		2.42	0.8*	
P	254.1	76.7	30.2	723.8	199.6	27.6
<u>Summer</u> (J,J,A)						
T	18.1	0.81		17.7	0.17*	
P	39.4	20.5	52.1	192.6	45.7	23.7

T = mean temperature (°C)

P = total precipitation (mm)

SD = standard deviation (°C)

CV = coefficient of variation (%). (Calculated only for precipitation).

* = temperature variances of model and observed data are significantly (0.05 level) different on the F-test.

GP region averaged for the three grids (referred to as grand spatial means on the table) and for the three individual grids. Table 2 presents the same but for winter and summer seasonal values rather than annual values. Tables 3, 4, and 5 present annual and seasonal values for the GL, SE, and WC grids, respectively. The GP region is discussed first, where the effect of spatial aggregation is analyzed.

It can be seen from Table 1 that the grand spatial mean annual average modeled and observed temperatures are very close in value, but that the variability (indicated by the standard deviations) of the modeled data is lower than that of the observed data (significantly lower at the 0.05 level on the basis of the F-test for equality of variances). Modeled results for precipitation clearly show the tremendous over estimation of total amounts (off by up to a factor of five), but the relative variability (indicated by the coefficient of variation) is similar to that of the observed data. This may be fortunate if it means that a simulation error in the absolute amount of precipitation would not imply an error in model sensitivity to climatic forcing. This remains to be investigated.

Values for the individual three grids show results qualitatively similar to those for the grand spatial means. Mean temperatures are within one or two degrees C of observed values, and standard deviations within 0.5°C of the observed. However, the direction of model error is not the same at all three grids. At Grid I the model is cooler than the observations. Moreover, the errors of the individual grids are larger than those of the three grid aggregation. Again, the modeled variability is significantly less than that of the observed data. The statistics of precipitation for each grid reflect the direction of error inconsistency seen in the temperature statistics, i.e., two grids underestimate precipitation variability, while the third overestimates it.

Looking at seasonal values for the grand spatial means of temperature and precipitation (Table 2), it can be seen that seasonal temperatures for winter and summer are well simulated, although the model is slightly too cool in the summer. Decreases in variability from winter to summer are well simulated for both temperature and precipitation. Again, this may be a good sign for forecasting climatic changes even if means are somewhat in error.

The seasonal statistics for each grid square of the GP region are of course less similar (modeled and observed) than for the averaged grid values, but the values are still quite close. The direction of error, however, is not the same at each grid square. In winter, for example, the simulated temperature is slightly too cold at grid I but slightly too warm at grids II and III. Again the model variability of temperature, indicated by the standard deviations, is slightly lower than that of the observed temperatures, at all three grids for both summer and winter.

Although we deliberately chose an eastern slope midcontinental region without much sub-grid scale spatial heterogeneity as the primary area of analysis to minimize the anchoring effect of oceanic temperatures or mesoscale effects of topography, it is still likely that model variability may be slightly lower because Chervin's (1986) control run was designed to exclude variability of oceanic surface temperatures.

At the GL grid (Table 3) the annual model temperature is quite accurate compared to observed as is the temperature variability (no significant difference according to the F-test at the 0.05 level). The relative variability of precipitation (indicated by the coefficient of variation) is also very accurate. In winter, although the model mean temperature is too low, the variability of temperature is relatively similar to that of the observed data. The variability of precipitation is also quite similar. In summer the model is slightly too warm, but the variability of temperature is again well reproduced. The variability of precipitation, however, is overestimated by the model. Note that the seasonal compensating errors in mean temperature account for the model's (ostensible) accuracy in reproducing the annual mean temperature.

At the SE grid (Table 4) the model overestimates the mean annual temperature by 3.4°C , whereas the variability is relatively well simulated (not significantly different at the 0.05 level). Precipitation, as has consistently been the case, is overestimated, but the variability of precipitation is reasonably well reproduced, the coefficient of variation being 12.0% for observed data and 9.9% for the model. The seasonal statistics indicate that the error in the annual mean temperature value of the model is a result of the very high error in

Mearns

reproducing the winter mean temperature (Table 4). The temperature variance is fairly well simulated, but is less than that of the observations. The simulation of the variability of winter precipitation is again relatively accurate. In summer, the model variability of temperature is again less than the observed, whereas the variability of precipitation of the model is higher than observed.

At the WC grid (Table 5) the model accurately reproduces the mean and standard deviation of temperature and the variability of precipitation on an annual basis. However, temperature variability is underestimated in both winter and summer. We speculate that the low model variability in winter could be due to the fixed SSTs but that the low variability in summer is due to the fixed soil moisture. The relative variability of precipitation is greatly underestimated in summer. Perhaps the model underestimation of the coefficient of variation of precipitation at this west coast grid is associated with the absence of interannual SST anomalies in the model.

In summary, the Chervin model either successfully reproduces the interannual variability of temperature (as at the GL grid) or underestimates it (at the GP grids, SE grid, and WC grid). The seasonal decrease in variability of temperature from summer to winter is well reproduced at all grids. Regarding precipitation, the relative variability (as measured by the coefficient of variation) is in general well simulated, although there is an occasional overestimation by the model. Aggregating over the three grid boxes in the GP region produces in general better comparisons with observations than for the individual grids, and directions of error of the three GP grids are not consistent.

CHAPTER 4

INTERCOMPARISONS OF THREE CCM VERSIONS AND OBSERVED DATA

COMPARISONS OF MEAN CONDITIONS: TEMPERATURE AND PRECIPITATION

Table 6 presents comparisons of annual and seasonal mean conditions (temperature and precipitation) simulated by the three models and observations for the four grids. Statistics of interannual variability cannot be analyzed because there are too few years of simulated data (Washington and Dickinson runs). The Chervin model is consistently the most accurate in predicting mean annual temperatures. In terms of mean annual precipitation totals, however, it is consistently the least accurate. The Washington model is in general the least accurate in terms of temperature, but is the most accurate in terms of total precipitation at GP III and GL. It is perhaps not surprising that a model that predicts sea surface temperature with a mixed layer ocean would not simulate temperatures as well as the other models which have prescribed observed SSTs. The Dickinson model best simulates total annual precipitation at the WC and SE grids. The Washington model also is the least accurate in winter and summer temperatures at GP III and GL. In terms of seasonal distribution of precipitation (i.e., percentage of annual total occurring in winter and summer) none of the models fare very well. However, the high winter, low summer precipitation cycle of the WC grid is generally captured by all models. The Washington model fails (relative to observed as well as to the other models) to reproduce the winter low-summer high precipitation regime of GP III and GL.

On the basis of mean annual and seasonal comparisons, no one model is clearly superior to the other two regarding the accurate reproduction of all these measures of the climate at these locations. Reasons for these contrasts will be explored in future research efforts.

RELATIVE HUMIDITY

Relative humidity comparisons are made among the three models because we anticipated significant differences among the models, since their surface hydrology packages are so different and this would certainly affect the modeling of surface relative humidity. We first present a detailed analysis of the Chervin version relative humidity including a display of histograms, and then compare these results with those of Washington and Dickinson.

The Chervin modeled average daily time series of relative humidity for the four regions compare poorly with the observed values, which are presented in Figure 14. In the GP and GL regions the modeled series form the mirror image of the observed series. At GP the observed series reaches its maximum values (approx. 70%) in winter when the modeled series experiences its minimum (approx. 50%). There is a greater range of values (summer vs. winter) in the simulated data, particularly at the GL grid. At the more humid SE grid, where the seasonal cycle of relative humidity is muted, discrepancies are less serious. The model values show very little variability. The strongest seasonal cycle in the observed data is found at the WC location, where values range from about 85% in winter to 40% in summer. The model curve is virtually flat at 70% again pointing out the models inability to simulate the seasonal cycle. Again, given the errors that fixed soil moisture could introduce, perhaps the discrepancy should be anticipated.

The poor results at GP are further highlighted in the selected monthly histograms (Figure 15). The distributions of the modeled data are greatly shifted relative to observed data in most months. The observed distributions are roughly normal for all months, whereas the distributions formed from the modeled data depart significantly from the normal distribution for most months (April-October). In addition, some model distributions such as that of July, are much narrower than those formed from observed data, and thus exhibit a narrower range and less variability. At the GL grid (Figure 16, 4 selected months), the model distributions also differ from the observed, but reduced variability in the model data is only seriously in evidence in the summer months (e.g., July as shown in Figure 16). At the SE grid, the reduced variability of model data is again seen

Mearns

Table 6. Four Grids - Multicomparisons of CCM Model Version and Observed Mean Temperature and Total Precipitation Statistics

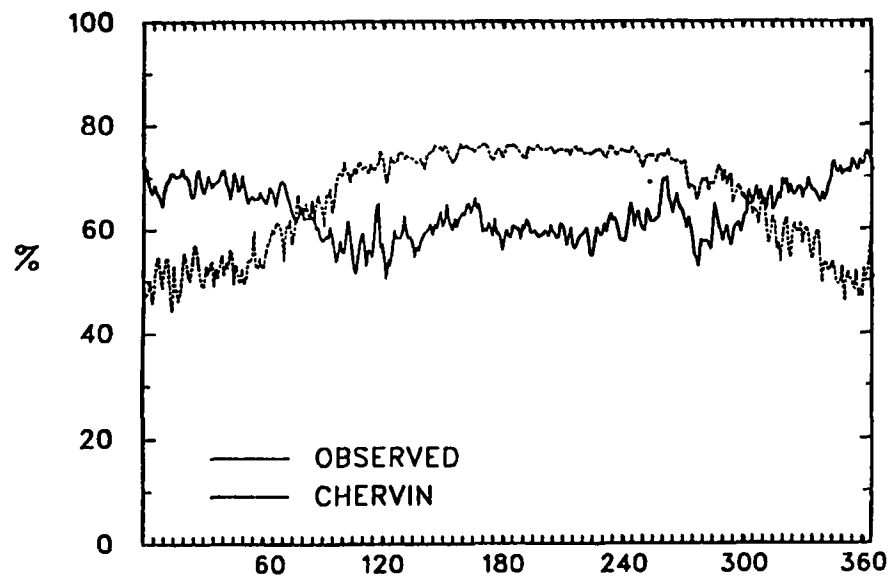
	Observed	CCM Model		
		Chervin	Wash	Dick
SOUTHEAST (SE)				
<u>Annual</u>				
Mean Temperature (°C)	16.6	20.0	20.1	21.5
Total Precipitation (mm)	1137.2	3085.5	589.1	1401.8
<u>Winter</u>				
Mean Temperature (°C)	7.4	14.1	14.8	16.0
Total Precipitation (mm)	1137.2	3085.5	589.1	1401.8
<u>Summer</u>				
Mean Temperature (°C)	25.5	25.9	24.2	26.6
Total Precipitation (mm)	317.0	786.4	75.7	346.9
GREAT PLAINS (GP III)				
<u>Annual</u>				
Mean Temperature (°C)	12.8	13.4	17.6	15.3
Total Precipitation (mm)	725.7	2690.8	931.3	1287.5
<u>Winter</u>				
Mean Temperature (°C)	0.4	1.7	3.5	2.9
Total Precipitation (mm)	81.3	541.8	291.7	270.3
<u>Summer</u>				
Mean Temperature (°C)	24.9	23.8	29.3	26.1
Total Precipitation (mm)	276.9	877.7	194.4	498.4
GREAT LAKES (GL)				
<u>Annual</u>				
Mean Temperature (°C)	9.0	9.3	16.2	12.6
Total Precipitation (mm)	887.4	3345.4	849.1	1902.4
<u>Winter</u>				
Mean Temperature (°C)	-3.1	-6.6	-1.2	-2.7
Total Precipitation (mm)	187.2	640.0	250.5	319.8
<u>Summer</u>				
Mean Temperature (°C)	20.5	22.8	31.7	26.6
Total Precipitation (mm)	254.9	1105.4	156.4	616.6
WEST COAST (WC)				
<u>Annual</u>				
Mean Temperature (°C)	10.1	10.1	13.7	14.3
Total Precipitation (mm)	553.2	1792.8	707.4	652.1

Table 6 (continued).

		CCM Model		
	Observed	Chervin	Wash	Dick
<u>Winter</u>				
Mean Temperature (°C)	2.6	2.4	5.3	4.2
Total Precipitation (mm)	254.1	723.8	340.6	207.6
<u>Summer</u>				
Mean Temperature (°C)	18.1	17.7	24.4	26.4
Total Precipitation (mm)	39.4	192.6	15.7	24.7

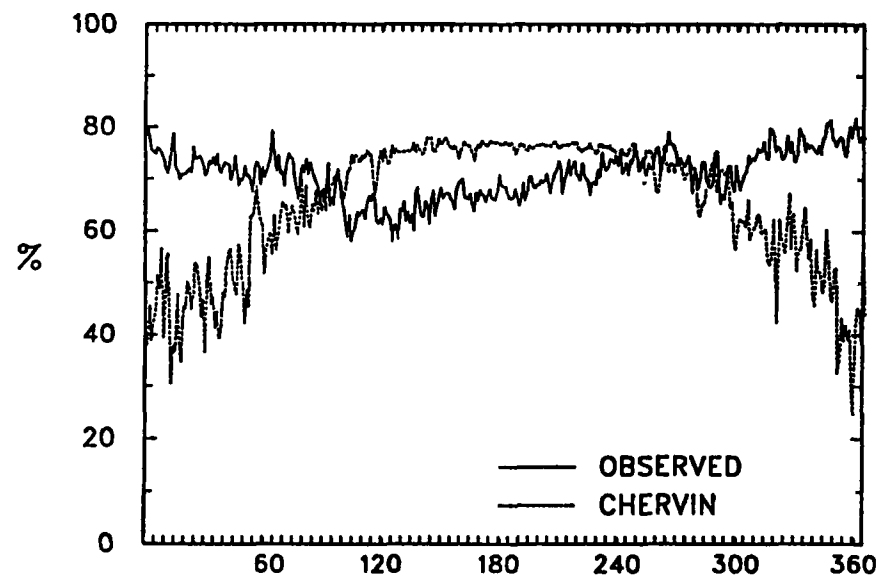
T = temperature
Chervin = Chervin CCM version
Wash = Washington CCM version
Dick = Dickinson CCM version

GP123

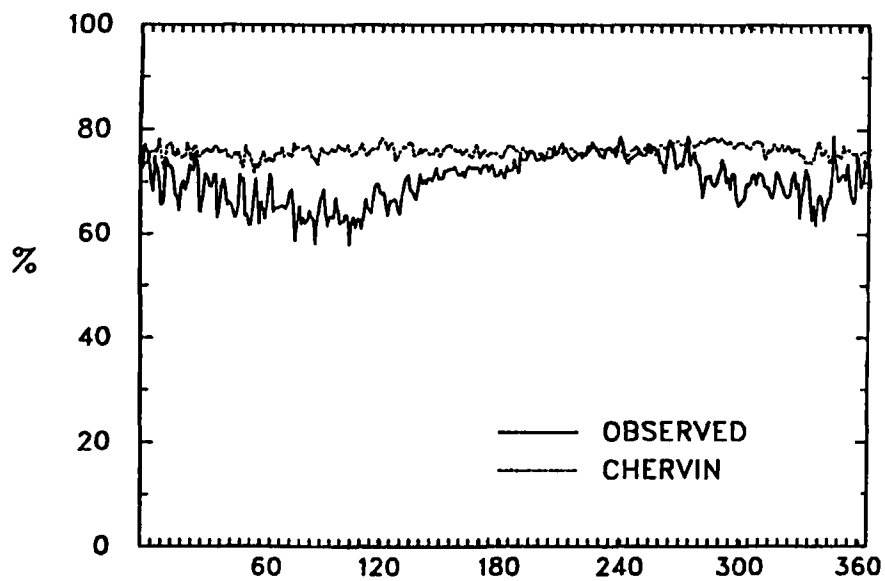


SOEAST

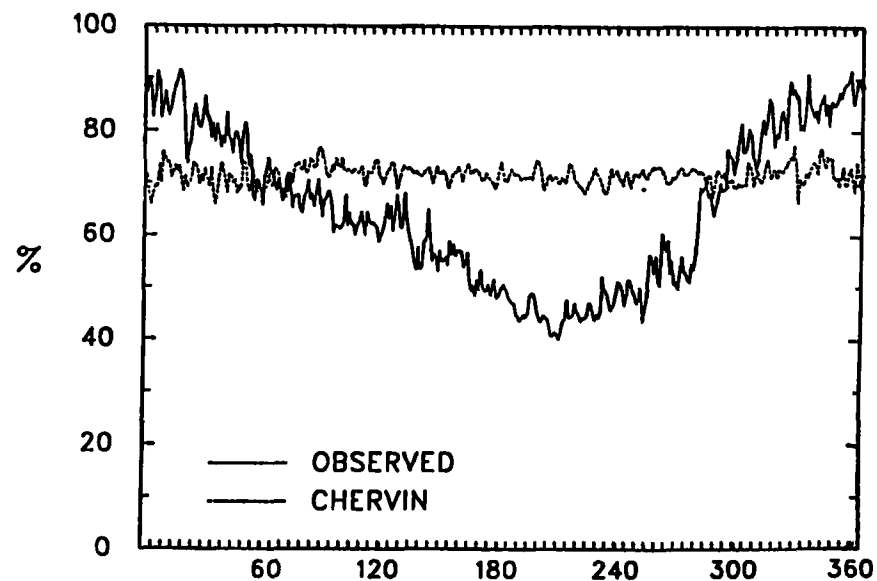
GTLAKES



WCOAST



DAYS



DAYS

Means

Figure 14. Daily average relative humidity for an 18-year average, Chervin vs. observed for four seasons.

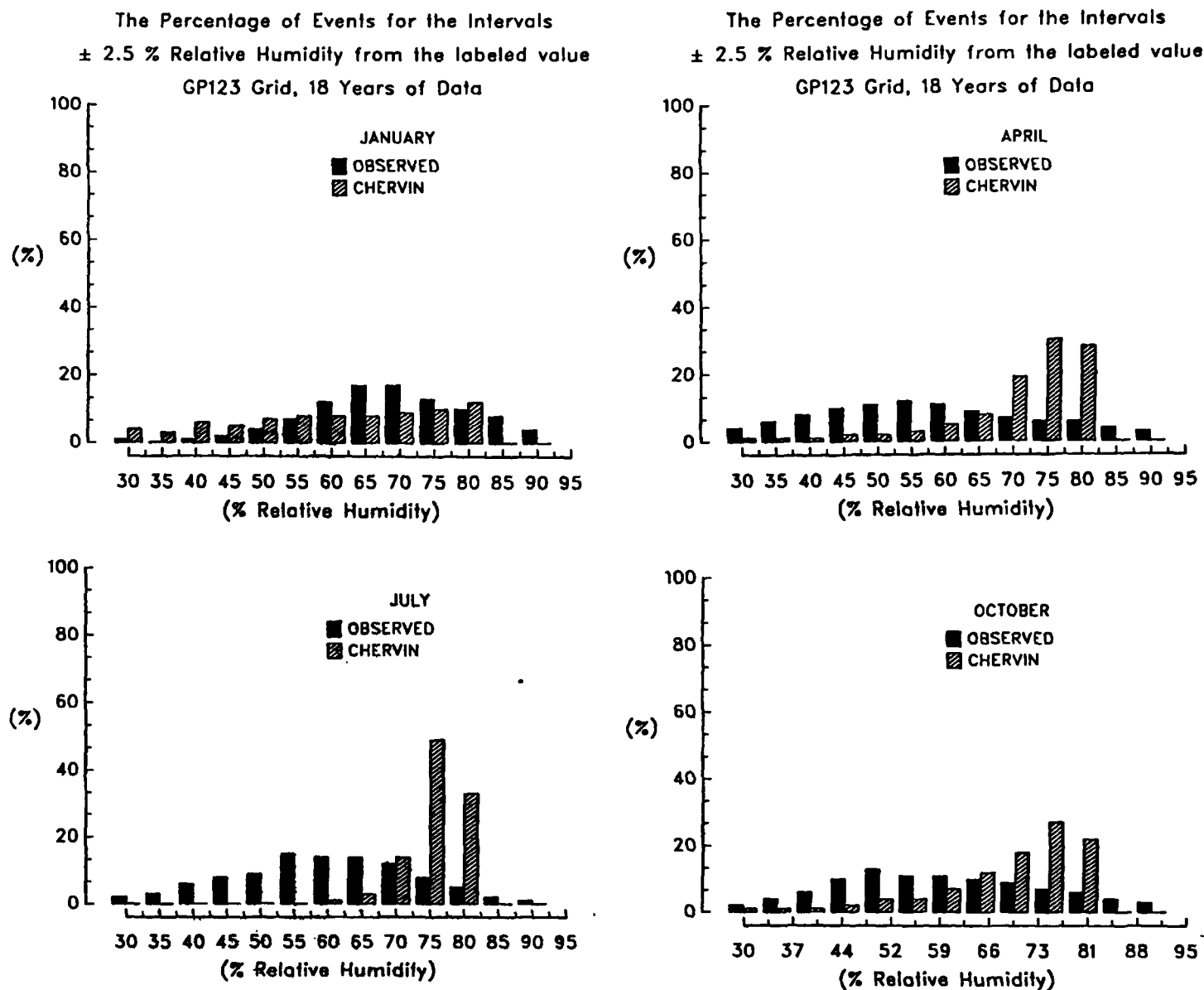


Figure 15. Histograms of relative humidity (18 years) for the three GP grids, four selected months, Chervin model vs. observed.

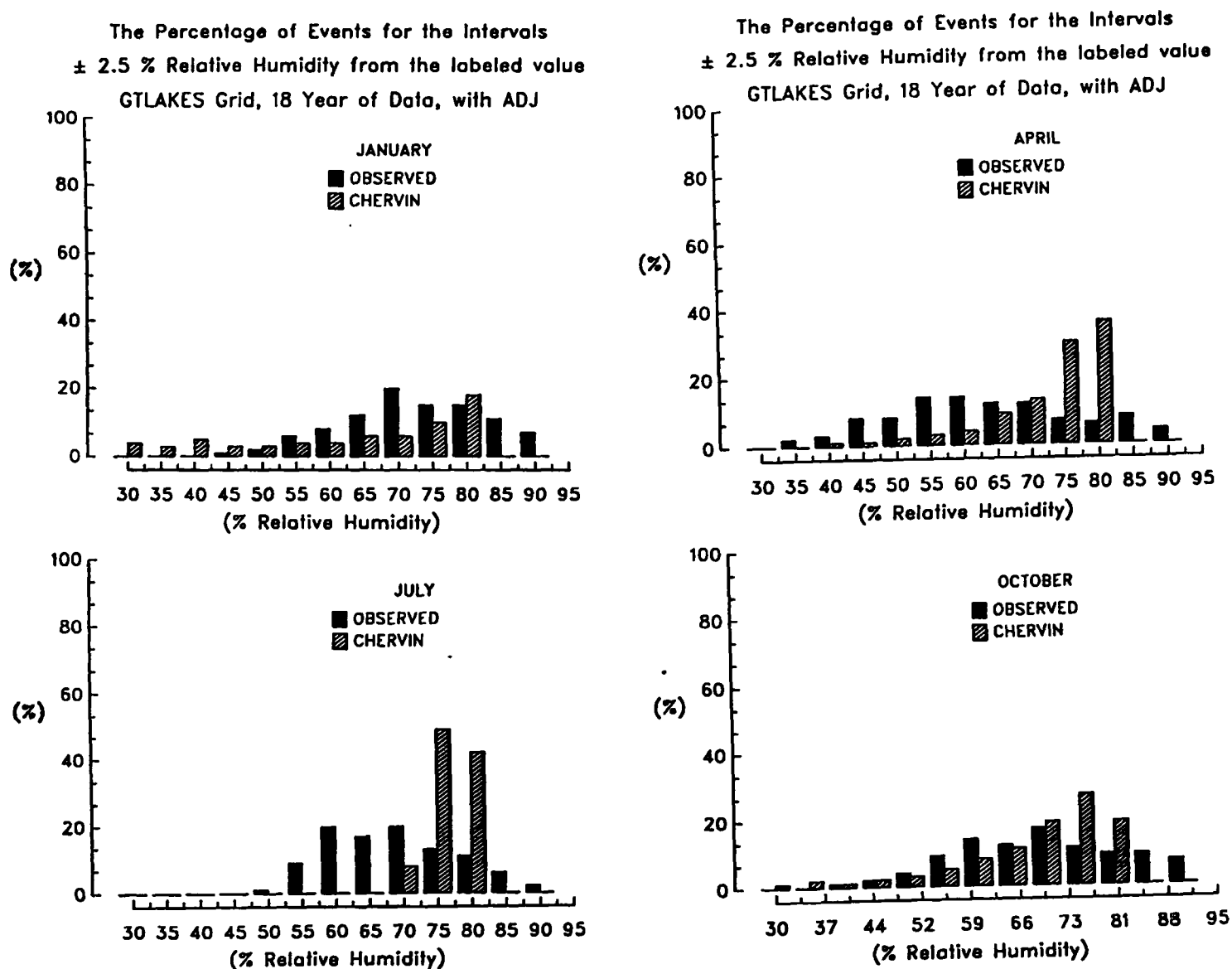


Figure 16. Histograms of relative humidity (18 years) for the GL grid, 4 selected months, Chervin model vs. observed.

in all months (Figure 17). It is difficult to even speculate on why the SE relative humidity should be both too large and not variable enough relative to the observed humidity. Perhaps the proximity to the Atlantic Ocean, coupled with horizontal diffusion is responsible. The absence of a diurnal cycle in CCM0 could be another factor.

These results may reinforce the speculation offered earlier, i.e., that fixed soil moisture is a major cause of the discrepancies. In the GP and GL regions, winter/spring season soil moisture and relative humidity are usually high, and warm season, especially late summer values, are usually low. The fixed soil moisture at 25% of field capacity would thus cause too little evaporation, too low relative humidity, (perhaps) too few clouds and too warm temperatures in the winter/spring and exactly the opposite in late summer. Such diagnostics are consistent in pointing to the fixed hydrology as a potential cause of the late winter/late summer discrepancies evident in the model for the GP and GL regions.

We present here a brief comparison of average daily relative humidity of the Washington and Dickinson versions and contrast them with the Chervin version results. Both the Washington and Dickinson results are more accurate (compared to observations) than those of the Chervin version. The Washington version (Figure 18) reproduces fairly well the seasonal cycle of relative humidity at the SE and WC grids. However serious discrepancies are still found at the other two grids. Late summer minima are produced by the model at both locations which have no correspondence in the observations. The Dickinson model is the most accurate of the three models (Figure 19). The overall shapes of the relative humidity curves are successfully reproduced at each grid. However, the Dickinson version also produces too much daily variability which is seen as "noise" on the plots. The relative success of the Dickinson and Washington version is first of all a result of the interactive surface hydrology used in both models (although the parameterizations are not the same). Furthermore, the overall success of the Dickinson model is most likely due again to the superior treatment of surface interactions and the inclusion of a diurnal cycle. The cause of the much higher variability of relative humidity for Dickinson's model is not immediately obvious, but is partially related to the smaller sample size (three years) compared to the Chervin output. The effect of vegetation on the hydrologic cycle, which is included in the Dickinson model could also contribute to the high day-to-day variability. These conclusions, however, must be accepted with caution, since the observed relative humidity is generally based on one station observation, and, in the case of the GL grid, on one that is not even located within the grid area (see Figure 1).

DAILY VARIABILITY OF TEMPERATURE

The daily variance of temperature is first discussed qualitatively by comparing temperature histograms (3 models and observed) for January and July at the SE and GL grids (Figures 18 and 19). The Dickinson model results exhibit the lowest variability, indicated by its comparatively narrow distributions. Washington and Chervin model results are fairly comparable, showing relatively greater variability compared to both Dickinson and observed data. A possible explanation for the lowered daily temperature variability of the Dickinson model concerns the more physically and biologically comprehensive surface energy balance used, which includes consideration of soil heat capacity, an issue briefly mentioned above in the description of the Dickinson model.

Quantitative analysis of daily temperature variance is more complex than analysis of interannual variance because of the need to consider the effect of autocorrelation in the time series. Autocorrelation refers to the condition that the temperatures in the series are not independent one from another but tend to be correlated over time. Katz (1984, 1988) has developed a statistical method by which valid statistical comparisons of daily variance may be performed. This method controls for the effect of autocorrelation by removing the autocorrelation influence and creating a new time series of effectively uncorrelated daily temperatures. The variance of this new series (known as the innovation variance) is then statistically analyzed via Z scores which compare the two innovation variances by taking the difference of their natural logarithms. (Natural logarithms are used to improve the normal approximation for moderate sample sizes). Removal of the autocorrelation effect requires the representation of the time series as some order autoregressive process. The appropriate order is selected via the Bayesian Information Criterion (BIC) (Schwarz, 1978). The mathematical details of the statistical method are presented in the appendix (1).

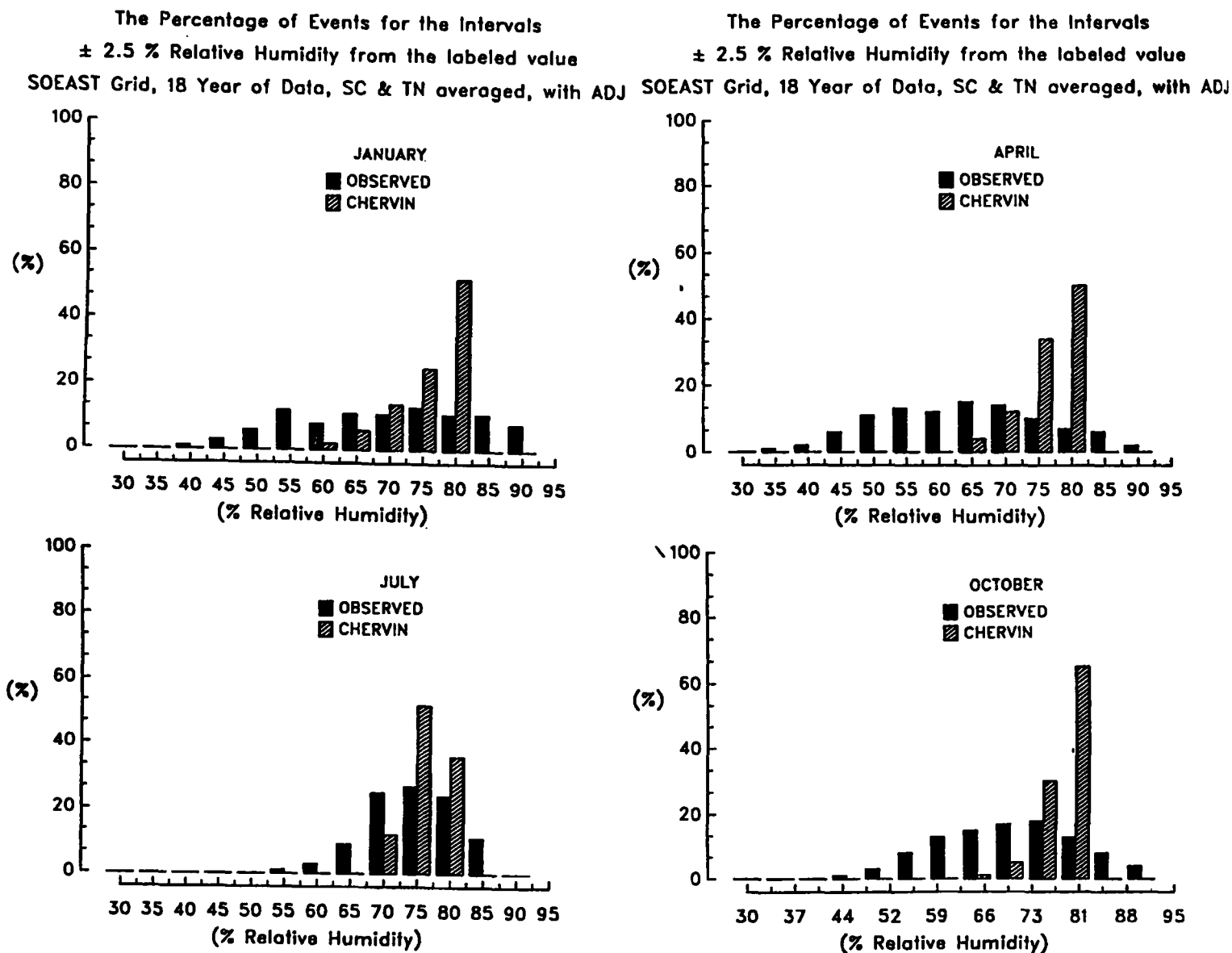
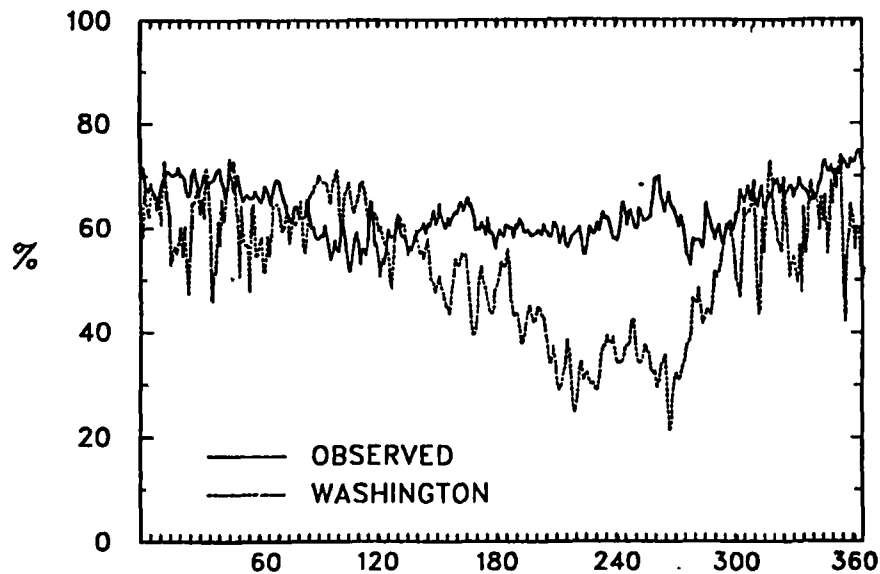
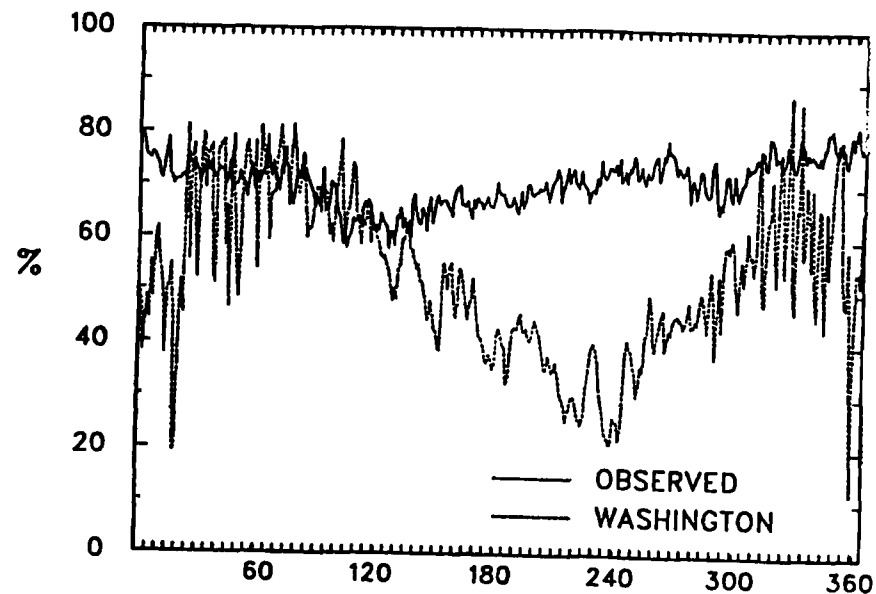


Figure 17. Histograms of relative humidity (18 years) for the SE grid, 4 selected months, Chervin model vs. observed.

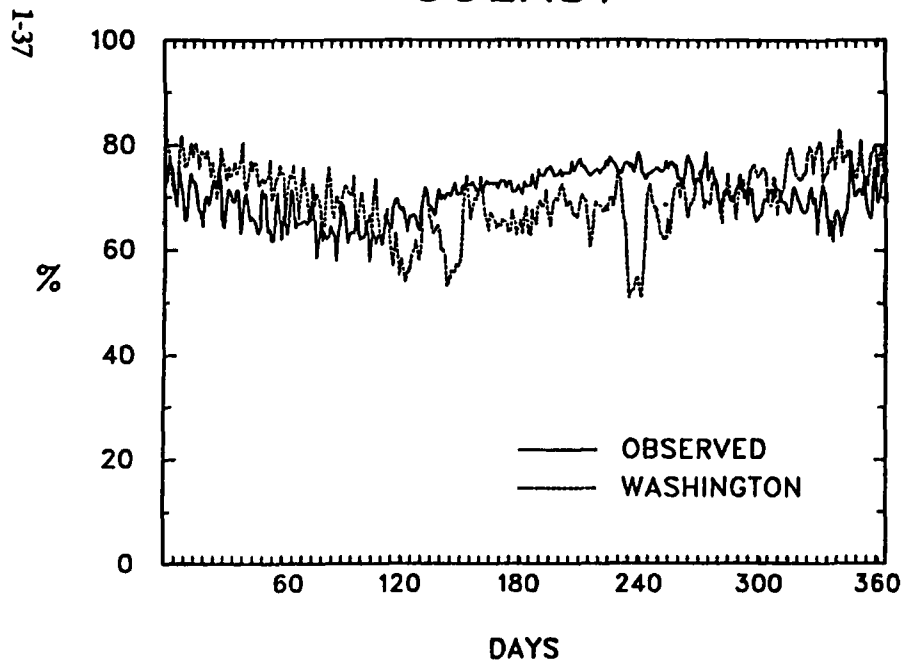
GP123



GTLAKES



SOEAST



WCOAST

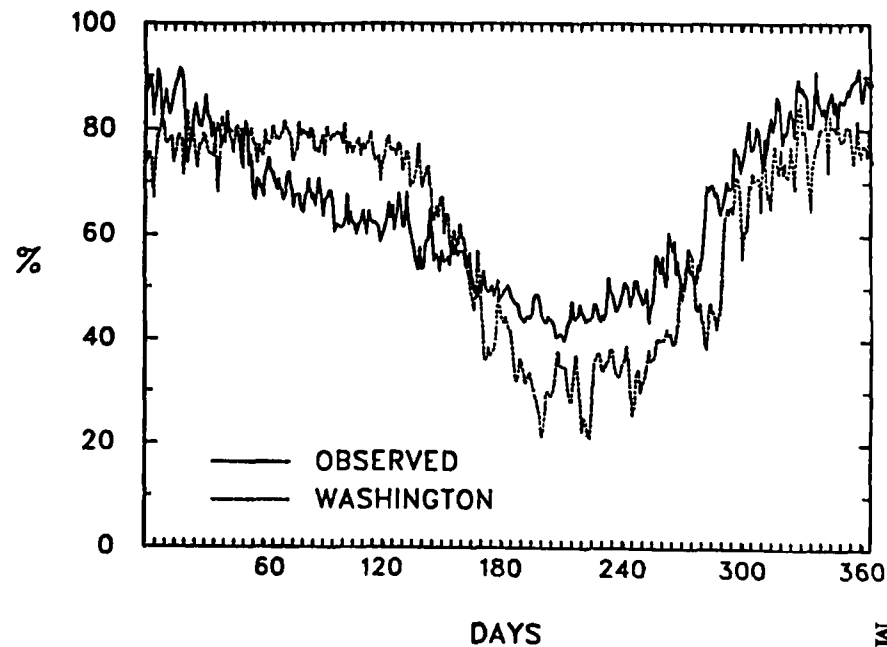
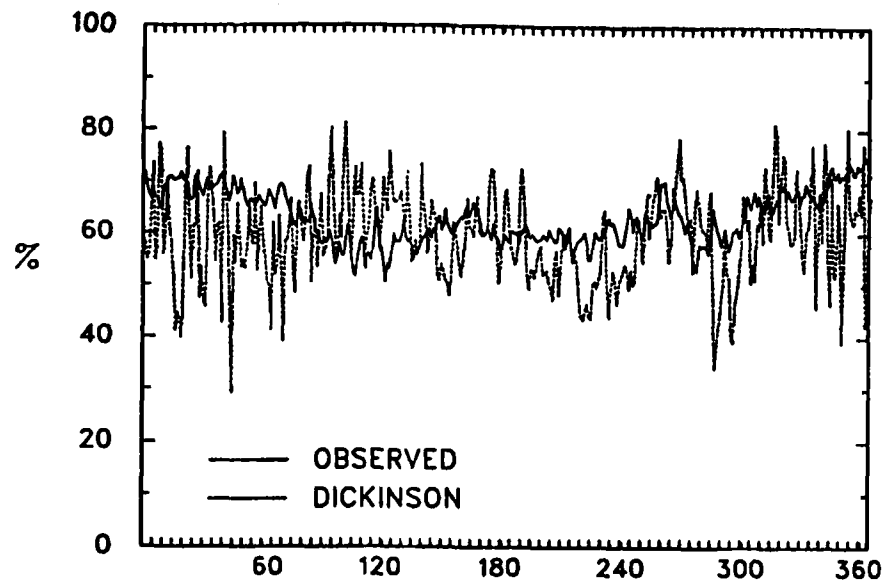
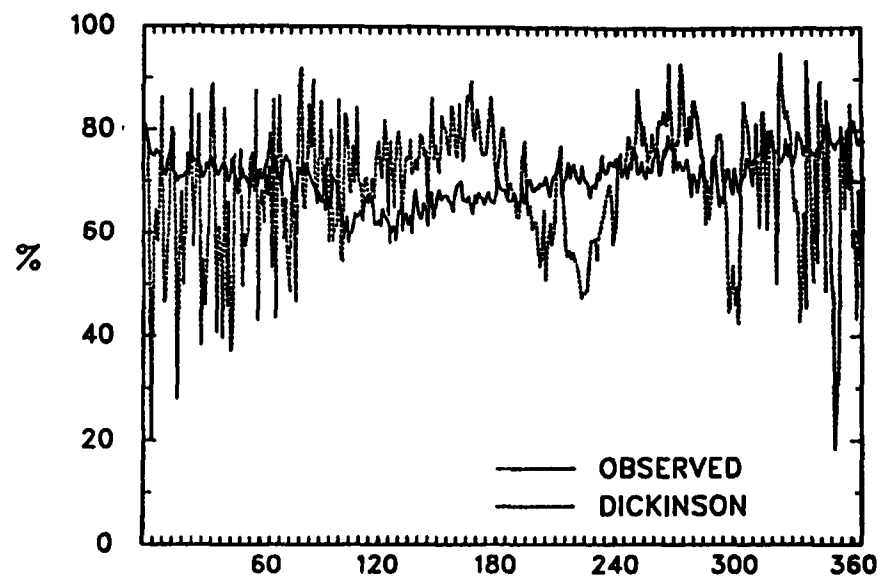


Figure 18. Daily average relative humidity for an 18-year average, Washington model vs. observed.

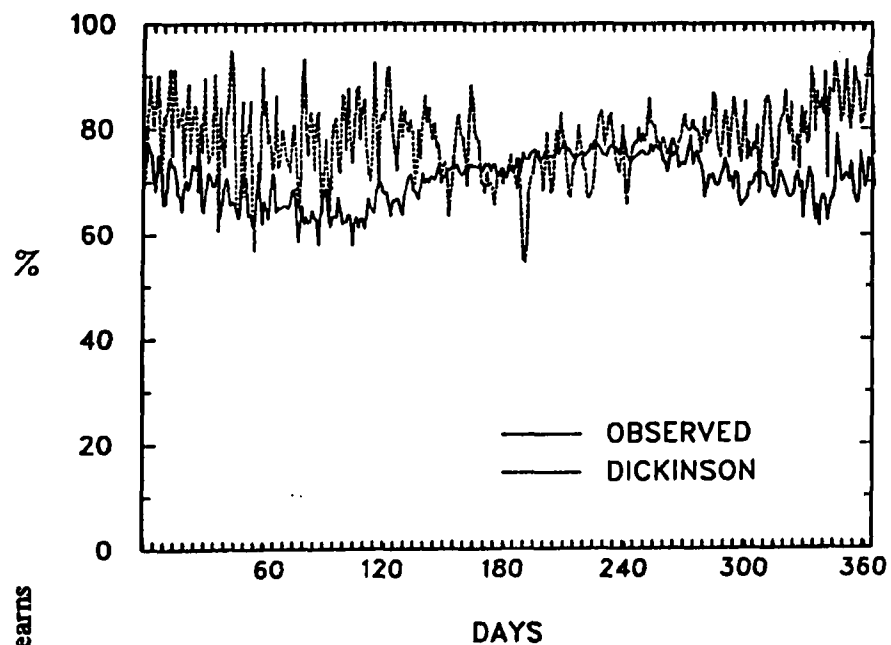
GP123



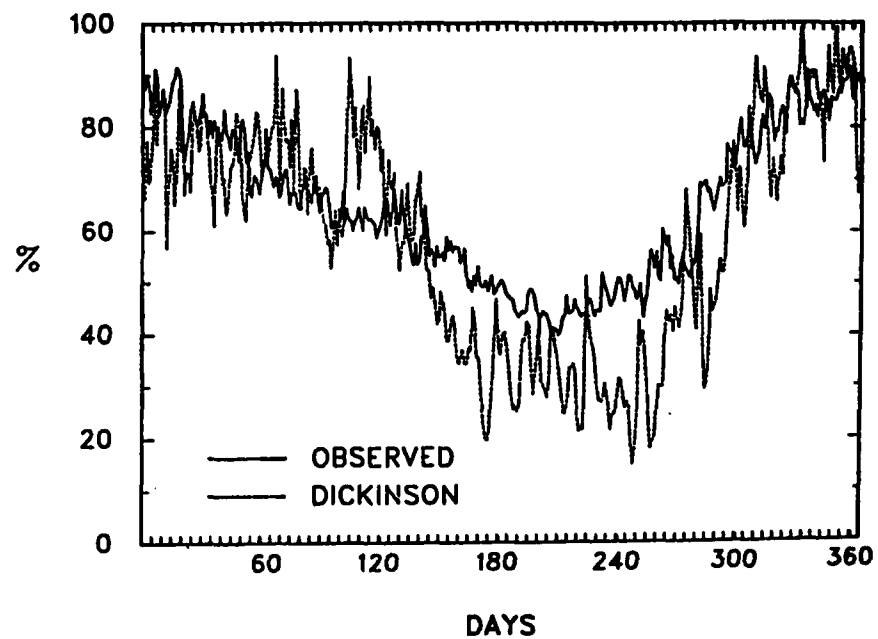
GTLAKES



SOEAST



WCOAST



Means

Figure 19. Daily average relative humidity for an 18-year average, Dickinson model vs. observed.

Daily temperature variances were tested for January and July at the GP III, SE, GL, and WC grids. Table 7 presents relevant results for all three CCM versions and observed data. We discuss the results for Chervin's version first so as to contrast the daily variance results with the interannual variance results presented in Chapter III.

At the GP III grid, the model daily variance for January is significantly higher (at the 0.05 level) than that of the observed data, whereas the July model variance is not significantly different from the observed. Note also that different autoregressive model orders are selected according to the BIC criterion, which reflects different autocorrelation structures. The first order autocorrelation coefficient (which indicates the relative dependence of one day's temperature upon the previous day's) for the model series in January is significantly lower than the observed, which is consistent with the innovation variance results. At the SE grid, the daily variability of the model time series (as measured by the innovation variance) is greater than the observed series in both January and July, as is the case at the WC grid. The greatest discrepancy occurs at the GL grid in January where the model innovation variance is seven times greater than the observed. This extreme overestimation may again relate to the lack of moderating effects of the Great Lakes in the modeled temperatures. In contrast, the model very successfully reproduces the autocorrelation function, the sample variance and hence the innovation variance at the GL grid in July.

Note that as with the interannual variability, the reduction in daily variance from winter to summer is well simulated at all locations.

These results on daily temperature variability contrast with the interannual variability results where model variability tended to be lower than observed at these grids in winter and in summer. The direction of the daily variance error (i.e., too high) may be related to the absence of soil heat capacity in the surface energy budget calculations or absence of a diurnal cycle and attendant night time temperature inversions. Further analysis (for more months and at more grids) will be necessary to completely evaluate the nature of daily temperature variance in the Chervin version of the CCM. So far it must be concluded that the model overestimates daily temperature variance.

The results for Washington and Dickinson are not as clearcut as those for the Chervin model, because there are only three simulated years available, but some overall tendencies can be identified. The Dickinson model is often more successful than both the Washington and Chervin models in accurately reproducing daily variability, based on the tests of equality of the innovation variances. The innovation variances of the Dickinson model temperatures do not significantly differ from those of the observed data in five of the eight cases. The variance is too low in two cases and too high in only one case. The Washington model successfully reproduces the variance in only three of the eight cases and is too large in the other five cases, and the Chervin model variance is too large in six of the eight cases. Hence, it can be said that the Dickinson model has the lowest temperature variance, followed by the Washington and Chervin models. It should be noted that the Dickinson model is not the most successful at reproducing the monthly temperature means although it is the most successful in reproducing the daily variances. It is perhaps not surprising that the Dickinson model is most successful in reproducing the daily variance if we are correct in our speculation as to why the Chervin model (as well as the Washington model) tends to overpredict variance, that is that the neglect of surface heat capacity allows rapid temperature variations with cloudiness, etc. Also, these models (especially Chervin's) use simple surface hydrology.

DAILY PRECIPITATION VARIABILITY

The daily variability of precipitation is difficult to analyze due to the positively skewed nature of the distribution. Comparisons of standard deviations can be very misleading. Moreover, comparisons must be made on both frequency of occurrence and intensity. One of the most useful means of comparing distributions of daily precipitation is through the box plot display (Tukey, 1977). In this display, the box height indicates the interquartile range, a horizontal line through the box indicates the median, and the box whiskers (extreme ends) indicate the maximum and minimum of the distribution. Other quantiles can also be indicated, such as the 90th

Mearns

Table 7. Daily Temperature Variance Statistics (°C) Chervin, Washington, and Dickinson Versions of the CC Control Runs Versus Observed

	<u>Order</u>	<u>Mean (°C)</u>	<u>Lag 1 Coeff.</u>	<u>Sample Variance</u>	<u>Innovation Variance</u>
GREAT PLAINS (GP III)					
<u>January</u>					
Observations	3	-1.2	0.73	38.2	15.6
Chervin	2	0.0	0.52	78.2	51.5*
Washington	4	0.7	0.70	41.2	20.0
Dickinson	2	0.3	0.46	21.9	15.9
<u>July</u>					
Observations	3	26.0	0.79	8.4	2.9
Chervin	2	24.3	0.73	7.8	3.1
Washington	2	28.1	0.89	15.7	2.2
Dickinson	2	25.6	0.81	9.4	2.6
SOUTHEAST (SE)					
<u>January</u>					
Observations	3	7.0	0.76	29.3	10.8
Chervin	3	13.3	0.56	35.1	21.4*
Washington	2	13.7	0.71	23.2	9.5
Dickinson	4	15.7	0.55	12.7	7.3*
<u>July</u>					
Observations	3	26.1	0.76	2.4	0.8
Chervin	3	26.2	0.63	2.9	1.7*
Washington	2	24.1	0.71	3.2	1.5*
Dickinson	2	26.9	0.60	1.1	0.6
GREAT LAKES					
<u>January</u>					
Observations	4	-4.0	0.74	30.4	12.4
Chervin	4	-8.9	0.54	126.3	84.8*
Washington	3	-3.8	0.61	44.9	27.7*
Dickinson	1	-5.3	0.53	37.8	27.6*
<u>July</u>					
Observations	3	21.6	0.72	7.2	3.0
Chervin	3	24.0	0.72	8.0	3.3
Washington	2	31.5	0.84	16.2	4.3*
Dickinson	3	27.9	0.69	3.6	1.5*

Table 7. (continued)

	<u>Order</u>	<u>Mean</u> <u>(°C)</u>	<u>Lag 1</u> <u>Coeff.</u>	<u>Sample</u> <u>Variance</u>	<u>Innovation</u> <u>Variance</u>
WEST COAST (WC)					
<u>January</u>					
Observations	3	1.2	0.85	17.0	4.4
Chervin	3	1.7	0.66	24.8	13.4*
Washington	2	4.5	0.76	17.9	7.6*
Dickinson	1	3.3	0.67	9.3	5.3
<u>July</u>					
Observations	2	19.6	0.77	4.7	1.8
Chervin	3	18.2	0.80	12.4	3.5*
Washington	3	25.2	0.82	16.9	3.8*
Dickinson	3	28.1	0.86	12.3	2.3

Order = selected order of autoregressive process

Lag 1 Coeff = 1st order autocorrelation coefficient

* = model innovation variance significantly different from observed (0.05 level)

at WC, percentile. Figures 20a-d present box plots of the distribution of daily precipitation aggregated on a seasonal basis for the three model versions and observations for the four grids. The distributions are formed from the subset of rain day data (i.e., precipitation amounts less than 0.1 mm are not included). Rainfall frequency (i.e., percentage of raindays for each season) is indicated by the numbers to the left near the upper quartile of each box plot.

The results for Chervin's version have been already basically presented in the probability functions (Figures 10-13). Additionally, it is clear from the box plots that this model version greatly overestimates variability as measured by the interquartile range, maximum values, and skewness. These results are somewhat uninteresting since they largely follow from the fact that all precipitation amounts are overestimated to begin with. Comparisons of the Dickinson version, Washington version, and observed distributions are on the whole more interesting.

The Dickinson version also tends to produce greater variability compared to the observations. In general the model interquartile ranges are much greater than those of the observations, even when the medians are quite similar (as at GP III, Figure 20a). Maximum values are also usually greater, and the distributions are more skewed. This last condition means that a greater portion of the data are small precipitation events. In general the distributions differ most in the distance from the median to the upper quartile, i.e., the upper half of the data is too dispersed (variable). This is not always the case, however. In fall at GP3, the distributions are very similar regarding these measures, and the Dickinson model even has a lower maximum than the observations. In winter the Dickinson model is clearly less variable than the observations, except that the distribution is more skewed.

The Washington model, in general, is the most successful in reproducing the daily variability of precipitation of the observations. This model version produces the lowest errors in simulating the maximum values (e.g., winter at GL). The interquartile ranges are not as overestimated as in the case of the Chervin and Dickinson models, but some are slightly too large. There also is a tendency for the Washington model to produce more positively skewed distributions (e.g., summer at GL; spring at WC). There are cases where the daily variability is somewhat less than the observations, such as the fall at GL and WC.) At the SE grid (Figure 20c) all

Mearns

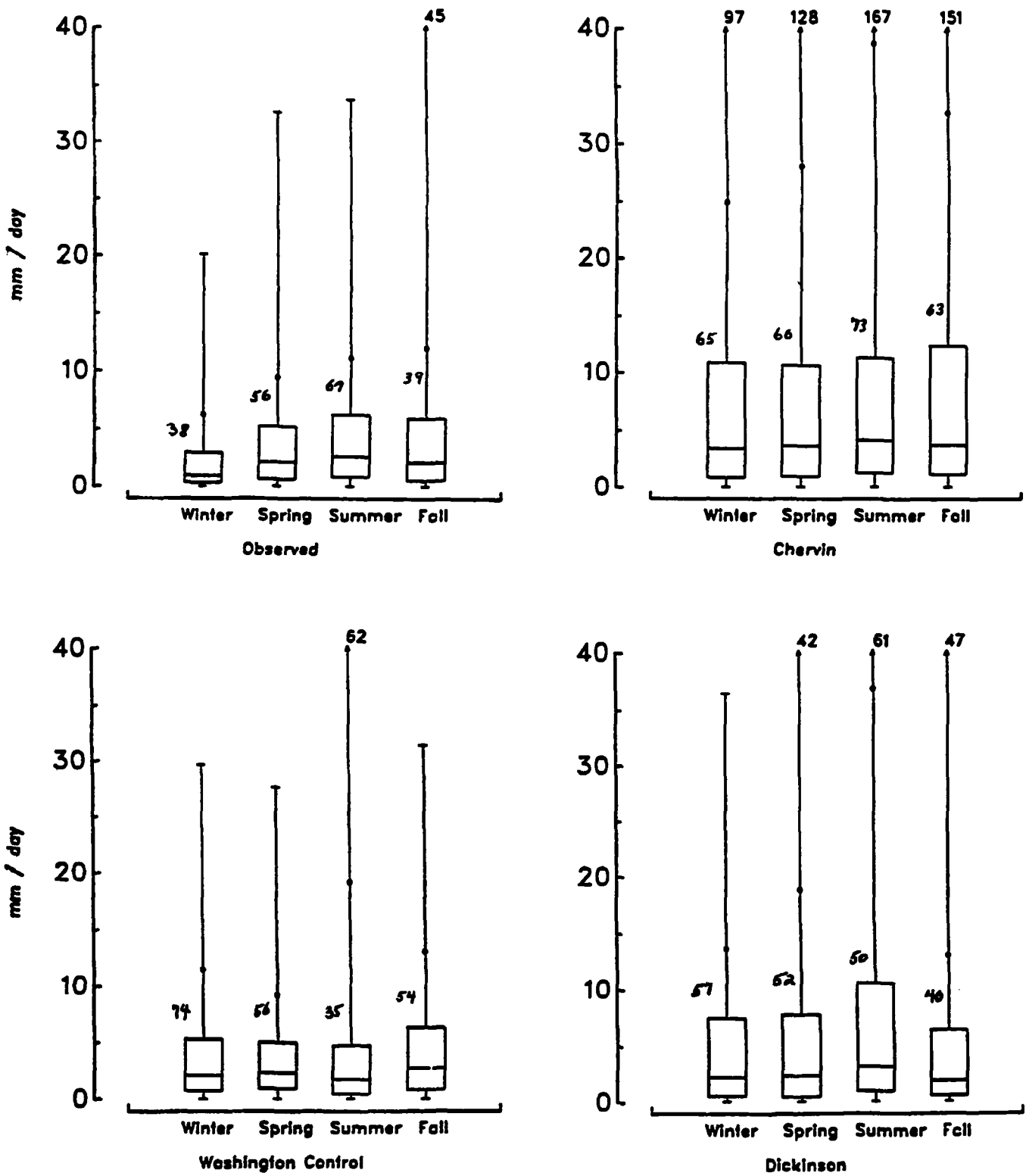


Figure 20a. Box plots of daily precipitation, GP III grid, four seasons; observed, Chervin, Dickinson, and Washington models. Numbers on left side of each box plot are % rain days.

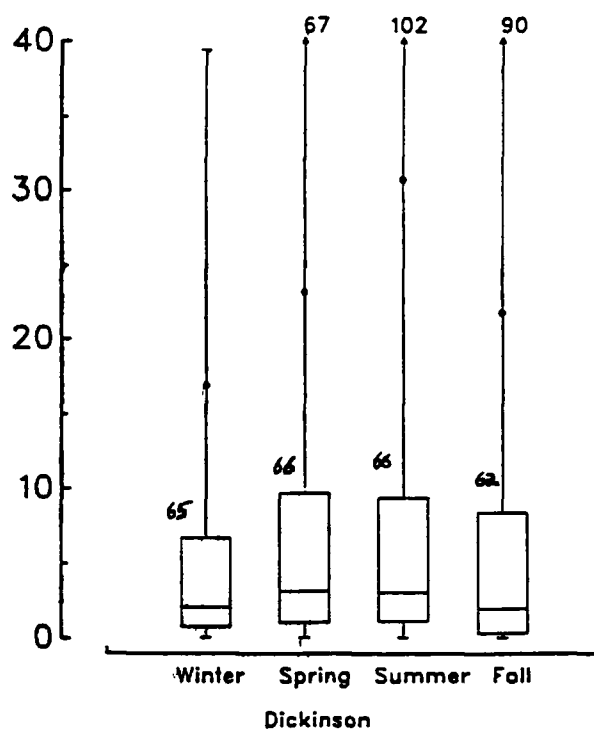
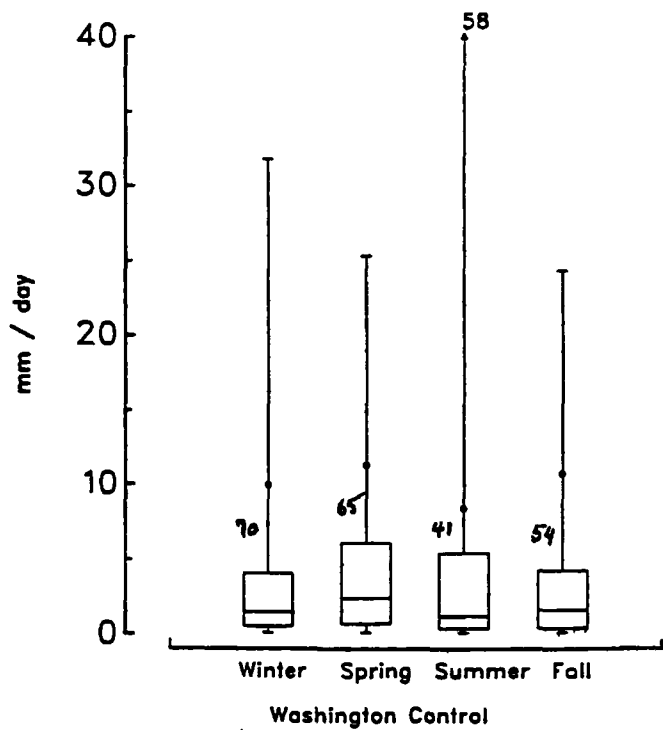
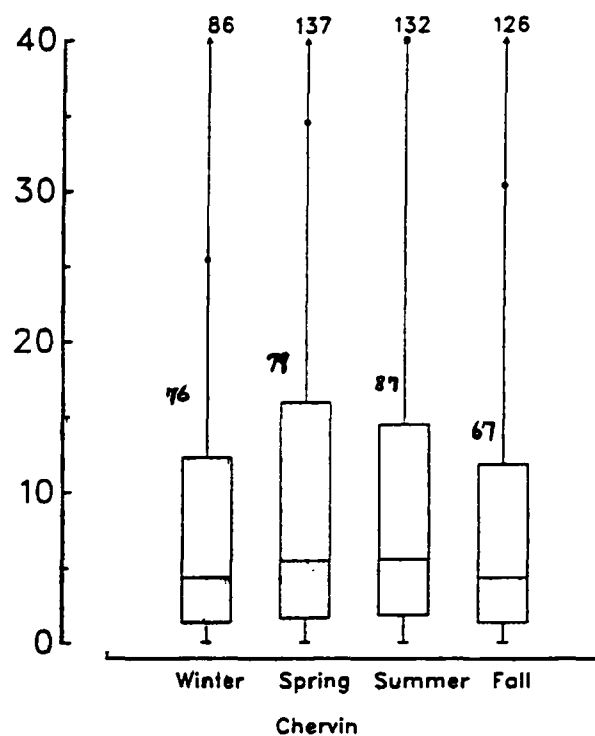
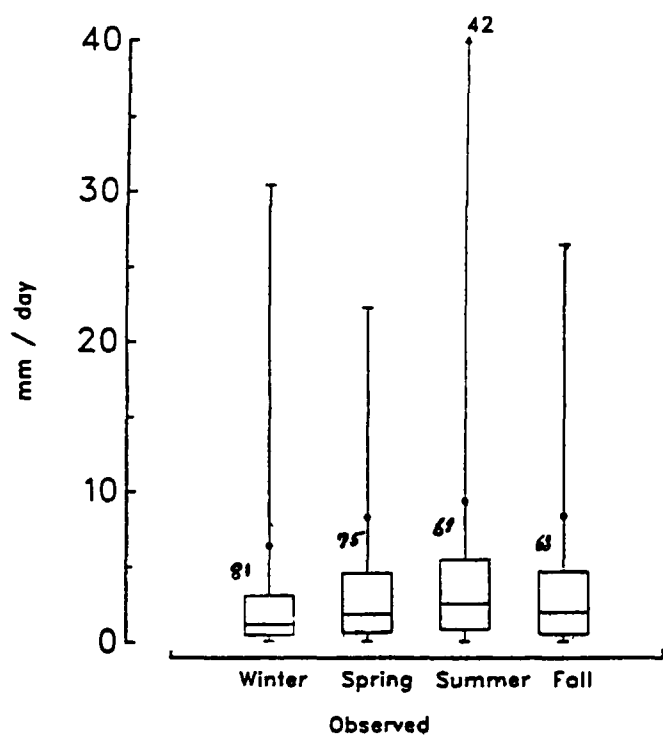


Figure 20b. Box plots of daily precipitation, GL grid, four seasons; observed, Chervin, Dickinson, and Washington models. Numbers on left side of each box plot are % raindays.

Mearns

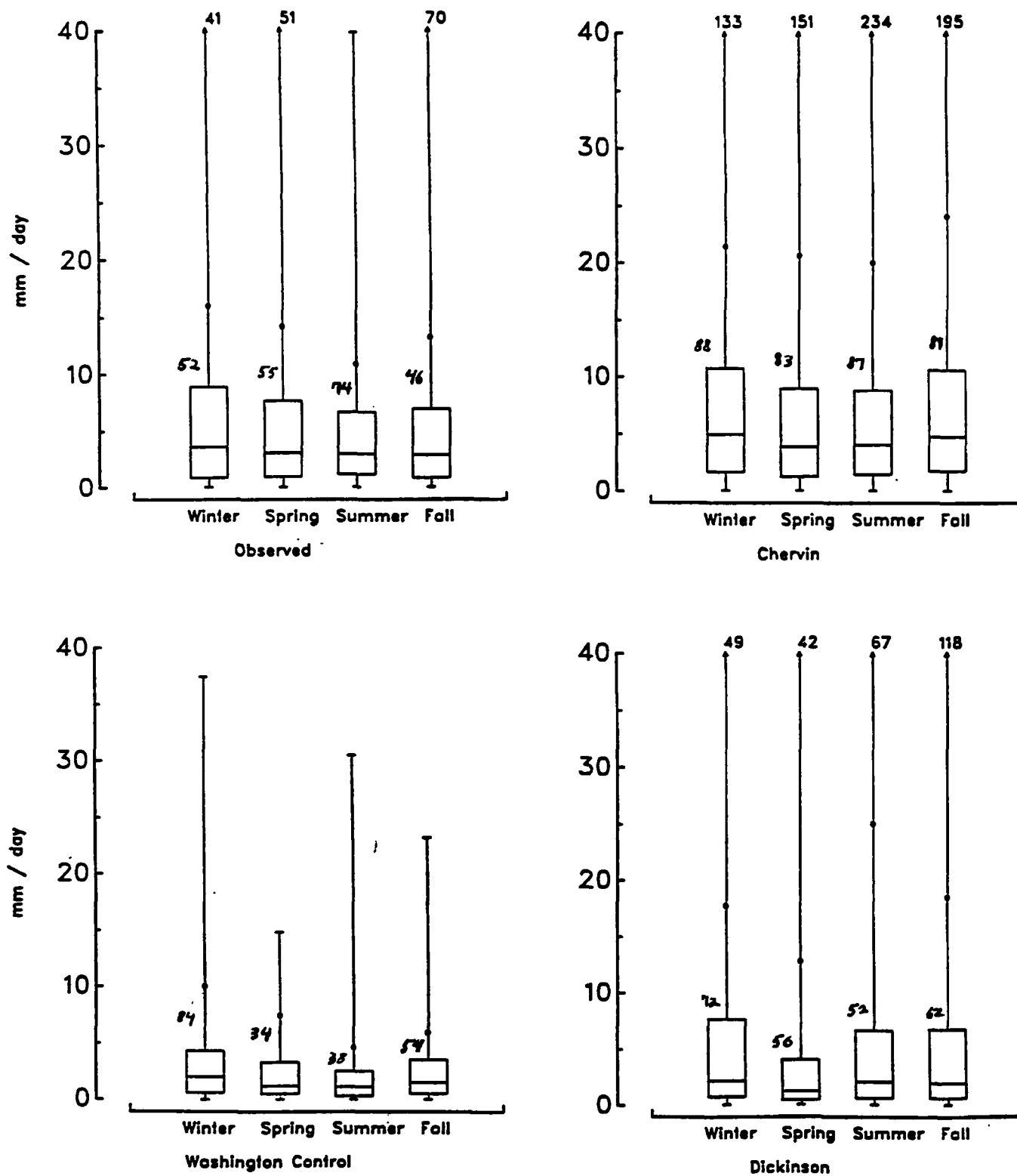


Figure 20c. Box plots of daily precipitation, SE grid, four seasons; observed, Chervin, Dickinson, and Washington models. Numbers on left side of each box plot are % raindays.

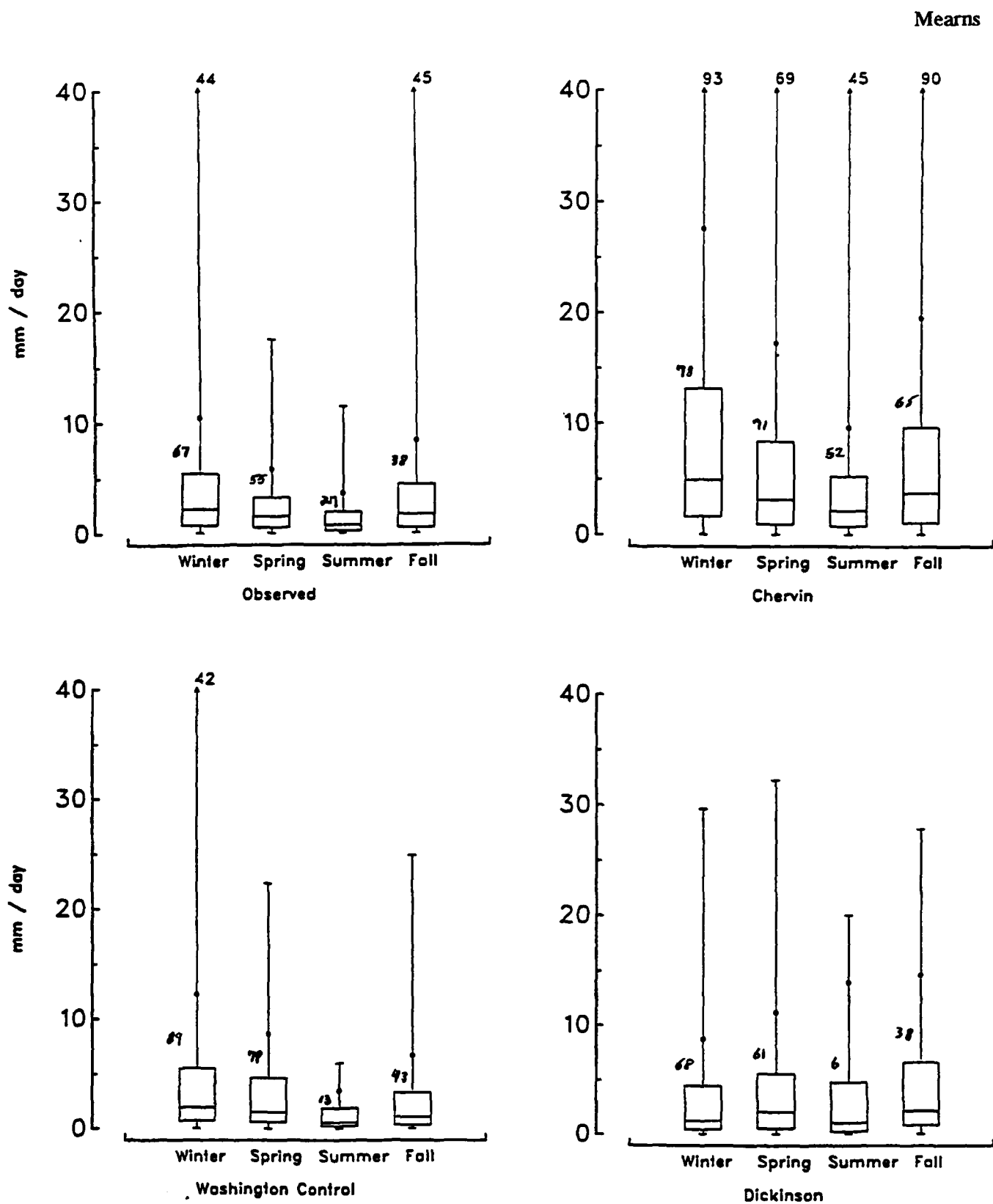


Figure 20d. Box plots of daily precipitation, WC grid, four seasons; observed, Chervin, Dickinson, and Washington models. Numbers on left side of each box plot are % raindays.

Mearns

Table 8. Daily Precipitation Distribution Interquartile Ranges (mm): Observed, Dickinson, Washington, and 2xCO₂.

	<u>Winter</u>	<u>Spring</u>	<u>Summer</u>	<u>Fall</u>
GREAT PLAINS (GP III)				
Observed	2.3	4.6	5.4	5.4
Dickinson	6.9*	7.3*	9.6	5.8
Washington	4.6*	4.1	4.3	5.5
2xCO ₂	5.1	4.2	6.5*	7.0*
GREAT LAKES (GL)				
Observed	2.6	3.9	4.6	4.1
Dickinson	5.9*	8.6*	8.2*	8.0*
Washington	3.6**	5.4**	5.0	3.8
2xCO ₂	5.5*	3.9	4.5	5.2
SOUTHEAST (SE)				
Observed	8.0	6.7	5.5	6.1
Dickinson	6.9	3.6*	6.0	6.1
Washington	3.7*	2.8*	2.2*	3.0*
2xCO ₂	3.1	3.1	1.9	3.5
WEST COAST (WC)				
Observed	4.7	2.7	1.7	3.9
Dickinson	4.0	5.0*	4.5*	5.7*
Washington	4.8	4.0*	1.6	3.0
2xCO ₂	5.1	3.1	2.8*	4.4

* - Significantly different from observed value at the 0.05 level, for Washington and Dickinson cases; significantly different from Washington (control) for 2xCO₂ case.

** - Significantly different from observed at the 0.1 level.

measures of variability indicate that the Washington model underestimates variability. However, since the model generally underestimates all precipitation amounts at this location, it would be difficult to say that the variability, separate from the errors in the mean, is actually underpredicted.

A quantitative comparison of interquartile ranges of observed, Dickinson, Washington, and 2xCO₂ daily precipitation distributions are presented in Table 8. The 2xCO₂ values in the table will be discussed in the next section. Significant differences between model values and observed values, on the basis of the interquartile range statistical test (see appendix 2), are indicated on the table by asterisks. On the basis of this test, the Washington model accurately reproduces the observed interquartile range in 10 of the 16 cases, overpredicts in 2 of the 16 and underpredicts in 4. However, it should be remembered that the underprediction of total precipitation for all seasons at the SE grid results in the low variability in all four of these cases. If one considers the relative variability (in this instance the interquartile range relative to the median), then the Washington model variability at the SE grid is very similar to that of the observations in all seasons. The Dickinson model underpredicts or

accurately predicts the interquartile range at the SE grid (all seasons), the WC grid in winter, and the GP III grid in the fall. All other cases are overpredictions.

The results for the SE grid for all models form an interesting pattern. In terms of the observations, comparing the four grid regions, highest amounts and greatest variability are found at this location; the models consistently come closest to observations at the SE grid, and do not overpredict precipitation as much as they typically do at the other grids. Perhaps this relative "underprediction" arises from the difficulty a 15-wave model has in reproducing intense precipitation events associated with hurricanes or small scale coastal cyclones.

In terms of estimation of precipitation frequency, the Washington model consistently underestimates the percentage of raindays in summer at all locations, and underestimates raindays in all seasons at GL. Aside for GL, winter raindays are overestimated at the other grids. Other seasons and locations show no overall tendencies.

There is less of a pattern of rainfall frequency errors in the Dickinson model. The only tendency is that of underestimation of raindays in summer (all locations except GL). Otherwise, there is a mix of over and under predictions at different locations and different seasons. Rainfall frequencies are relatively accurate in one third of the cases.

It is very difficult to even speculate on the causes of these results for precipitation. For example, we already mentioned the problem of grid or subgrid scale storms. Additionally, Dickinson's model contains a diurnal cycle which could well alter the frequency of convective and large scale precipitation events, particularly in the afternoon when humid synoptic conditions prevail. Unfortunately, such diagnostic information is not available on the model history tapes we have used.

CHAPTER 5

PILOT STUDY OF CONTROL VS. CO₂ PERTURBED RUNS

We include here a preliminary analysis of changes in temperature and precipitation under a scenario of doubled CO₂, using the output from Washington's control and doubled CO₂ runs for the four grids, each case consisting of three year runs. Of the three CCM versions discussed here, the Washington model is the only one for which doubled CO₂ experiments have been performed. Again, interannual variability could not be analyzed because the 3-year time series are too short. However, examination of daily variance of temperature and precipitation is presented.

Table 9 displays seasonal and annual mean values for temperature and precipitation for the control and doubled CO₂ cases. As is typical for GCMs, there is an annual temperature increase of between 2 and 3°C. The increase is distributed rather evenly in all four seasons at WC and SE, whereas winters experience larger increases at the two inland grids (GP III and GL). On an annual basis precipitation increases between 22 and 26% at three grids, but experiences a slight (2%) decrease at the SE grid. There are also potentially important changes in the seasonal distribution of precipitation. At the GL and SE grids, a smaller percentage of the annual total occurs during the summer in the CO₂ perturbed case (e.g., from 13% to 6% at SE). Increased percentages are obtained in the fall and spring. The WC area may benefit from redistribution since a slight increase in percentage occurs there in summer. Seasonal redistributions of precipitation are important to consider from a climate impacts point of view, particularly for agriculture.

Figure 21 presents histograms of temperature for 4 months for the control and perturbed cases at the SE grid. What is most striking in this figure is the similarity in the distributions between the two cases. Aside from the shift in the mean, there are no other visually obvious changes, except for a slight decrease in range for the 2xCO₂ case in October. This condition is underlined by the statistics comparing daily temperature variance of the control and perturbed runs for four months (Table 10) for the four locations. There are only two cases out of the 16 where the innovation variances of the perturbed climate temperatures are significantly (at the 0.05 level) different from the control: in October at the SE grid where the innovation variance decreases (reflected in Figure 21) and in October at the GP III grid where the innovation variance increases in the perturbed case. In the latter case an interesting condition exists where the sample variance decreases while the innovation variance increases. In fact in 5 of the 16 cases, the direction of change of innovation and sample variances is in opposite directions. This indicates the importance of the effect of autocorrelation on the sample variance and its effect on physically meaningful measures of variability, such as the frequency of extreme events. It should also be noted that noise in the data may also be partially responsible for the contrary directions. In the case of October at GP III, the first order autocorrelation coefficient decreases significantly, whereas the means of the two series are virtually the same.

It should be kept in mind that the lack of significant differences in innovation variances may be related to the relatively small sample size of the Washington runs (only three years of data), which limits the power of the statistical tests (i.e., the likelihood of accepting the null hypothesis when in fact it is false). These results may in fact be reflecting the lack of power. Longer time integrations of runs will be necessary to resolve this issue.

Without regard to significance levels, it can be said that the innovation variances decrease in half the cases and increase in half, whereas in 10 out of 16 cases the sample variances increase. From this information and that in the preceding paragraph, it is obvious that no clear conclusions can be drawn. No general statement can be made regarding the direction of change of daily temperature variability under CO₂ warmed climate conditions for three years of data from the Washington model at the locations investigated.

These results contrast with those of Wilson and Mitchell (1987), who used the same statistical tests on the innovation variances presented here. They concluded that daily temperature innovation variances significantly decreased in winter at two grid box locations in Europe. Decreases in spring were also recorded but were not statistically significant. However, it should be noted that here we are comparing the results of two structurally

Table 9. Control vs. Doubled CO₂ Mean Temperature and Total Precipitation Statistics (Washington CCM)

	<u>Annual</u>	<u>Winter</u>	<u>Spring</u>	<u>Summer</u>	<u>Fall</u>
SOUTHEAST (SE)					
<u>Temperature (°C)</u>					
Control	20.1	14.8	18.5	24.2	22.7
2xCO ₂	22.1	17.1	20.2	26.6	24.7
<u>Precipitation (mm)</u>					
Control	589.1	295.3	85.3	75.7	132.7
2xCO ₂	575.9	211.5	120.9	35.0	208.4
GREAT PLAINS (GP III)					
<u>Temperature (°C)</u>					
Control	17.6	3.5	18.3	29.3	18.9
2xCO ₂	20.0	7.4	19.6	32.1	20.8
<u>Precipitation (mm)</u>					
Control	931.3	291.7	203.2	194.4	242.0
2xCO ₂	1179.5	357.6	243.9	232.2	345.8
GREAT LAKES (GL)					
<u>Temperature (°C)</u>					
Control	16.2	-1.2	16.2	31.7	17.6
2xCO ₂	19.4	3.7	17.2	34.9	21.6
<u>Precipitation (mm)</u>					
Control	849.1	250.5	267.1	156.5	175.0
2xCO ₂	1032.5	391.0	305.0	109.2	227.3
WEST COAST (WC)					
<u>Temperature (°C)</u>					
Control	13.7	5.3	9.8	24.4	15.0
2xCO ₂	16.3	7.4	12.5	27.3	17.7
<u>Precipitation (mm)</u>					
Control	707.4	340.6	248.2	15.7	102.9
2xCO ₂	867.5	359.2	250.1	37.1	220.5

different GCMs (NCAR spectral CCM vs. U.K. Met Office grid point model) at different locations (U.S. vs. Europe) and across different time intervals (a season vs. one month). That these results do not agree is thus unrevealing. Moreover, it cannot be assumed that variability of climate variables would change in the same direction in different regions.

In conclusion, all that can be legitimately stated is that our preliminary analyses of the Washington model results do not support the finding that daily temperature variability tends to decrease with climate warming.

Mearns

Table 10. Daily Temperature Variance Statistics ($^{\circ}\text{C}^2$) Washington Control vs. $2\times\text{CO}_2$

		SE		GP3		GL		WC	
		Sample	Innov	Sample	Innov	Sample	Innov	Sample	Innov
JAN	Control	23.2	9.5	41.2	20.4	44.9	27.7	17.8	7.6
	$2\times\text{CO}_2$	20.5	8.4	33.8	20.6	54.8	34.6	19.2	10.2
APR	Control	8.3	5.1	22.3	6.8	41.0	16.8	9.6	4.6
	$2\times\text{CO}_2$	15.1	5.0	24.1	9.2	26.3	12.8	9.4	3.6
JUL	Control	3.2	1.5	15.7	2.2	16.2	4.3	16.9	3.8
	$2\times\text{CO}_2$	3.3	1.2	19.6	3.6	17.1	4.7	20.2	2.7
OCT	Control	9.1	2.8	39.2	6.8	45.3	16.2	17.4	7.2
	$2\times\text{CO}_2$	4.0	1.6*	34.8	14.6*	26.2	15.3	26.8	10.1

Sample = sample variance; Innov = innovation variance.

JAN = January, APR = April, JUL = July, OCT = October.

* = $2\times\text{CO}_2$ innov. variance is significantly different from control variance at 0.05 level.

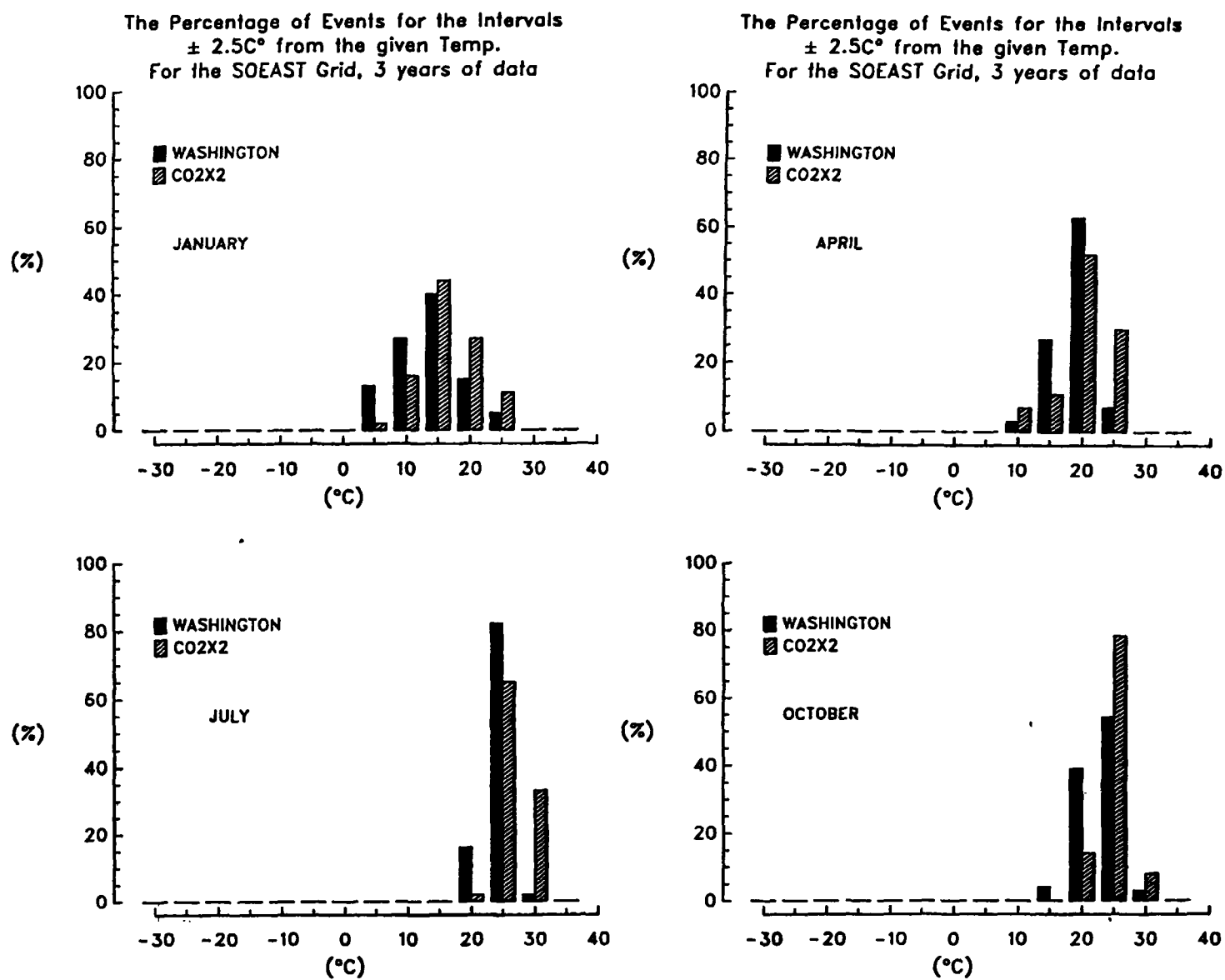


Figure 21. Histograms of daily temperature ($^\circ\text{C}$), Washington control and $2\times\text{CO}_2$, SE grid, 4 selected months.

Mearns

There is, however, a problem in drawing credible conclusions regarding change in daily temperature variance under climate change conditions, when the models do not reproduce actual variability very well, i.e., the model variability is usually quite significantly larger than observed variability. Any relationship between the direction of error of control run vs. observations and possible "errors" in predicting variability under climate change remains to be explored.

As described in Chapter 4, it is difficult to summarily compare daily variability of precipitation since variability can be operationally defined in so many ways, such as by the standard deviation, maximum values, changes in occurrence frequency, transitional probabilities, and other distribution characteristics, such as the interquartile range. First, changes in rainfall frequency, and high extremes are presented. Then again we present box plots of seasonal distributions of precipitation for the control and doubled CO₂ runs of the Washington version (Figure 22). Comparisons are made of the degree of skewness, maximum values, and interquartile range. Quantitative comparison of interquartile ranges is provided in Table 8.

At GP III percentage raindays increases in summer and spring and maximum values increase in all seasons but summer. At the GL grid percentage raindays, the maximum value, and percentage greater than 20 mm/day all decrease in summer, whereas these three quantities increase in the winter and spring. At the SE grid percentage of rain days decreases in the summer but increases in the spring and fall. Contrasts at the WC grid are not very striking, except that there is a slight increase in rain days and maximum values in all seasons but winter.

At the GP III grid (Figure 22a) under doubled CO₂ conditions maxima are clearly higher in three seasons and virtually the same in the other (summer). In winter, summer, and fall the interquartile ranges are greater in the doubled CO₂ case, but slightly less in the spring. From Table 8, the interquartile range increases are significant (at the 0.05 level) in the summer and fall. Ninetieth percentiles are greater in winter, spring, and especially fall. On the basis of these measures, daily variability clearly increases in three seasons, and increases at least on the basis of higher maximum values in the other (spring). Variability increases most clearly in fall,

At GL variability results are more mixed. Maxima are greater in all seasons except summer but interquartile ranges are significantly greater only in winter. The doubled CO₂ distributions are clearly more skewed only in spring. Fall and winter are clearly more variable whereas the measures indicate mixed results for summer and spring.

At the SE grid, both summer and winter are less variable based on these measures although in summer the data are more skewed (higher proportion of low rainfall events). In fall and spring all measures indicate greater variability. Interquartile ranges are greater, but not significantly so (Table 8).

At the WC grid, winter, summer, and fall are more variable based on these measures, but fall most clearly. In spring, although there is a higher maximum, all other measures point to reduced variability.

In summary then, there are indications of greater daily variability of precipitation in the 2xCO₂ runs in most seasons at most locations (fall everywhere). Only in three of the total 16 seasons is daily precipitation unambiguously less variable (summer and winter at GL and spring at WC). There is also a greater frequency of precipitation under doubled CO₂ conditions in 10 of the 16 season-locations.

In summary, the changes in daily temperature variability under the doubled CO₂ conditions are not very striking at these particular grids. There is clearer indication of greater variability of precipitation, but ambiguities remain. We need much longer time series to provide adequate sampling for analysis of both daily and interannual variability.

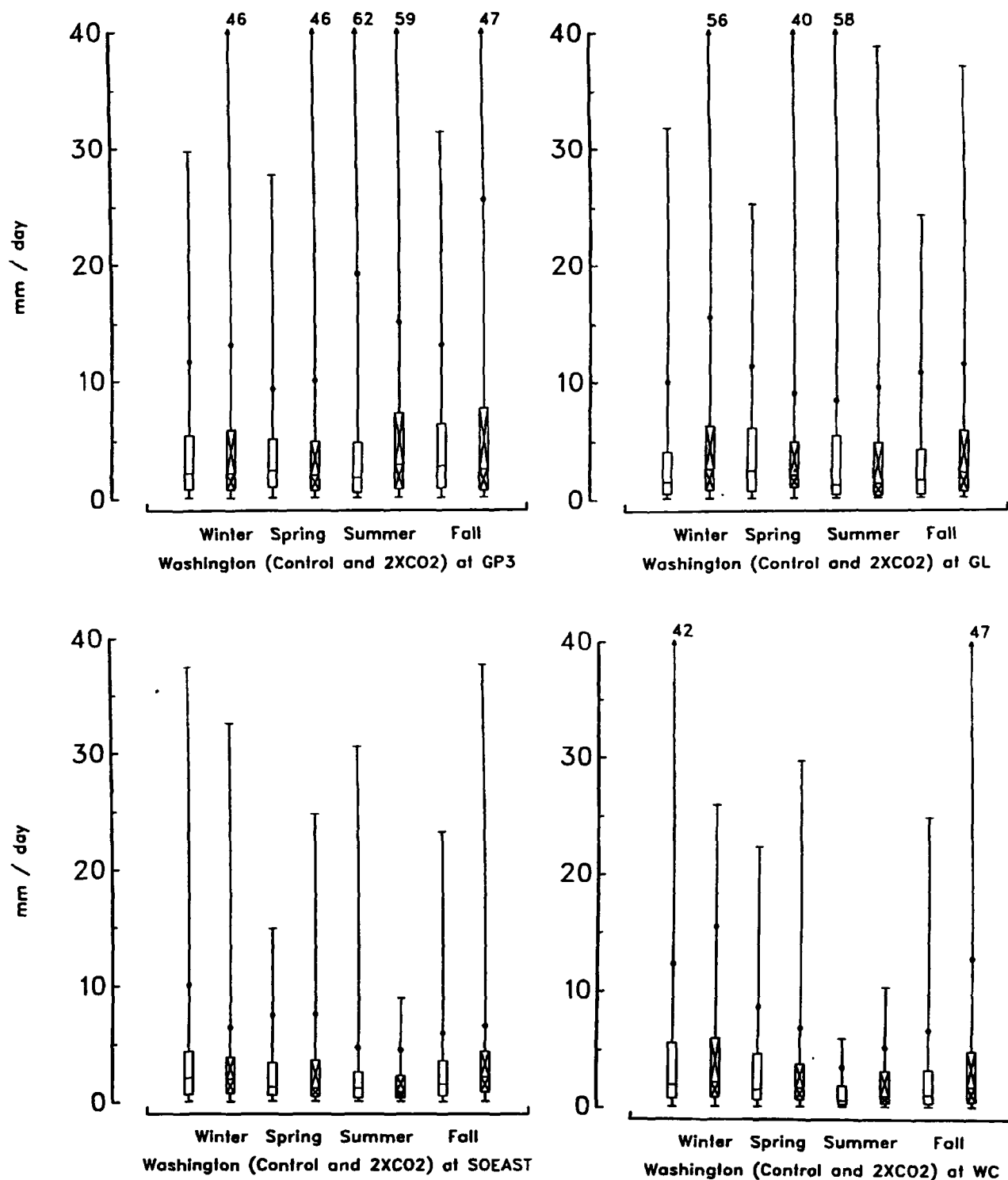


Figure 22. Box plots of daily precipitation, (a) GP III and GL grids (b) SE and WC grids, control (blank boxes) and 2xCO₂ (patterned boxes). Solid dot = 90th percentile; arrow with number = off scale maximum value.

CHAPTER 6

SUMMARY AND CONCLUSIONS

This study has presented analyses of comparisons of interannual and daily variability in GCM generated time series of climate variables and observed climate time series in four regions of the United States. Variables included temperature, precipitation, relative humidity, and absorbed solar radiation. An examination of the effect of spatial aggregation of grid boxes on model errors in these variables is included for the Great Plains region. In a more limited study involving temperature and precipitation (as well as some brief comments on relative humidity) at the four locations, several control runs of different versions of the NCAR GCM are compared. Finally, a preliminary investigation of changes in temperature and precipitation, both mean and variance, under a climate change scenario is presented. Results may be summarized as follows.

Interannual variability of temperature is generally underestimated or properly predicted by the 20-year simulation using the Chervin version of the CCM in all four regions. Interannual variability of precipitation as measured by the coefficient of variation is generally in reasonable agreement with observed data, although it is occasionally overestimated. This may be an encouraging result for the credibility of predicting climatic changes given the large inaccuracy of the control run precipitation results in terms of absolute amounts. As expected from sampling considerations, spatial aggregation of grids tends to improve results. When individual grids are examined, directions of errors among the grids are often inconsistent (especially for precipitation variability). From our preliminary results for temperature, it appears that the Chervin model overestimates daily temperature variance. Solar radiation daily variance comparisons are not particularly interesting. However, there are important and inconsistent regional contrasts in the direction of mean errors for solar radiation.

Comparisons of different CCM versions with observed data for mainly temperature and precipitation produced more interesting results. There is considerable difference in how well the models reproduce mean total precipitation for the four locations, ranging from the very good results of Dickinson's and Washington's models (at different grids), to the overestimation of Chervin's model at all four locations. The Dickinson model produced lower daily variability of temperature than the other two models or even occasionally than the observations and was most successful in reproducing present daily variability. In the Chervin model surface relative humidity is poorly simulated at all grids, and the daily variability is greatly underestimated. The Dickinson model most successfully reproduced the annual cycle of relative humidity at all four grids, but also displayed higher variability of relative humidity than the Chervin or Washington version. The reasons for these discrepancies have yet to be explored in depth, but, as we speculated, are likely related to different degrees of realism in the land surface parameterizations.

Regarding daily precipitation variability, Chervin's model greatly overpredicted the absolute variability, but this is strongly tied to the much higher total precipitation amounts predicted by the model. Dickinson's model does a better job of accurately reproducing daily precipitation variability, but there is still a tendency for overprediction. Washington's model is by far the most accurate in reproducing observed variability. There are also underpredictions, but these are generally related to Washington's underprediction of total precipitation amount at the SE grid.

The preliminary investigation of the change in daily temperature variability under doubled CO₂ conditions produced both increases and decreases in variance, but most of these changes were statistically insignificant at all four locations for the three years of simulation available. Precipitation change results varied according to location, e.g., from decreases in summer at the southeast (SE) and Great Lakes (GL) location to increases in percentage of raindays in the summer in the Great Plains (GP III). Daily precipitation variability increased more often than not on the basis of distribution characteristics such as skewness and the interquartile range. Extreme high precipitation events increased in all locations. Measures of the dispersion of the distributions (e.g., interquartile range) indicated greater variability of daily precipitation under doubled CO₂ conditions. It is clear that more analysis involving a greater number of grids and longer time series will be necessary to fully investigate various measures of variability changes with changed climate.

We plan to continue our statistical examination of variability in models of different structure in order to help interpret existing CO₂ versus control cases. We also hope to perform CO₂-perturbed experiments with improved versions of the CCM such as those now being developed by Dickinson (described above) and S.L. Thompson (which includes an interactive thermodynamic ocean and surface hydrology). While estimating the effect of trace gas increases on various variability measures is our ultimate goal, many intermediate steps are needed to explain the variability performance of various structurally different versions of the CCM, and their comparison with observations.

It is obvious from our results so far that further improvements in GCMs are needed in order to accurately reproduce regional mean climate and related climate variability. Among these would be higher horizontal resolution so as to capture regional influences on climate, such as the Great Lakes; improved moisture transport, condensation, and rainout parameterizations which would take into account potential effects on precipitation variability (i.e., improving on spectral advection); improvements in interactive surface hydrology (e.g., BATS) which appears to improve reproduction of surface relative humidity; inclusion of soil heat capacity which improves the reproduction of daily temperature variability. Other improvements not directly suggested by our results include the coupling of complete ocean-atmosphere models which would improve the reproduction of interannual variability, and the modeling of sub-gridscale phenomenon such as thunderstorms and hurricanes which would contribute to better modeling of precipitation variability. The above list is far from exhaustive, but includes main areas of improvement which would ameliorate the models' ability to reproduce climate variability on various timescales. Only when this is accomplished can we place much faith in GCM forecasts of variability changes with a perturbed climate.

Despite the strong reservations we have placed on the qualitative and quantitative inferences in this study because of limited amounts of simulation data, we have given the detailed analyses anyway. It is our hope that future studies (ours and those of other GCM investigators) will include analyses of variability similar to those presented here as a routine part of GCM diagnostics.

APPENDIX 1

STATISTICAL TESTS OF DIFFERENCES IN VARIANCE OF SURFACE TEMPERATURE

The test statistic used to determine differences in variance of surface temperature is taken from Katz (1988). The procedures described below address two important problems encountered when trying to test variances of atmospheric time series: autocorrelation of the time series and departures from the assumption of normality. In regard to the first problem, tests are not performed on the variance of the original time series, but rather on the innovation variance, which may be considered the variance remaining after the effect of autocorrelation has been removed. The innovation variance is formed by fitting an AR(p) process (autoregressive process of order p) to the time series. The residuals (or innovations) from this process constitute the innovation variance:

$$\hat{a}_t = (X_t - \bar{X}) - \sum_{k=1}^p \hat{\phi}_k (X_{t-k} - \bar{X}), \quad t = 1, 2, \dots, n, \quad (A1)$$

where \hat{a}_t is the t th residual, X_t is the t th element of the time series of length n , \bar{X} is the time average of the series, and $\hat{\phi}_k$, $k = 1, 2, \dots, p$, are estimates of the autoregression coefficients. An unbiased estimator of the innovation variance is then:

$$\hat{\sigma}_a^2 = \frac{1}{n - p - 1} \sum_{t=1}^n \hat{a}_t^2, \quad (A2)$$

and all symbols are as previously defined. The residual time series is referred to as the "prewhitened data."

The test statistic for determining if two innovation variances (1) and (2) are equal (i.e., the null hypothesis) is asymptotically normally distributed,

$$Z = \frac{\ln \hat{\sigma}_a^2(2) - \ln \hat{\sigma}_a^2(1)}{\{s^2[\ln \hat{\sigma}_a^2(1)] + s^2[\ln \hat{\sigma}_a^2(2)]\}^{1/2}}, \quad (A3)$$

where s is the standard error of $\ln \hat{\sigma}_a^2$, and is given by

$$s(\ln \hat{\sigma}_a^2) = \left[\frac{1}{n} (2 + \hat{\gamma}_2) \right]^{1/2}, \quad (A4)$$

where γ_2 is the sample kurtosis. The statistic (A3) is in terms of the logarithms to improve the Gaussian approximation for moderate sample size. Moreover, because this statistic has an adjustment for the sample kurtosis, procedures based on (A3) are robust against the innovations (i.e., the residuals) departing from the normal distribution.

The testing procedure begins with autoregressive model identification, i.e., the correct order is selected using some criterion such as the Bayesian Information Criterion (BIC) (Katz, 1982; Schwarz, 1978), which we used. Using (A1) the prewhitened time series are obtained, and the innovation variances are estimated using (A2). The test of significance (A3) is then applied to the two innovation variances, and significance levels determined. Here we used a significance level of 0.05 to establish significant difference between two variances.

APPENDIX 2

STATISTICAL TESTS OF DIFFERENCES BETWEEN INTERQUARTILE RANGES

Given two sets of ordered data of daily precipitation, with interquartile ranges $IQR(1)$ and $IQR(2)$, the test statistic for determining if the interquartile ranges are equal (i.e., the null hypothesis) is asymptotically normally distributed,

$$Z = \frac{IQR(2) - IQR(1)}{\{s^2[IQR(2)] + s^2[IQR(1)]\}^{1/2}}, \quad (A5)$$

where $s^2(IQR)$ is the variance of the interquartile range IQR , i.e., the variance of the difference between the upper and lower quartiles (UQ and LQ). This can be expressed as

$$s^2(UQ - LQ) = s^2(UQ) + s^2(LQ) - 2cov(UQ, LQ), \quad (A6)$$

where $cov(UQ, LQ)$ is the covariance of the upper and lower quartiles.

In general, the variance of the p th sample quantile, X_r , where $r = \text{approx. } np$, (n = sample size) is given by:

$$s^2(X_r) = \frac{p(1-p)}{n[f(\xi_p)]^2}, \quad (A7)$$

where $F(\xi_p)$ is the distribution function, ξ_p is the p th population quantile (i.e., $F(\xi_p) = p$), and $f = F'$, the density of the population (Kendall and Stuart, 1967). An estimate of $\frac{1}{f(\xi_p)}$ is given by:

$$\frac{1}{f(\xi_p)} \approx S_{m,r} = \frac{1}{(2m/n)}(X_{r+m} - X_{r-m}), \quad (A8)$$

where n is the sample size and m is some distance from r (Hall and Sheather, 1988). Then substituting for $\frac{1}{f(\xi_p)}$ in (A7) we have

$$\hat{s}^2(X_r) = p(1-p)S_{m,r}^2/n, \quad (A9)$$

where \hat{s}^2 is the estimated variance. Hence, in the case of the variance of the interquartile range, setting $UQ-LQ$ equal to $X_{nu} - X_{nl}$ and substituting (A9) in (A6), we finally have

$$\begin{aligned} \hat{s}^2(IQR) = & 1/n[p_1(1-p_1)S_{m,ru}^2 + p_2(1-p_2)S_{m,rl}^2 \\ & - 2p_1(1-p_2)S_{m,ru}S_{m,rl}] \end{aligned} \quad (A10)$$

For the interquartile range, $p_1 = 1/4$, $p_2 = 3/4$ and we use $m = n/8$, which is consistent with the approach of McGill et al. (1978) for determining confidence intervals for medians. A significance level of 0.05 is used to determine significant difference between interquartile ranges.

REFERENCES

- Bates, G.T., and G.A. Meehl. 1986. The effect of CO₂ concentration on the frequency of blocking in a general circulation model coupled to a simple mixed layer ocean model. *Monthly Weather Review* 114:687-701.
- Bourke, W. 1974. A multi-level spectral model. I. Formulation and hemispheric integrations. *Monthly Weather Review* 102:687-701.
- Bourke, W., B. McAvaney, K. Puri, and R. Thurling. 1977. Global modeling of atmospheric flow by spectral methods. *Methods in Computational Physics* 17:267-324.
- Chervin, R.M. 1986. Interannual variability and seasonal predictability. *Journal of the Atmospheric Sciences* 43:233-251.
- Chervin, R.M. 1981. On the comparison of observed GCM simulated climate ensembles. *Journal of the Atmospheric Sciences* 38:885-901.
- Dickinson, R.E., A. Henderson-Sellers, P.J. Kennedy, and M.F. Wilson. 1986. Biosphere-Atmosphere Transfer Scheme (BATS) for the NCAR Community Climate Model. NCAR Technical Note 275. Boulder, CO: National Center for Atmospheric Research.
- Hall, P., and S.J. Sheather. 1988. On the distribution of a studentized quantile. *J. Royal Statistical Society (B)* 50:381-391.
- Hansen, J., I. Fung, A. Lacis, S. Lebedeff, D. Rind, R. Ruedy, G. Russell, and P. Stone. 1988. Global climate changes as forecast by the Goddard Institute for Space Studies three-dimensional model. *Journal of Geophysical Research* 93(D8):9341-9364.
- Katz, R.W. 1982. Statistical evaluation of climate experiments with general circulation models: A parametric time series modeling approach. *Journal of Atmospheric Science* 39:1446-1455.
- Katz, R.W. 1984. Procedures for Determining the Statistical Significance of Changes in Variability Simulated by an Atmospheric General Circulation Model. Climate Research Institute Report No. 48. Corvallis, OR: Oregon State University.
- Katz, R.W. 1988. Statistical procedures for making inferences about changes in climate variability. *Journal of Climate* 1:1057-1068.
- Kendall, M.G., and A. Stuart. 1967. *The Advanced Theory of Statistics*. 2nd edition. Volume 1: Distribution theory. New York, NY: Hafner Publishing Co.
- Lowe, P.R. 1976. An approximating polynomial for the computation of saturation vapor pressure. *Journal of Applied Meteorology* 16:100-103.
- Manabe, S., and D.G. Hahn. 1981. Simulation of atmospheric variability. *Monthly Weather Review* 109:2260-2286.
- McGill, R., J.W. Tukey, and W.A. Larsen. 1978. Variations of box plots. *American Statistician* 32:12-16.
- Mearns, L.O., R.W. Katz, and S.H. Schneider. 1984. Extreme high-temperature events: Changes in their probabilities with changes in mean temperature. *Journal of Climate and Applied Meteorology* 23:1601-1613.
- Parry, M.L. 1978. *Climatic Change, Agriculture and Settlement*. Folkstone, U.K: Dawson.

- Reed, D.N. 1986. Simulation of time series of temperature and precipitation over eastern England by an atmospheric general circulation model. *Journal of Climatology* 6:233-257.
- Schwarz, G. 1978. Estimating the dimension of a model. *Annals of Statistics* 6:461-464.
- Schwarz, H.E. 1977. Climatic change and water supply: How sensitive is the Northeast? In: *Climate, Climate Change and Water Supply*. Washington, DC: National Academy of Sciences, pp. 111-120.
- Tukey, J.W. 1977. *Exploratory Data Analysis*. Reading, MA: Addison-Wesley.
- Washington, W.M., and G.A. Meehl. 1984. Seasonal cycle experiment on the climate sensitivity due to a doubling of CO₂ with an atmospheric general circulation model coupled to a simple mixed-layer ocean model. *Journal of Geophysical Research* 89(D6):9475-9503.
- Wilson, C.A., and J.F.B. Mitchell. 1987. Simulated climate and CO₂-induced climate change over Western Europe. *Climate Change* 10:11-42.
- Williamson, D.L., J.T. Kiehl, V. Ramanathan, R.E. Dickinson, and J.T. Hack. 1987. Description of NCAR Community Climate Model (CCM1). NCAR Technical Note 285. Boulder, CO: National Center for Atmospheric Research.

CHANGE IN CLIMATE VARIABILITY IN THE 21st CENTURY

by

**D. Rind
Goddard Space Flight Center
Institute for Space Studies
2880 Broadway
New York, NY 10025**

and

**R. Goldberg
Institute for Global Habitability
Columbia University
New York, NY 10027**

and

**R. Ruedy
Sigma Data Service Corporation
2880 Broadway
New York, NY 10025**

Interagency Agreement No. DW80932629-01-1

CONTENTS

	<u>Page</u>
ACKNOWLEDGMENTS	iii
FINDINGS	2-1
CHAPTER 1: INTRODUCTION	2-2
CHAPTER 2: MODEL AND CLIMATE CHANGE EXPERIMENTS	2-3
CHAPTER 3: MEAN VALUES	2-4
CHAPTER 4: YEAR-TO-YEAR VARIABILITY	2-10
CHAPTER 5: DAILY VARIABILITY	2-15
CHAPTER 6: VARIABILITY OF THE DIURNAL CYCLE	2-28
CHAPTER 7: DISCUSSION	2-30
CHAPTER 8: CONCLUSIONS	2-33
REFERENCES	2-34

ACKNOWLEDGMENTS

We thank Frank Abramopoulos, who helped with statistical tests, and William Weinstein who helped with computing. We also thank Linda Mearns and Stephen Schneider for their interest and encouragement in the course of this work, and Thomas Karl for useful comments in review. This research was supported by the United States Environmental Protection Agency, while climate modeling at GISS is supported by the NASA Climate Program Office.

FINDINGS¹

As climate changes owing to the increase of greenhouse gases, there is the potential for climate variability to change as well. The change in variability of temperature and precipitation in a transient climate simulation, where trace gases are allowed to increase gradually, and in the doubled CO₂ climate is investigated using the GISS general circulation model. The current climate control run is compared with observations and with the climate change simulations for variability on three time-scales: interannual variability, daily variability, and the amplitude of the diurnal cycle. The results show that the modeled variability is often larger than observed, especially in late summer, possibly owing to the crude ground hydrology. In the warmer climates, temperature variability and the diurnal cycle amplitude usually decrease, in conjunction with a decrease in the latitudinal temperature gradient and the increased greenhouse inhibition of radiative cooling. Precipitation variability generally changes with the same sign as the mean precipitation itself, usually increasing in the warmer climate. Changes at a particular grid box are often not significant, with the prevailing tendency determined from a broader sampling. Little change is seen in daily persistence. The results are relevant to the continuing assessments of climate change impacts on society, though their use should be tempered by appreciation of the model deficiencies for the current climate.

¹Although the information in this report has been funded wholly or partly by the U.S. Environmental Protection Agency under Interagency Agreement No. DE80932629-01-1, it does not necessarily reflect the Agency's views, and no official endorsement should be inferred from it.

CHAPTER 1

INTRODUCTION

The increasing concentration of greenhouse gases in the atmosphere has led to the likelihood of substantial climatic warming in the coming decades. The climate perturbation is usually expressed in terms of the change of the mean value of specific parameters, such as temperature or precipitation. However, in many instances, a change in climate variability would have as great an influence as a change in the mean. This is especially true for biologically oriented processes, such as tree growth or agriculture, where killing frosts or anomalous heat waves can destroy the crop regardless of the "mean temperature" for the month or year. Solomon and West (1985) emphasized the lack of suitable projections of changes in climate variability as a limiting factor in evaluating the response of forests to the projected climate change. As implied by this opinion, were variability to change as climate warms, it would likely alter the impact of the greenhouse warming on society.

The United States Environmental Protection Agency (EPA) is currently studying the potential effects of climate change on various aspects of society, including agriculture, forestry, and water resources (EPA, 1988). The EPA study uses climate change results for the monthly mean temperature and precipitation as calculated by several different general circulation models (GCMs). However, the study assumes variability will not change from its present magnitude. This was done out of necessity, since no systematic study of possible alterations in variability had been undertaken. The variability change produced by the GCMs was not used directly, since there had also been no study of how realistic their variability was for the current climate simulation. Thus interannual and daily variations were taken from observed data for a 30-year time period, and the models' monthly mean climate change values were simply appended to them. It was recognized that this conservative approach might well underestimate the influence of the projected climate changes, in the sense that many of society's processes are inherently arranged with the current variability in mind. In an attempt to determine whether the GCMs could be used for an estimate of the change in variability, and what change would have resulted, the following study was undertaken.

The GISS GCM was one of the models providing data for the climate change assessments. Results used were from both the GISS doubled CO₂ run with its current climate control, and a transient climate change experiment in which trace gases are increased gradually. To assess how well this model can simulate the observed variability we compare model and observed interannual and daily variations of temperature and precipitation for the four geographic areas of concern in the EPA analysis: southeast United States, the Great Lakes region, the Southern Great Plains, and the West Coast. We also compare how the variability for these time scales is altered in the climate change simulations. We then repeat these comparisons for the diurnal cycle variation of temperature. The results of this study provide a first estimate of how variability changes with climate change.

CHAPTER 2

MODEL AND CLIMATE CHANGE EXPERIMENTS

The model used is the GISS GCM (Hansen et al., 1983) run at the $8^\circ \times 10^\circ$ resolution. The model numerically solves the conservation equations for mass, momentum, energy, and moisture. It includes parameterizations for rain and snow generation, cloud cover, short wave and long wave radiation, surface fluxes, etc., and uses two ground layers for surface hydrologic calculations. For climate change experiments, the ocean temperatures are allowed to adjust but ocean heat transports, required to produce current sea surface temperatures, are specified as unchanged. Uncertainties in climate models' cloud cover, ground hydrology, and ocean parameterizations induce uncertainties in model responses to climate change forcing.

The model has been run for both doubled CO_2 experiments (Hansen et al., 1984), and the transient climate change, in which trace gases are allowed to accumulate gradually, and the climate change is calculated for the next 100 years. This transient experiment has been reported in several different forums (Hansen et al., 1987, 1988), and the results reported here correspond to a trace gas growth scenario in which current trends are continued into the future unchanged. Both climate change experiments will be used in this analysis, depending on the availability of model output for the various time-scales of variability.

CHAPTER 3

MEAN VALUES

Temperature and precipitation results will be reported for the four areas of the United States which are the focus of the EPA climate-change effects study. The four grid box regions for the $8^\circ \times 10^\circ$ resolution model are shown in Figure 1, along with the cities that are used for comparison purposes (Table 1). We present in Table 2(a,b) a comparison of the model and observed temperature and precipitation for the 4 months, with observations obtained by averaging values for the nine cities within or in the proximity of each of the grid boxes. The reason for choosing nine cities will be discussed in Chapter 4. The model results are averages over 10 model years (10 independent samples) for the control run, doubled CO_2 study, and transient experiments decades.

We evaluate the statistical significance of the differences between the model and observations, and the model and climate change experiments, by using the first moment test variate (Chervin, 1981), which equals the difference in mean values divided by the square root of the sum of the squares of the standard deviations. Standard deviations for observations, current climate, and doubled CO_2 climate are given in Table 3. We use the hypothesis that there is no difference between the means, and reject it at the a priori selected significance level of 5%, for a two-sided critical region. Cases in which the hypothesis is rejected, and thus values can be determined to be significantly different, are indicated by an asterisk in Table II. Note that even if we cannot prove a significant difference, it does not necessarily indicate that the model is reproducing the current temperatures or precipitation. It may be that we simply do not have enough data to disprove the assumption. Thus in the cases where the differences are not significant, we must simply say we cannot reject the hypothesis (rather than accepting it).

Model monthly mean temperatures (Table 2a) are significantly different from the observed during summer and fall. In these seasons the model is consistently cooler, due most likely to the ground hydrology scheme which keeps too much moisture in the ground in summer (Hansen et al., 1983). As the winter temperatures are more accurately reproduced, the model tends to underestimate the seasonal temperature cycle by 15-20%.

Model monthly mean precipitation values (Table 2b) are generally realistic for the southeast and Great Lakes grid boxes, while they tend to overestimate the rainfall for the west coast and southern Great Plains. These discrepancies will affect the precipitation distributions discussed below.

Thus as indicated in Table 2, in about half the cases the model produces significantly different mean temperature and precipitation values when compared with observations. This properly raises doubts about the validity of model-produced changes in these fields, as well as changes in variability. We return to this question in the discussion section; here we simply note that the model discrepancies must be borne in mind when evaluating the results.

The current climate control run utilized the atmospheric composition of 1958. Also shown in Table 2 are the model-predicted changes for the decades of the 2010s, 2030s, 2056-2065, and the equilibrium doubled CO_2 results. The annual average global mean warming for the 2010s was about 1°C relative to the control run, for the 2030s about 2°C , and for 2056-2065 about 4.2°C . Close to one-half of the temperature changes in the 2010s are significant, while temperature changes in later decades and for the doubled CO_2 climate are usually so.

The doubled CO_2 results are averages for years 26-35 from the experiment, when the atmosphere was 4.2°C warmer and temperature was no longer changing. In that respect it can be compared with the values for 2056-2065, in which the warming was reached in a transient mode. Cases in which the two temperatures are significantly different are indicated by a plus sign in Table 2; several of the cases fall into this category, with the equilibrium doubled CO_2 changes being smaller than that for the decade around 2060. In the cases which lack significant differences, there is no consistent sign of the difference. For the purposes of the following discussion we will look upon the experimental results for the 2060 time period as being similar to those for equilibrium doubled CO_2 .

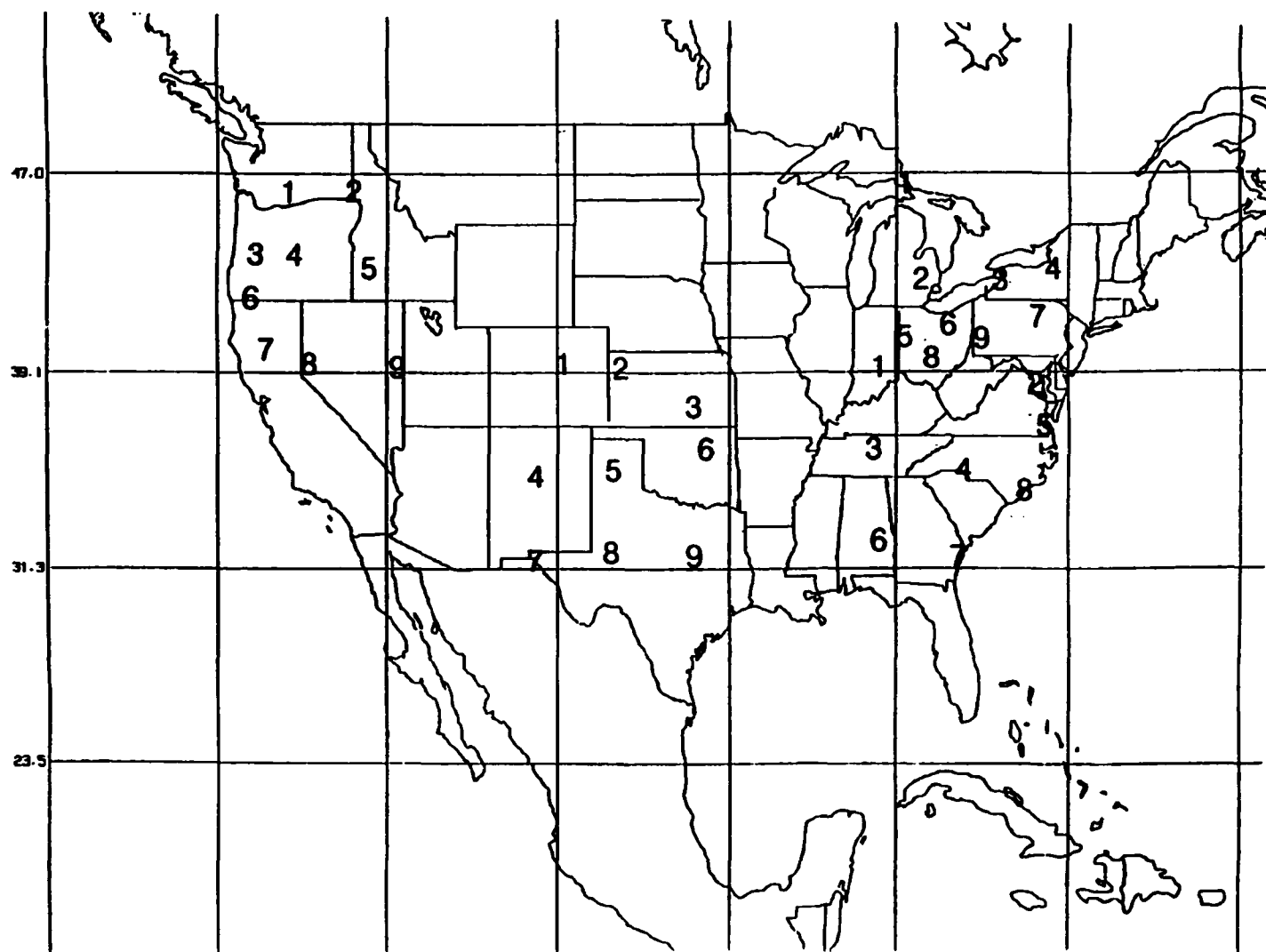


Figure 1. Location of grid boxes for model results, and cities from which observed data has been used for comparison. The cities corresponding to the numbers are listed in Table 1.

Table 1. Stations Used to Obtain Grid Box Averages

SOUTHERN GREAT PLAINS (31-39°N, 95-105°W)		SOUTHEAST (31-39°N, 75-85°W)	
1. DENVER	6. TULSA	1. INDIANAPOLIS	6. MONTGOMERY
2. GOODLAND	7. EL PASO	2. WASHINGTON	7. SAVANAH
3. WICHITA	8. MIDLAND	3. NASHVILLE	8. WILMINGTON
4. ALBUQUERQUE	9. WACO	4. CHARLOTTE	9. COLUMBUS
5. AMARILLO		5. NORFOLK	
WEST COAST (39-47°N, 115-125°W)		GREAT LAKES (39-47°N, 75-85°W)	
1. YAKIMA	6. MEDFORD	1. SLTE ST. MARIE	6. CLEVELAND
2. LEWISTON	7. RED BLUFF	2. FLINT	7. WILLIAMSPORT
3. EUGENE	8. RENO	3. BUFFALO	8. COLUMBUS
4. REDMOND	9. ELY	4. SYRACUSE	9. PITTSBURG
5. BOISE		5. FT. WAYNE	

Table 2a. Monthly Average Mean Temperatures (°C)

MONTH	LOCATION	OBS TEMP	CURRENT TEMP	2010s Δ T	2030s Δ T	~2060 Δ T	2xCO2 Δ T
JANUARY	S.G.PLAINS	2.32	-0.07	1.87	3.07*	5.39*	5.0*
	SOUTHEAST	2.79	4.40	2.10	1.71	4.74*	4.0*
	WEST COAST	-0.08	-1.23	1.38	3.71*	4.17*	6.0*
	GRT.LAKES	-4.79	-2.72	0.06	1.84	5.16*	6.0*
APRIL	S.G.PLAINS	14.30	14.08	0.44	4.06*	5.32*	5.0*
	SOUTHEAST	14.46	14.36	2.31*	5.07*	5.79*	4.0**
	WEST COAST	8.59*	6.85	1.82*	2.43*	5.58*	6.0*
	GRT.LAKES	8.41	7.52	1.45	3.08*	3.52*	5.0**
JULY	S.G.PLAINS	26.80*	20.50	1.19*	1.84*	4.84*	4.0*
	SOUTHEAST	25.60*	22.86	1.68*	2.44*	4.57*	3.0*
	WEST COAST	21.40*	16.84	0.60	3.55*	4.14*	3.0*
	GRT.LAKES	21.69*	18.61	2.06*	2.89*	3.75*	4.0*
OCTOBER	S.G.PLAINS	15.55*	12.83	1.52	1.76	6.24*	7.0*
	SOUTHEAST	15.49	15.28	1.51	3.01*	4.80*	5.0*
	WEST COAST	10.84*	8.21	1.72	3.42*	4.96*	5.0*
	GRT.LAKES	10.88*	6.41	2.15*	2.81*	5.89*	4.0**

Table 2b. Monthly Average Precipitation (mm d⁻¹)

MONTH	LOCATION	OBS PREC	CURRENT PREC	2010s Δ P	2030s Δ P	~2060 Δ P	2xCO2 Δ P
JANUARY	S.G.PLAINS	0.46*	2.08	-0.07	0.00	1.12*	-0.76+
	SOUTHEAST	2.83	2.85	-0.29	-0.96	-0.41	0.27
	WEST COAST	2.18*	4.03	-0.19	0.08	0.13	0.93
	GRT.LAKES	2.04*	2.98	-0.79	-0.81	-0.43	0.07
APRIL	S.G.PLAINS	1.31	1.93	1.44	1.36	1.39	-0.47
	SOUTHEAST	2.93	2.27	0.77	-0.50	0.25	0.54
	WEST COAST	0.94*	2.40	-0.16	-0.02	-1.19	0.04+
	GRT.LAKES	2.73	2.08	-0.15	-0.34	0.14	0.25
JULY	S.G.PLAINS	1.99*	4.31	-0.43	-0.23	-0.33	1.05
	SOUTHEAST	4.07	4.51	-0.21	0.25	0.06	1.60
	WEST COAST	0.25*	1.54	0.41	0.09	0.73	0.14
	GRT.LAKES	2.82	2.44	0.01	0.70	-0.16	0.61
OCTOBER	S.G.PLAINS	1.22	0.57	0.03	0.57	0.27	0.02
	SOUTHEAST	2.14	1.87	1.57	-0.39	0.19	-0.06
	WEST COAST	0.91	1.40	0.59	-0.55	0.39	0.57
	GRT.LAKES	2.16	1.62	0.04	0.04	0.32	-0.25

Table 3a. Interannual Standard Deviations of Temperature (°)

GRID BOX		JAN	FEB	MAR	APR	MAY	JUN	JUL	AUG	SEP	OCT	NOV	DEC
S.G. PLAINS	OBS	2.0	2.0	1.9	1.4*	1.2	1.2	1.1	0.9	1.3	1.4	1.5	1.5
	CONT	3.1	2.7	2.2	2.5	1.3	1.1	0.9	1.3	1.5	2.1	2.4	2.5
	2CO2	2.1	1.9	1.7	1.2*	0.7*	1.0	1.1	0.9	2.0	1.9	1.5	2.3
	STD	0.7	0.7	0.5	0.5	0.3	0.3	0.4	0.5	0.5	0.4	0.8	0.6
SOUTHEAST	OBS	2.3	2.3	2.1	1.2*	1.4	1.0	0.7*	0.8*	1.1	1.4	1.3	1.9
	CONT	3.0	2.3	2.2	2.4	1.9	0.9	1.3	3.1	1.2	2.0	1.4	2.9
	2CO2	2.1	1.9	1.7	1.2*	0.7*	1.0	1.1	0.9*	2.0	1.9	1.5	2.3
	STD	0.3	0.6	0.5	0.4	0.3	0.2	0.3	0.7	0.5	0.5	0.7	0.4
WEST COAST	OBS	2.1	1.7	1.2	1.4	1.3	1.3	0.9	1.3*	1.5*	1.1*	1.3	1.5
	CONT	2.2	2.4	1.7	1.6	1.2	1.3	1.5	4.2	3.0	2.5	2.1	1.3
	2CO2	1.7	2.1	2.2	1.2	1.5	1.3	1.6	3.5	2.6	2.7	2.4	2.3
	STD	0.7	0.6	0.4	0.4	0.4	0.6	0.5	0.7	0.6	0.5	0.5	0.4
GREAT LAKE	OBS	2.4	2.5	2.0	1.4	1.7	1.1	1.0	1.1	1.3	1.7	1.5	2.2
	CONT	3.0	1.8	1.7	2.3	2.0	1.5	1.3	1.7	1.8	1.8	1.4	2.2
	2CO2	1.5*	1.8	1.8	1.3	1.6	1.0	1.1	1.6	1.4	1.8	1.9	2.5
	STD	0.6	0.7	0.6	0.4	0.4	0.3	0.5	0.7	0.4	0.3	0.5	0.5

Table 3b. Interannual Standard Deviations of Precipitation (mm d⁻¹)

GRID BOX		JAN	FEB	MAR	APR	MAY	JUN	JUL	AUG	SEP	OCT	NOV	DEC
S.G. PLAINS	OBS	0.3*	0.3*	0.6*	0.6*	0.7*	0.7	0.8	0.6	0.9*	0.8	0.5*	0.4*
	CONT	1.0	1.2	1.7	1.5	1.4	1.0	1.2	1.0	0.4	0.6	1.2	0.8
	2CO2	0.9	1.5	1.4	1.9	1.4	2.0*	1.9	1.3	1.0*	1.5*	0.8	0.7
	STD	0.4	0.3	0.3	0.6	0.4	0.3	0.3	0.2	0.2	0.3	0.2	0.2
SOUTHEAST	OBS	0.7*	0.9	0.8*	0.8	0.7*	0.8	0.9*	0.8*	1.2	0.9	0.8*	0.8
	CONT	1.5	1.5	1.5	1.2	1.9	1.2	1.9	2.0	1.6	1.4	1.7	1.4
	2CO2	1.9	1.7	2.0	2.0	1.9	1.5	1.9	2.0	2.0	1.9	1.9	1.6
	STD	0.3	0.2	0.5	0.4	0.5	0.4	0.3	0.3	0.6	0.4	0.3	0.4
WEST COAST	OBS	0.8*	0.7	0.5	0.5*	0.5*	0.4*	0.1*	0.3*	0.3	0.6	0.9*	1.1
	CONT	1.6	1.2	0.6	1.5	1.3	1.2	0.9	0.6	0.3	0.9	1.7	1.5
	2CO2	0.9*	1.6	1.5*	1.2	1.5	1.9	0.6	0.8	0.2	1.4	2.0	1.9
	STD	0.3	0.6	0.2	0.2	0.2	0.3	0.1	0.2	0.1	0.2	0.5	0.3
GREAT LAKE	OBS	0.7	0.7	0.7	0.7	0.8	1.0	0.6*	0.8*	0.8	1.0	0.7*	0.7
	CONT	1.0	0.5	1.2	0.8	1.3	1.4	1.2	1.5	1.0	0.8	1.3	1.2
	2CO2	1.1	0.8	1.3	1.5*	1.4	1.0	1.5	1.1	0.7	1.7*	1.0	0.9
	STD	0.2	0.2	0.3	0.3	0.2	0.4	0.3	0.1	0.4	0.2	0.3	0.2

The precipitation changes (Table 2b) are not significant, although the doubled CO₂ or equivalent 2060 changes usually indicate increased rainfall: 23 of the 32 cases shown for these time periods have increased precipitation. From standard binomial probability testing for increase versus decrease, this or higher percentages of increase would occur less than 1% of the time simply by chance. As discussed in more detail (Rind, 1988a) the 10-year average changes are generally on the order of one (interannual) standard deviation regardless of the size of area averaging. Such differences would require integrations for many years to establish their significance. We will see this tendency repeated throughout the study: individual results often show little significant change, although a majority of the results show the same sign of the change. Note also that as the doubled CO₂ and 2060 precipitation differences are not significantly different, we again treat the two simulations as being similar.

Given this character of the modeled climate change, we now investigate the model's variability compared to the observed, and indicate how variability changes as the climate warms. The time-scales of variability are investigated in inverse order, starting with the longest accessible scale of year-to-year variability, then daily, and finally the diurnal cycle amplitude.

CHAPTER 4

YEAR-TO-YEAR VARIABILITY

How does the modeled year-to-year variability compare with observed variability? We compare the model variability from a 100-year control run for the present climate (Hansen et al., 1988) with the interannual variability obtained from the stations shown in Figure 1/Table 1 for the 1951-1980 time period. The results of this comparison are given in Table 3a for the relevant areas. To determine significant differences, we evaluate the second-moment test variate, equal to the square root of the F statistic, from the ratio of model to observed standard deviations (Chervin, 1981). Following Chervin, we determine the significance at the a priori selected 10% significance level using the hypothesis of equal variances. Significant differences are again indicated by an asterisk. For comparison we also show the standard deviation of the 10-year standard deviation, determined by breaking the 100-year run up into 10 equal intervals. Note again the test allows us only to determine whether significant differences exist between the model and observations, and not to prove that the model is actually reproducing the current climate values.

Overall the modeled and observed temperature variability are in good agreement, statistically different at the 10% level in only 7 of the 48 cases. However, the model in summer generally overestimates the variability, even if the magnitude of the difference is not significant. The modeled surface air temperatures in summer are sensitive to the ground hydrology parameterization, which is very crude in this and most other climate models. It would appear to allow for greater variability in soil moisture and surface air temperature than occurs in the real world, an effect which is exaggerated by August when the ground can become completely dry in the model owing to continual evapotranspiration (the parameterized vegetation does not completely shut off moisture loss before the ground dries out entirely).

The comparison between model and observed interannual variability of rainfall is shown in Table 3b. In almost half the cases the values are significantly different, with the model variability generally larger than observed; this is especially true in the areas and seasons where mean precipitation amounts were overestimated (e.g., West Coast in summer, Southern Great Plains in winter, Table 2b). With excessive precipitation there is more scope for variability. However, even in other regions, the modeled values are generally too high. The model produces one value for rainfall each time step over the entire grid box; thus either it rains or it does not. In the observations, it can rain at one station and not another, and the result is to smooth the grid box average value and reduce variability. When we reduced the number of stations used for assessing the observed variability from nine to five, precipitation variability increased by some 33%, while temperature variability was relatively unchanged. This indicates the uncertainty that must be attached to the "observed" interannual precipitation variability for a grid box as a whole. Again, the deviation of the modeled variability from observed will likely affect the confidence that can be placed in the climate change assessments.

What should we expect for changes in the interannual standard deviation of temperature and precipitation as climate warms? If there are physical reasons for expecting changes, then we can establish an a priori expectation of sign change. We begin with temperature, and discuss precipitation later in this chapter.

Climate models have been unanimous in predicting that high latitudes should warm more than lower latitudes (e.g., Schlesinger and Mitchell, 1987). High latitudes have greater static stability, so that low level warming is trapped near the surface, rather than being convected to higher altitudes as occurs in the tropics. Furthermore, snow and sea ice melting at higher latitudes reduces the surface albedo, allowing more solar radiation to be absorbed, and leading to greater heat ventilation from the oceans during winter.

Because of this latitudinal variation in temperature change, the temperature differential between low and high latitudes is expected to decrease, a result which again holds true in the different climate models (e.g., Rind, 1987). Were the latitudinal temperature differences to be completely eliminated (as is apparently the case for Venus), temperature variability on all time scales would tend toward zero; the variability currently results from the advection of cold and warm pools of air into a region, pools which accumulate at high and low latitudes

respectively. All that would be left to provide for advective temperature changes would be land/ocean or other longitudinal temperature contrasts. As the equilibrium doubled CO₂ climate reduces the latitudinal temperature contrasts, this should lead to reduced temperature variability in the future.

In addition, the synoptic scale systems of high and low pressure which are responsible for advecting different air masses into a region gain their energy from the latitudinal temperature gradient via the baroclinic process. As this temperature gradient decreases, so should the energy of these systems, as has been seen in doubled CO₂ climate studies (Rind, 1987). Again, this should result in reduced temperature variability.

With these expectations in mind, numerous studies have been made, looking for a trend in variability as climate has warmed over the past century (e.g., Angell and Korshover, 1978; Barnett, 1978; Ratcliffe et al., 1978; van Loon and Williams, 1978; Diaz and Quayle, 1980). None of these studies has found such a trend, although the warming over this time period, on the order of 0.6°C (Hansen and Lebedeff, 1987), has not been particularly large when compared with the projected future warming. Does the model show decreased variability as the climate warms?

In Table 3a, we show the monthly standard deviation of temperature for the last 10 years of both the current climate control run and the doubled CO₂ run on the 8° x 10° resolution. The significance of the changes at the 10% level are determined as discussed previously. In only six of the cases are the differences significant, although there is a general tendency for the expected reduced variability from January through April in the doubled CO₂ climate (13 of the 15 months which show changes from the four grid boxes have reductions, and all six of the significant changes show reduced variability).

To determine whether the tendency for reduced variability during winter would be evident in a broader sample, a comparison was made for 13 grid boxes over the United States for the months of January through April. In 70% of the approximately 50 cases the control run standard deviations were lower than those for the doubled CO₂ run. However, the grid boxes are not necessarily independent; Hansen and Lebedeff (1987) computed the correlation coefficient of annual mean temperature changes for pairs of randomly selected stations having at least 50 years of records. They found that for mid-latitudes, the correlation dropped off to 0.5 at approximately 1200-km separation, and to 0.1 at 3000-km separation. While those authors used the 1200-km distance as representative of independent data points, to absolutely guarantee that we are dealing with geographically independent regions, we look at grid boxes more than 3000 km apart (i.e., every fourth grid box).

Grid boxes 4000 km apart were chosen at random in the Northern Hemisphere extratropics (20-70°N) during winter, when the high latitude amplification of the temperature change is greatest (Hansen et al., 1984). In 60% of the 150 cases, the standard deviations decreased. Evaluating this result, standard binomial distribution theory shows that such a change, or even greater percentage reductions, would have occurred by chance less than 1% of the time. We show in Figure 2 the change of the standard deviation during January. As evident in the figure, and the fact that only 60% of the cases show a decrease, as well as the sampling for the United States, the reduction does not occur at all grid boxes in all winter months. However, there can be no doubt about the reality of the effect on the largest spatial scales; for the extratropics during winter, the latitudinal average surface air temperature standard deviation decreases in the doubled CO₂ climate more than 80% of the time. And in the months for which the climate change shows a decrease in the latitudinal temperature gradient (September through May), the interannual variability for the Northern Hemisphere as a whole decreases in every month in the warmer climate.

How should precipitation variability change as climate warms? An indication can be gained by comparing the model's variability relative to the observed with the model's mean values relative to observed. As noted above, where the model severely overestimates precipitation for the mean, it also does so for its variation, as greater magnitude differences between years are possible when rainfall values are greater. As climate warms, there is increased evaporation from the oceans, and an increase in the hydrologic cycle, with global rainfall higher by about 11% (Rind, 1988a,b). With all else the same, this should lead to increased variability, and the annual

Rind

global average variability does increase in the doubled CO₂ climate by some 3%. Diaz and Quayle (1980) failed to find any significant differences in precipitation variability between warm and cold decades, although the temperature changes were much smaller than is being considered here for doubled CO₂.

The standard deviation of monthly average precipitation in the climate change experiments is given in Table 3b. The results maintain the character we have seen throughout; on an individual basis, very few of the changes are significantly different (7 of the 48 cases). Overall, however, the expected tendency emerges, as 31 out of the 44 total months in which a change is recorded have increased variability in the doubled CO₂ climate. The tendency was particularly striking in the Southeast, in which the variability in the warmer climate did not decrease for any month of the year, including autumn, when the actual mean precipitation values decreased by 0.6 mm day⁻¹ (Rind, 1988a).

To look at a broader sample, we need to know the spatial scale for independent precipitation measurements. Rind and Lebedeff (1984) investigated the correlation coefficient between the precipitation trends for stations in the United States, and found that at a distance of 500 km the correlation had already dropped to 0.4. Diaz and Quayle (1980) have clearly shown that the changes in precipitation and precipitation standard deviation between different decades have smaller spatial scales than the corresponding temperature changes. Thus in this case we use 1000 km as the length scale for independent measurements. Referring to the 22 grid boxes over the United States and contiguous North America for the 12 months, 65% received precipitation increases in the doubled CO₂ climate (Rind, 1988a). Examination for variability changes indicated that out of the 264 cases, 62% showed increased variability, which would occur by chance (along with even higher percentages) less than 0.1% of the time. When the study is repeated using grid boxes 2000 km apart, increased variability still occurred with a probability which would have occurred by chance less than 1% of the time. On even larger spatial scales, the hemispheric and global standard deviations increased each month. The change in standard deviation is shown in Figure 3 for July. Again note that although general increases occur, there are some regions with decreased variability. When this figure is compared with the GISS model change in summertime precipitation in the doubled CO₂ climate (as shown in Schlesinger and Mitchell, 1987) it is evident that the largest changes in interannual variability occur in regions where there are large changes in the mean precipitation itself, and both the mean and variance changes have the same sign. Thus the near equality of percentage of locations which show increases in mean precipitation over the United States, and those which have increased variability, is not fortuitous.

When the change in variability is of the same sign as the change in the mean, it indicates that the change in relative variability is minimized, which may be important in some applications. To examine this issue more closely, the sign of the change of the mean was compared to the sign of the change in interannual variability for the grid boxes and months described above. In 50% of the cases, grid boxes over the United States and adjacent North America had increases in both quantities, while in 23% of the cases there were decreases in both. Thus in 73% of the cases the sign of the change in variability was the same as the sign of the change in the mean. Of the other 27%, 16% had increased mean precipitation but decreased variability.

To summarize the results of this section, at individual stations changes in the interannual standard deviation of temperature and precipitation were generally not significant. However, when a larger geographical region is considered, the number of independent grid boxes which show a decrease in interannual temperature variability and an increase in interannual precipitation variability in the doubled CO₂ climate is significant, with the changes noted 60-70% of the time. As emphasized by this value, as well as the results shown in Table 3 and Figures 2 and 3, the sign of these changes simply represent tendencies, not uniform results.

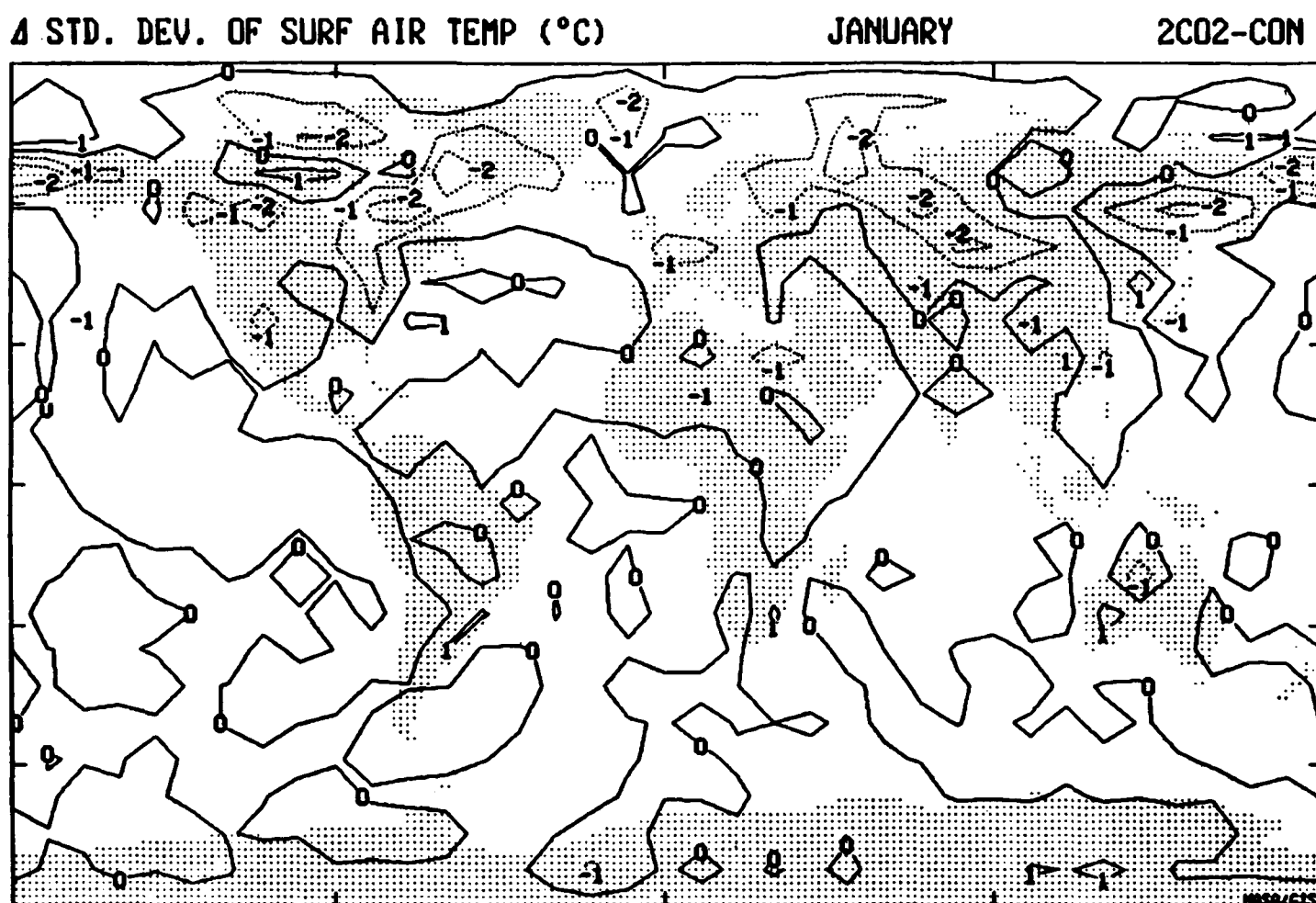


Figure 2. Latitude-longitude presentation of the change in the interannual standard deviation of surface air temperature in January, doubled CO₂ climate minus control. The tic marks indicate latitudes of 0°, $\pm 30^{\circ}$, and $\pm 60^{\circ}$, and longitudes of 0° and $\pm 90^{\circ}$.

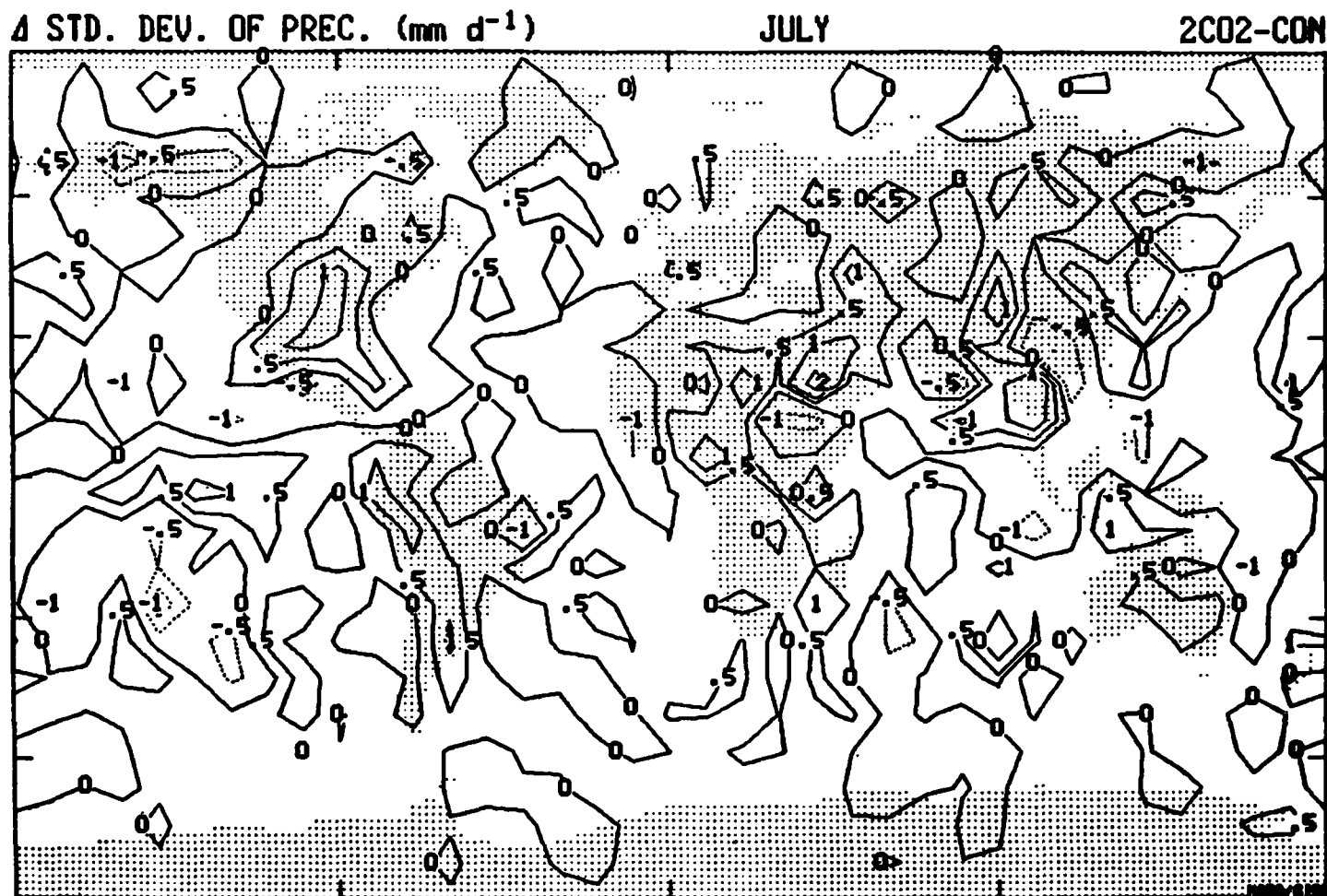


Figure 3. As in Figure 2 for the change in the interannual standard deviation of precipitation in July, doubled CO₂ climate minus control.

CHAPTER 5

DAILY VARIABILITY

In this section our interest is in comparing daily variations in temperature and precipitation, for observations versus the modeled current climate, and for the climate change experiments. For temperature, the daily mean value is compared with the monthly average value and the departure noted; the results are then tabulated for the length of the record, 30 years in observations, 10 years for the different model runs. The distribution of these departures can then be compared. While this technique is straightforward for the model values, in which a single temperature represents the entire grid box, the situation is not as clear for the observations.

How many stations are needed to produce a representative result for the area equivalent to the model grid box? In Figure 4, we compare the distribution of daily temperature departures from the monthly mean for 30 years of April data (1930-1960) when using 3, 5, and 7 stations respectively, for the Southern Great Plains in April. In each case the stations were widely distributed throughout the grid box. While some changes can be noted, the results are rather similar regardless of the number of stations used.

Comparisons were also made between the distributions of observed and modeled precipitation for the same grid boxes and months. Due to the importance of true drought episodes, the frequency of occurrence of absolutely no precipitation was recorded separately from very light precipitation. The distribution of precipitation as a function of number of stations is shown in Figure 5. Here the results are very different. As the station number is increased, the frequency of days with absolutely no rainfall decreases, and the frequency with light rainfall increases. This is not unexpected, since light rainfall occurs with significant spatial variability, and the more stations utilized, the better the chance of recording it. However, it does indicate that the comparison of observed and modeled rainfall distributions will depend on the number of stations utilized.

When the number of stations used was increased to nine, the resulting distribution in the test cases did not differ significantly from the distribution obtained with seven (with significance determined in the manner described below), for either temperature (compare Figure 4 with Figure 7, top left) or precipitation. The use of nine stations in each grid box thus appeared to be adequate for these purposes, although the more uniform the station distribution, the better the grid box representation. The stations are indicated in Figure 1; as is evident we also occasionally chose to use stations which were just outside the grid box, in order to secure a more area-wide representation of the results.

In comparing distributions of this sort, considerable problems are encountered when attempting to evaluate the significance of differences between them. Daily temperature values are unlikely to be independent, as some degree of persistence is prevalent for several days. The daily variance can be defined in terms of autocorrelation coefficients and an uncorrelated contribution. Katz (1984) provided a procedure for investigating the significance of the changes in the uncorrelated contribution. Wilson and Mitchell (1987) employed his technique, and found a significant decrease in the uncorrelated daily variance during winter.

However, our interest is not in the uncorrelated component, it is in the actual daily variation. As climate warms, and the latitudinal temperature gradient decreases, there is the potential for decreases in the mean zonal wind flow, leading to slower movement of synoptic scale systems. This might produce a change in persistence, which would contribute to the change in daily variations and would be an important component to recognize. The problem in including the correlated changes is that it reduces the number of independent data points being used, a factor which must be considered in the statistical evaluation.

Thus we adopted the following approach. We first calculated the autocorrelation function for the temperature and precipitation data sets for both observations and the different models experiments. An example of the observed and modeled temperature autocorrelation functions for the southeast grid box for April is shown

Rind

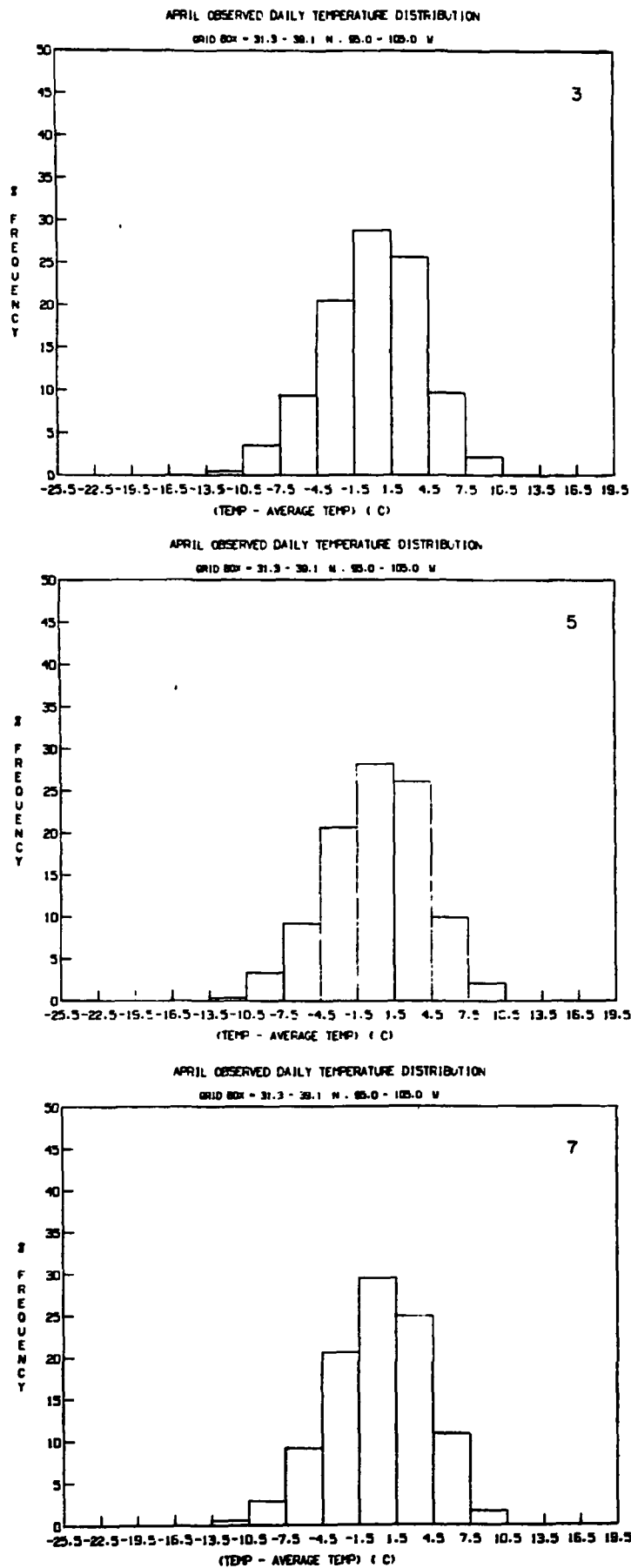


Figure 4. Distribution of observed daily temperature departures from monthly means for the Southern Great Plains grid box for 30 years of April data (1930-1960) using three stations (top), five stations (middle), and seven stations (bottom).

Rind

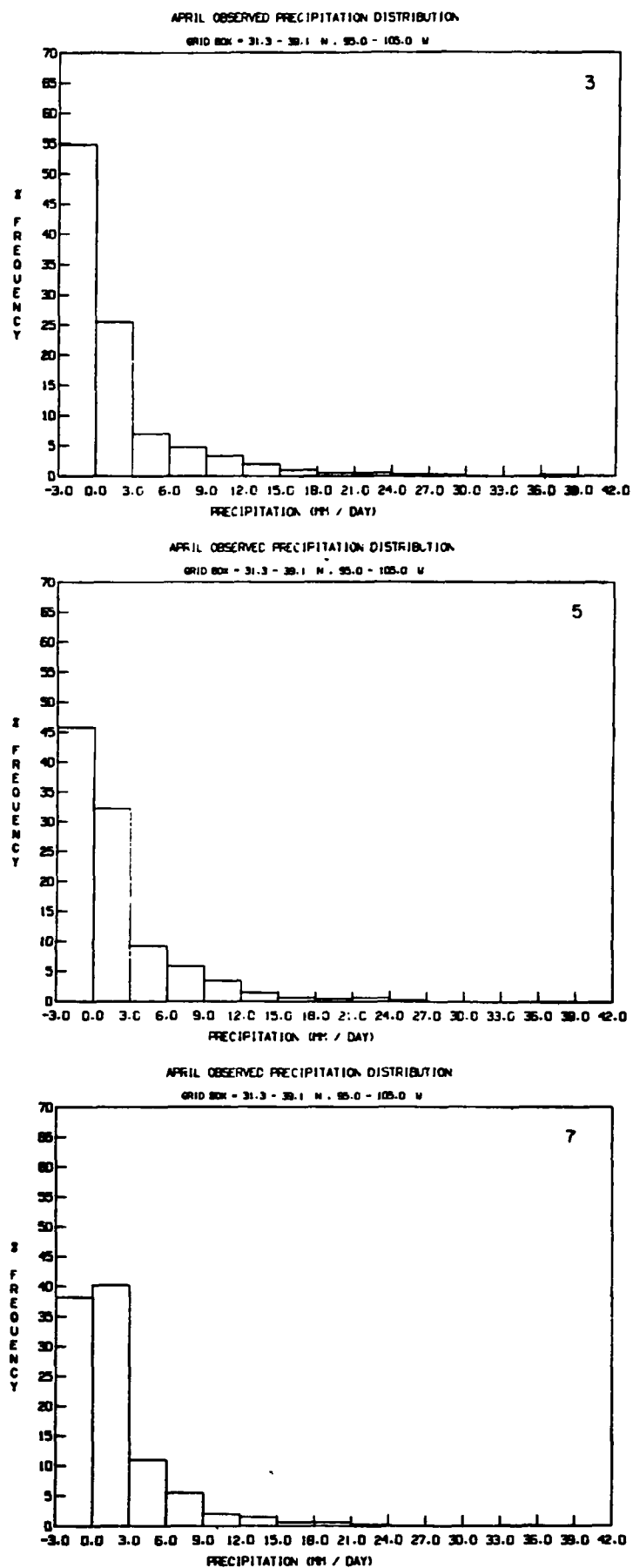


Figure 5. As in Figure 4, except for daily precipitation intensities.

in Figure 6. The area under the curve represents the persistence in the data set, in days. This value was calculated for each autocorrelation function, and is the value used to reduce the number of independent observations in the statistical tests described below.

The results of this analysis are presented in Table 4. Comparing the model with observations, there is a tendency for the model to have greater persistence, especially during the warm season, and more so for precipitation than temperature. The coarse grid used in this model might be expected to retard the movement of synoptic scale systems, increasing the time of persistence; and the simplified ground hydrology could set up stronger positive feedbacks to precipitation changes than exist in the real world. Note also the smaller persistence associated with precipitation; the persistence value of close to one day obtained for these regions for the observations is in agreement with the general independence of precipitation on the preceding day found by Chin and Miller (1980).

What happens as climate changes? As indicated above, the a priori assumption is that if warming and reduced latitudinal temperature gradient slows the zonal mean winds, synoptic scale systems might move more slowly and increase persistence in the future. In fact, while the latitudinal temperature gradient at the surface does decrease, the latitudinal temperature gradient aloft increases, as convection transports heat to the tropical upper troposphere. Thus in the GISS doubled CO₂ experiments the zonal kinetic energy actually increases slightly (Rind, 1987); thus it is not clear what to expect, and referral to the average persistence times shown in Table 4 indicates no obvious trend for either temperature or precipitation. As noted by Rind (1987), the change in zonal kinetic energy depends strongly on the degree of high latitude temperature change amplification produced in the model, and so may well be model dependent. This implies that changes in persistence may be so as well.

To compare distributions of data, several statistical methods are available. One can bin the data, as in Figures 4 and 5, and use the chi-squared test to evaluate whether the null hypothesis, that the two distributions arise from the same population, can be judged unlikely. The greater the difference in number for each grouping, the more likely the null hypothesis can be rejected. Alternatively, one can generate the distribution function of the continuous data set, and use the Kolmogorov-Smirnov (KS) test to evaluate differences (e.g., Knuth, 1969). In this study, we employ both techniques on the daily temperature and precipitation distributions. When we compare the results from the two techniques in the evaluations of significance at the 5% level (i.e., significant versus non-significant), the results were in agreement 84% of the time, with the same value for both temperature and precipitation. This lends confidence to the evaluation of significance; however, it must be mentioned that there are uncertainties in the calculation of the absolute value for the chi-squared test, such as the Yates' approximate correction for using discrete distributions of frequencies (Panofsky and Brier, 1968), and uncertainties associated with significance levels for large data sets with the KS test (Knuth, 1969). It is important to recognize that the characterization of significance is perhaps not as important as the nature of the similarities or differences.

To use the chi-squared statistic when the data set is not completely independent, the chi-squared value must be reduced by the fraction of the data which is correlated (Knuth, 1969). For example, in evaluating whether the distributions in Figure 4 are significantly different, the chi-squared value must be divided by 3, the value of persistence shown in Table 4 for temperature observations in the southeast grid box in April. When applied to this example, omitting categories in which the numbers are less than five (as noted by Panofsky and Brier, 1968), the result indicates that the three distributions are not significantly different, even at the 10% level. When correcting for lack of independence in the KS test, the number of observations (30 months x 30 days/month = 900) is reduced accordingly.

Comparisons were made between 30 years of observations (1951-1980) and 10 years of the control run for the transient experiment for the four grid boxes during the months of January, April, July, and October. (Here the fact that the degree of dependence in the distributions being compared differs (Table 4) implies that a weighted average correction must be applied.) The results show that the model and observed daily temperature variations about the monthly mean are rarely significantly different, occurring only once in the

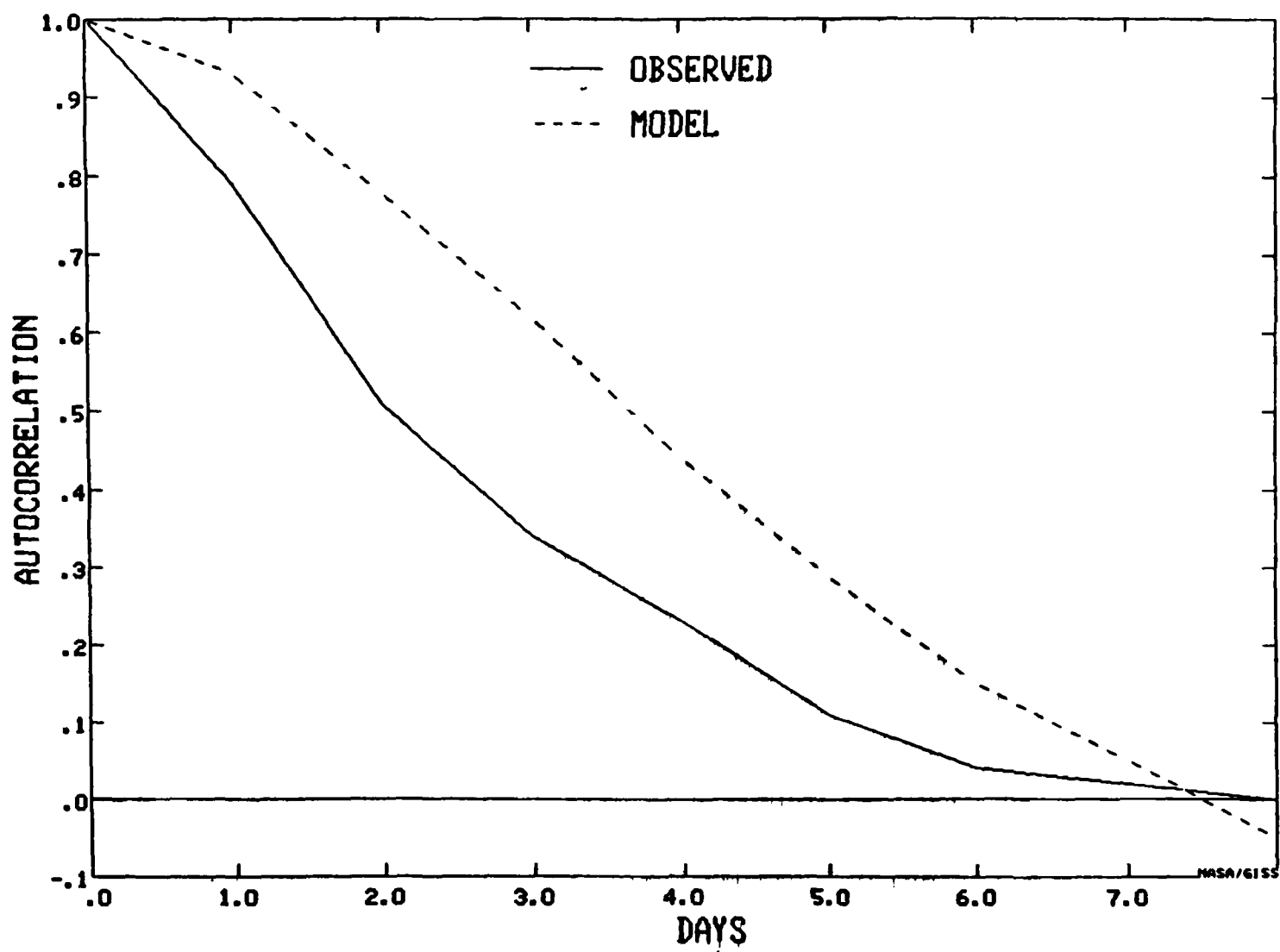


Figure 6. Autocorrelogram of observed and modeled daily temperatures for southeast grid box in April.

Table 4a. Daily Persistence of Temperature (days)

MONTH	LOCATION	OBS	CURRENT	2010s	2030s	~2060
JANUARY	S.G.PLAINS	2.72	2.26	2.10	1.90	2.20
	SOUTHEAST	2.17	2.35	2.76	2.25	2.69
	WEST COAST	2.94	2.46	2.26	2.67	2.27
	GRT.LAKES	2.32	2.25	2.28	2.21	2.47
APRIL	S.G.PLAINS	2.51	4.22	2.99	2.92	3.08
	SOUTHEAST	3.04	4.26	3.63	2.93	3.31
	WEST COAST	2.38	2.58	3.10	3.20	2.87
	GRT.LAKES	3.06	2.89	2.99	2.62	2.45
JULY	S.G.PLAINS	2.36	3.98	2.57	4.36	3.42
	SOUTHEAST	2.44	3.63	3.83	3.71	3.10
	WEST COAST	2.91	3.85	3.91	4.28	4.65
	GRT.LAKES	2.10	2.82	4.07	2.97	3.85
OCTOBER	S.G.PLAINS	3.32	3.50	2.82	3.95	3.86
	SOUTHEAST	3.00	4.04	3.49	3.79	3.19
	WEST COAST	3.01	2.54	3.26	2.97	3.14
	GRT.LAKES	2.42	3.60	2.82	3.64	3.79

Table 4b. Daily Persistence of Precipitation (days)

MONTH	LOCATION	OBS	CURRENT	2010s	2030s	~2060
JANUARY	S.G.PLAINS	1.24	1.78	1.76	1.48	2.34
	SOUTHEAST	1.17	1.80	1.96	1.80	1.68
	WEST COAST	1.76	1.95	2.14	1.77	1.94
	GRT.LAKES	1.14	1.64	1.70	1.51	1.78
APRIL	S.G.PLAINS	1.24	1.82	2.88	2.81	2.05
	SOUTHEAST	1.23	2.32	2.62	2.51	2.17
	WEST COAST	1.30	2.17	2.38	2.36	1.93
	GRT.LAKES	1.21	2.15	1.99	1.66	1.88
JULY	S.G.PLAINS	1.33	2.14	2.09	1.88	1.99
	SOUTHEAST	1.16	2.64	2.14	2.78	1.66
	WEST COAST	1.21	1.63	2.74	2.38	2.11
	GRT.LAKES	1.10	2.32	2.20	2.58	2.49
OCTOBER	S.G.PLAINS	1.47	1.86	1.96	1.71	3.28
	SOUTHEAST	1.27	2.39	2.22	2.21	2.31
	WEST COAST	1.66	2.48	1.95	1.92	2.81
	GRT.LAKES	1.30	1.73	2.13	2.08	2.28

at the 5% level. Shown in Figure 7 are distributions from observations (top) and model (bottom) for the Southern Great Plains (left) and the Great Lakes (right). Although the distributions are not significantly different, it is clear that the model produces days with greater temperature extremes than is observed. (Note that since we are using 30 years of observations and only 10 years of model results, the likelihood of finding extreme values is larger in the observations, contrary to the actual results.) This tendency occurs continually and implies that there are feedback processes in the real atmosphere that limit surface temperature deviations over a grid-box sized area which do not operate with the same magnitude in the model. The difference is not a function of the number of stations used for the observations: the results of Figure 4, for the same month and location, show that even with three stations the extreme temperatures are not recorded.

To determine how the daily temperature variability changes with climate, distributions were produced for the four grid boxes and months from the transient experiment results for the years 2010-2019, 2030-2039, and 2056-2065. As noted above, the first two time periods experienced global mean warming of about 1° and 2°C respectively, relative to the control run with the 1958 atmospheric composition, and during the last time period the global warming of 4.2°C was equivalent to the doubled CO₂ equilibrium warming with the GISS model. Comparison with the control showed that the model distributions did not in general differ from that for today, and there was no obvious progression as climate warmed. The results showed considerable individuality, both from month to month and as a function of location. The distributions for the southeast grid box for April are given in Figure 8; while changes occur, they are neither systematic nor significant.

Although the distributions may not generally differ significantly overall, a change in the occurrence of extreme temperature values could be important. The standard deviation of the values about the monthly mean give greater weight to extreme values, and so these have been calculated for the same cases. The results for observations, the current climate control run, and the climate change experiments are given in Table 5a. The asterisk indicates significance at the 10% level, calculated, as before, using the second-moment test variate (Chervin, 1981), correcting the number of independent data points from the persistence values shown in Table 4a. As expected, model values are greater than observed, due to the model's greater extremes.

The interannual variations showed that standard deviations generally decreased, but the changes at individual locations were usually not significant. The decrease was anticipated due to the reduction in latitudinal temperature gradient and eddy energy. The same processes could be expected to reduce daily temperature variations. The changes shown in Table 5a are of the same nature; they generally show decreases, but only occasionally are the changes significant. For the winter/early spring months of January and April decreases occur in 18 of the 24 cases. Were the locations geographically independent, this percentage of decrease would be significant at the 3% level, using binomial probabilities. As the southeast and Great Lakes grid boxes are contiguous, it would be necessary to consider a wider sample to make a firmer assessment.

Precipitation distributions were also tested. Comparison between the model and observations is affected by the fact that the monthly average precipitation may be very different from the observed for the grid box as a whole (Table 2b); similar differences in monthly average temperature were not a factor in the temperature comparison since the daily departures from each monthly mean temperature were being recorded. The precipitation difference could not be removed in a unique fashion: if the grid box had twice as much rainfall as observed, should each rainfall occurrence be reduced in intensity by a factor of two, or should the frequency of rainfall be changed? Rather than arbitrarily altering model values, we decided to evaluate the distributions as they were.

As can be seen in Table 2b, for the southeast and Great Lakes grid boxes, the model simulates the observed precipitation reasonably well. For the west coast and southern Great Plains grid boxes the model produces too much rain. Thus it could be expected that these latter two areas would have significantly different rainfall distributions from the model, and such is the case -- in three of the four seasons the model and observed precipitation distributions differed at better than the 5% level in those regions. In contrast, the Great Lakes grid box showed significant differences only once. Overall, model and observed values differed slightly more than one-half of the time.

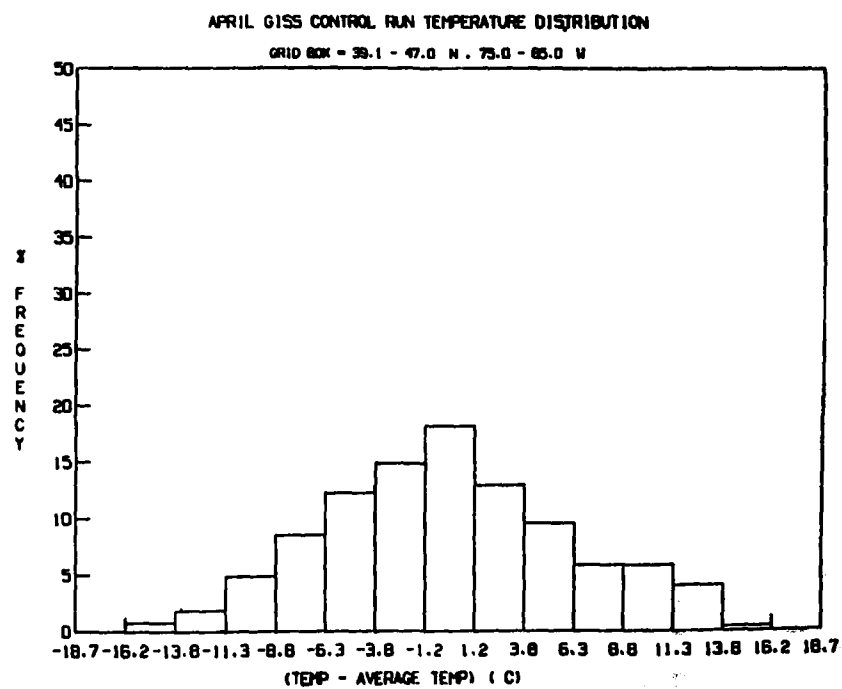
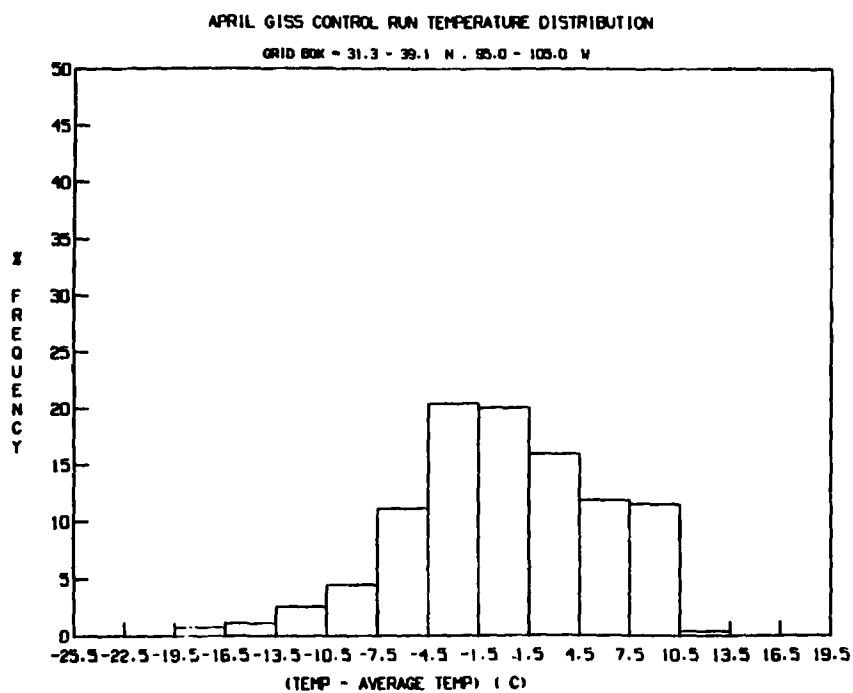
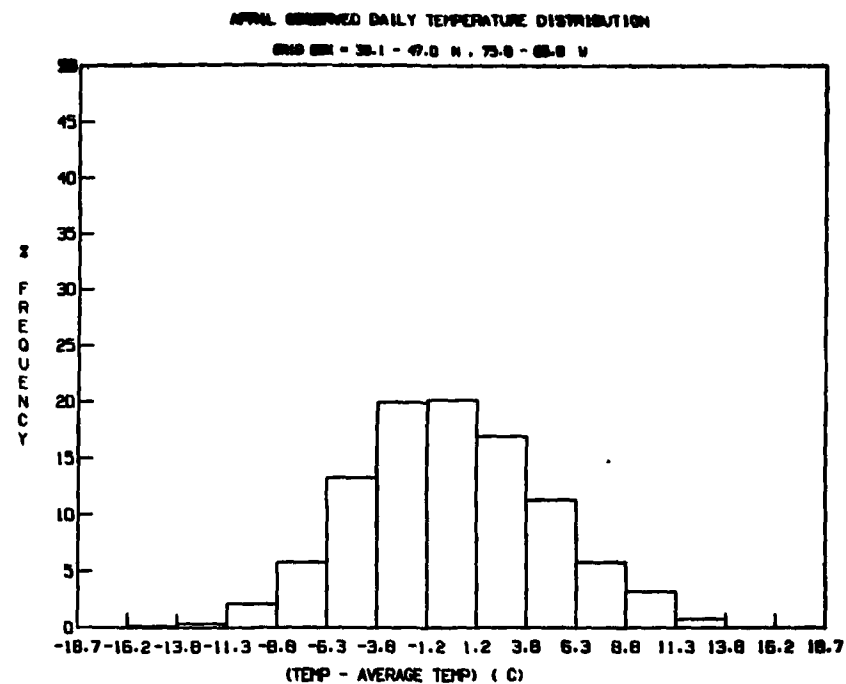
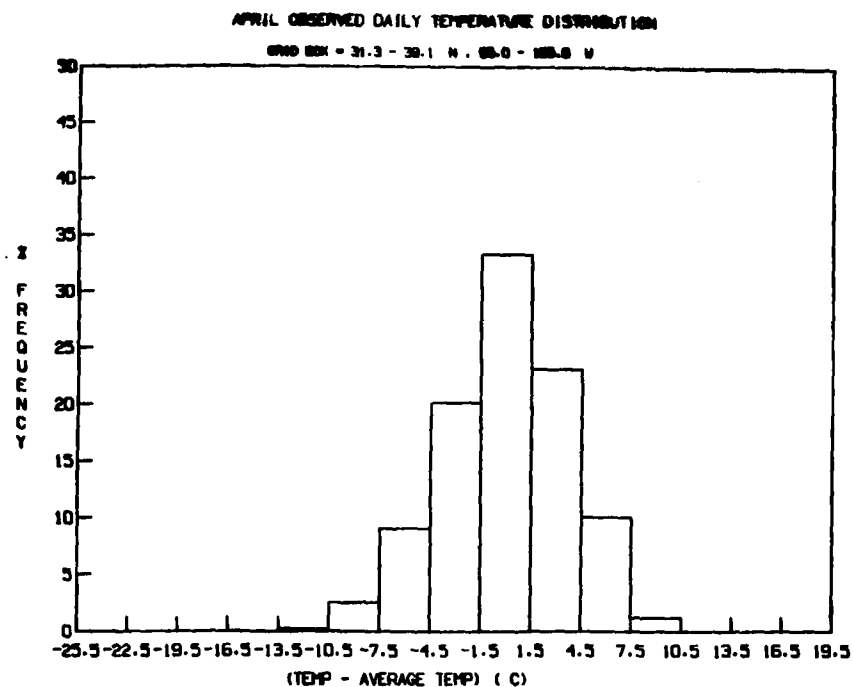


Figure 7. Observed (top) and model (bottom) daily temperature departure from the monthly mean for the Southern Great Plains in April (left), and the Great Lakes in April (right).

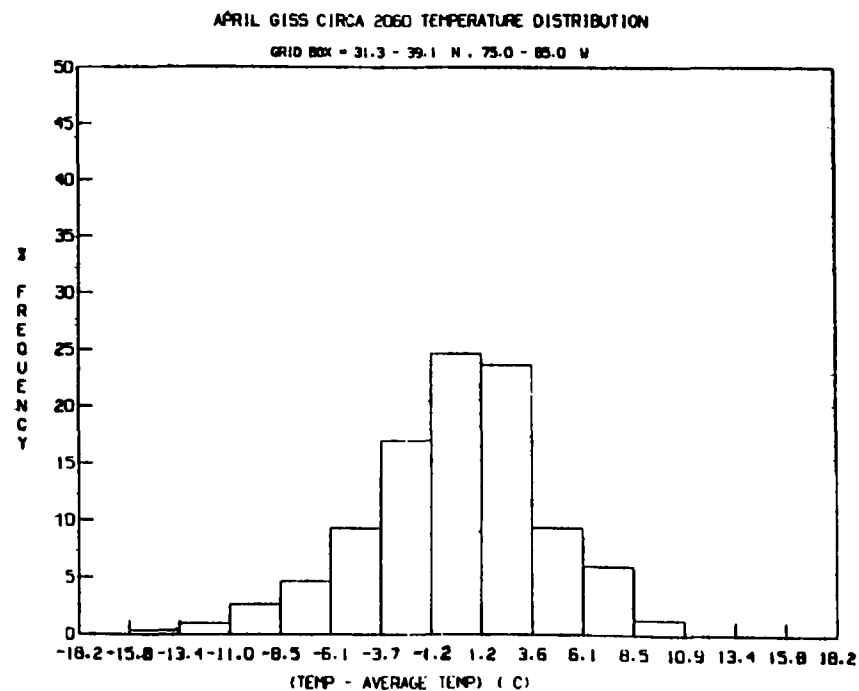
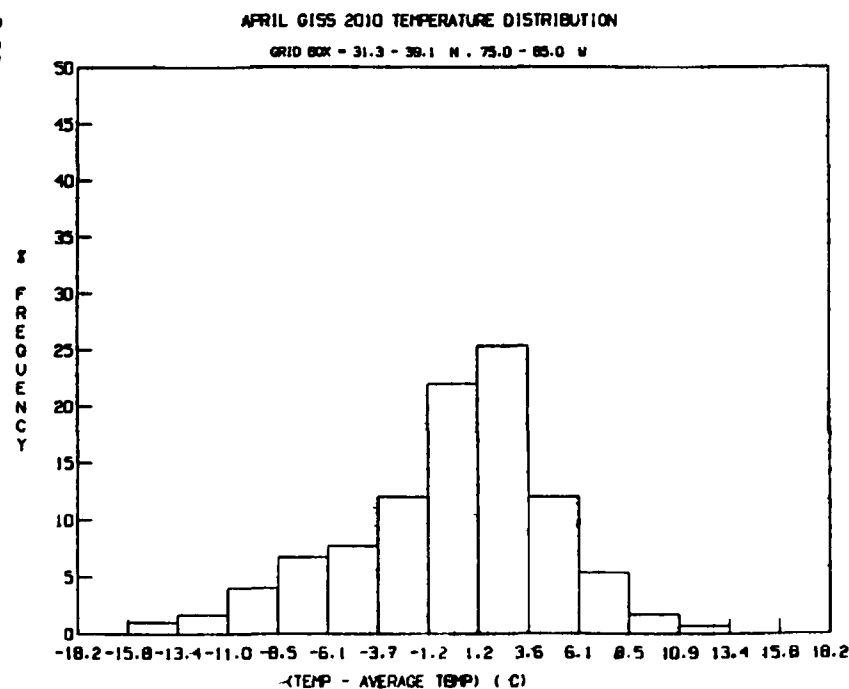
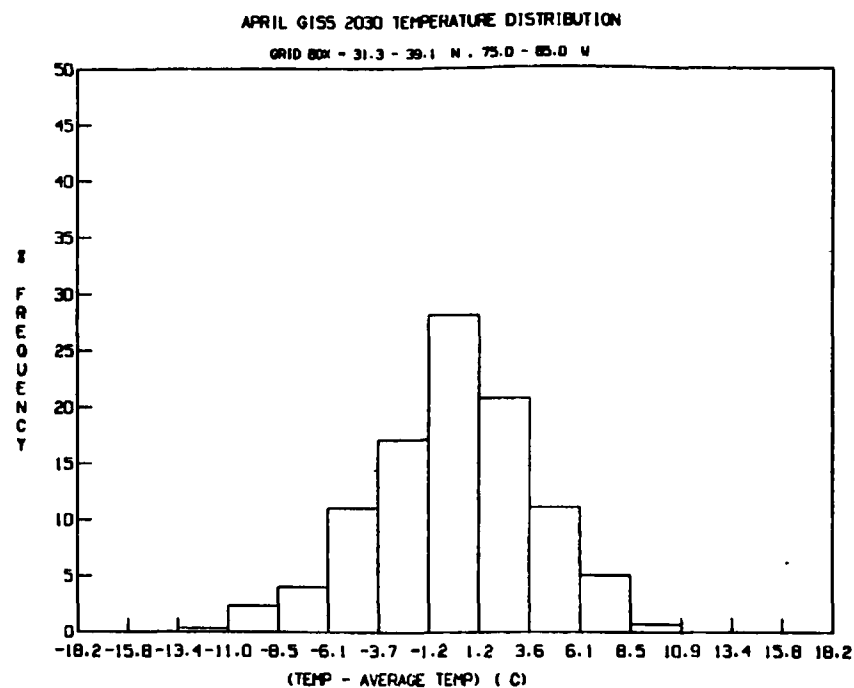
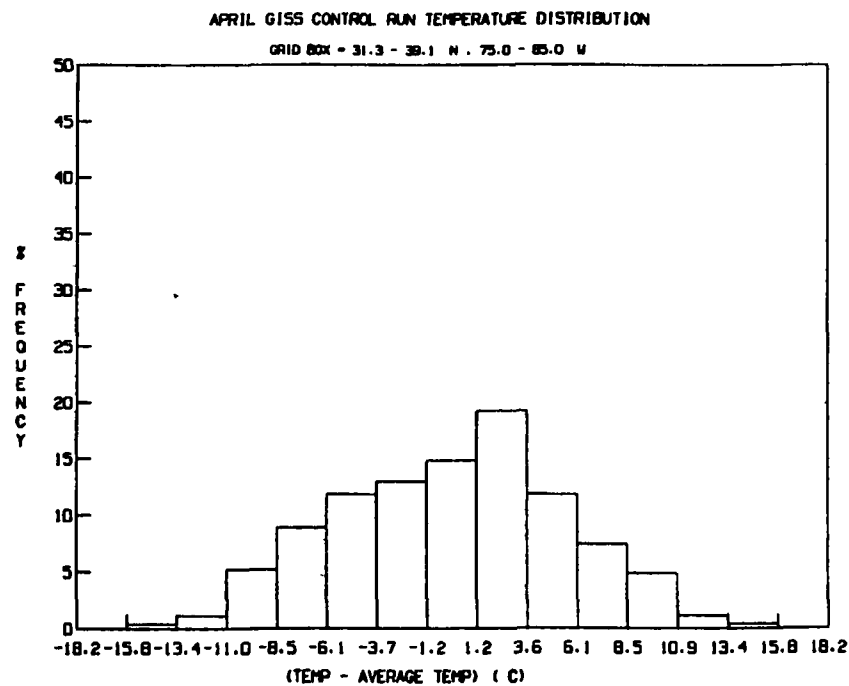


Figure 8. Distribution of daily temperature departure from the monthly mean for the southeast grid box in April for the current climate (top left), the 2010s (bottom left), the 2030s (top right), and 2056-2065 (bottom right).

Table 5a. Daily Temperature Standard Deviations (°C)

MONTH	LOCATION	OBS S.D.	CURRENT S.D.	2010s Δ S.D.	2030s Δ S.D.	~2060 Δ S.D.
JANUARY	S.G.PLAINS	4.81*	8.15	0.61	-1.19*	-0.83*
	SOUTHEAST	4.53*	6.90	-0.14	-1.14*	-0.23
	WEST COAST	3.63*	5.86	-0.61	0.05	-0.16
	GRT.LAKES	4.97	5.79	0.44	-0.33	-0.44
APRIL	S.G.PLAINS	3.72*	5.77	-0.57	-0.27	-0.80
	SOUTHEAST	3.71*	5.50	-0.65	-1.61*	-1.24
	WEST COAST	2.59*	4.29	0.77*	0.60	0.33
	GRT.LAKES	4.65*	6.15	-0.51	-0.26	-1.39*
JULY	S.G.PLAINS	1.74*	2.56	0.54	-0.19	0.18
	SOUTHEAST	1.50*	2.34	0.14	-0.22	-0.24
	WEST COAST	2.40*	3.56	0.03	0.54	0.28
	GRT.LAKES	2.38*	3.02	-0.48	-0.84*	-0.14
OCTOBER	S.G.PLAINS	3.79*	5.16	1.16*	0.97	1.35*
	SOUTHEAST	3.59*	5.21	-0.54	-0.25	-0.73
	WEST COAST	3.15*	6.51	-0.55	-0.30	-0.80
	GRT.LAKES	4.09*	5.46	-0.37	0.91	-0.06

Table 5b. Daily Precipitation Standard Deviations (mm d⁻¹)

MONTH	LOCATION	OBS S.D.	CURRENT S.D.	2010s Δ S.D.	2030s Δ S.D.	~2060 Δ S.D.
JANUARY	S.G.PLAINS	1.08*	2.80	0.05	0.05	1.68*
	SOUTHEAST	4.35	4.62	-1.20*	-1.35*	-0.85*
	WEST COAST	3.23*	4.55	-0.18	0.34	0.13
	GRT.LAKES	2.23*	4.06	-1.07*	-0.94*	-0.50*
APRIL	S.G.PLAINS	2.51*	3.26	0.94*	1.99*	1.17*
	SOUTHEAST	4.35*	3.85	0.95*	-0.15	0.81*
	WEST COAST	1.41*	2.76	0.07	1.02*	-0.12
	GRT.LAKES	3.85*	3.29	-0.43	-0.31	0.44
JULY	S.G.PLAINS	2.79	3.08	-0.10	-0.09	0.36
	SOUTHEAST	4.13*	3.31	0.28	0.29	0.11
	WEST COAST	0.57*	1.53	0.44*	0.24*	0.71*
	GRT.LAKES	3.68*	2.48	-0.06	0.72*	0.35
OCTOBER	S.G.PLAINS	2.75*	1.79	0.52*	0.34*	0.00
	SOUTHEAST	3.77	3.88	0.72*	-0.15	-0.28
	WEST COAST	1.86*	2.69	1.20*	-0.63*	1.34*
	GRT.LAKES	3.58*	2.26	0.52*	0.76*	0.95*

In the majority of cases, the model produced less days of light rain than did the observations. This is illustrated by the distributions for the southeast grid box in October (Figure 9, left). Note that it occurs even though the modeled mean monthly rainfall is only slightly less than observed (Table 2b). As shown in Figure 5, it is just this no rain/light rain distinction that is particularly dependent on the number of stations included in the observations. In the Great Lakes region, extreme rainfall values occur somewhat more frequently in observations in summer and autumn, as exemplified by the difference between the otherwise very similar distributions in July (Figure 9, right). Extreme values occur more frequently in the model in winter in all four regions. The difference in extreme events is evident in the standard deviations for the model and observations (Table 5b).

To determine the change in distribution as climate warms, similar analyses were made for the decades of the 2010s, 2030s, and 2056-2065. The distributions were significantly different about one-fourth of the time, with no general progression over the decades. Shown in Figure 10 are the distributions for the west coast in April, which has a steady increase in the days with no rain as the climate warms and dries.

Extreme events tended to vary, but an overall tendency does emerge. The assumption made for the interannual standard deviations was that the magnitude of variability would increase if precipitation did. As shown in Table 5b, the standard deviations in the climate change experiments were significantly different from the control more than one-half of the time with no general progression over the decades. (Note, however, that the use of the capital F distribution to evaluate significance in this case is not strictly valid, because the daily precipitation distribution does not have a bell-shaped appearance.) A comparison of Tables 2b and 5b indicates that the significant changes in variability coincided in sign with the change in mean precipitation.

In summary, the daily variability of precipitation tended to change with the same sign as the precipitation change itself, e.g., increasing when mean precipitation values did. Precipitation distributions changed significantly about one-fourth of the time, again influenced by mean value changes. Temperature variability on this time scale tended to decrease, but this cannot be proven statistically with the sample at hand, while temperature distributions showed no obvious change. Nor was there any obvious change in persistence as climate warmed.

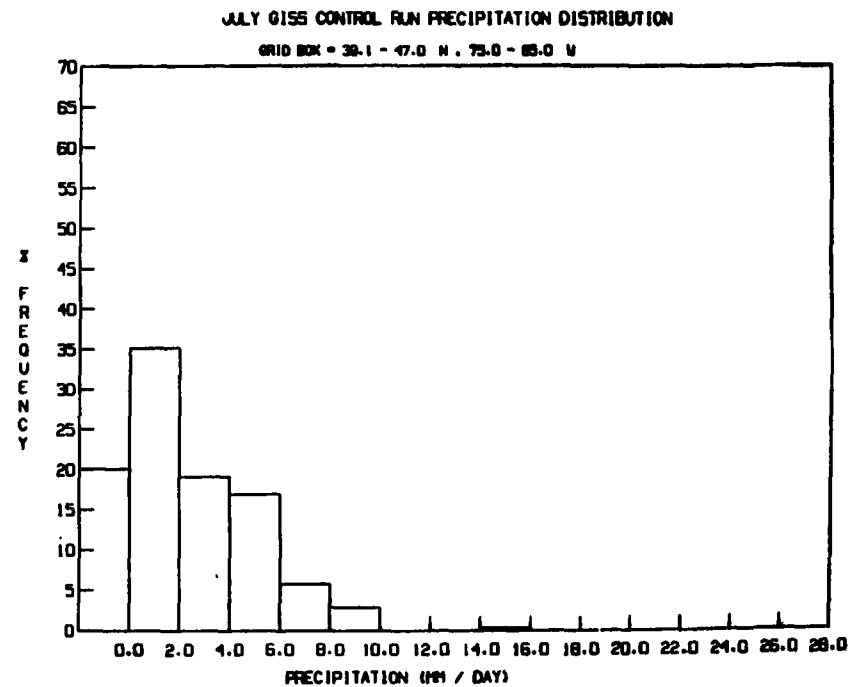
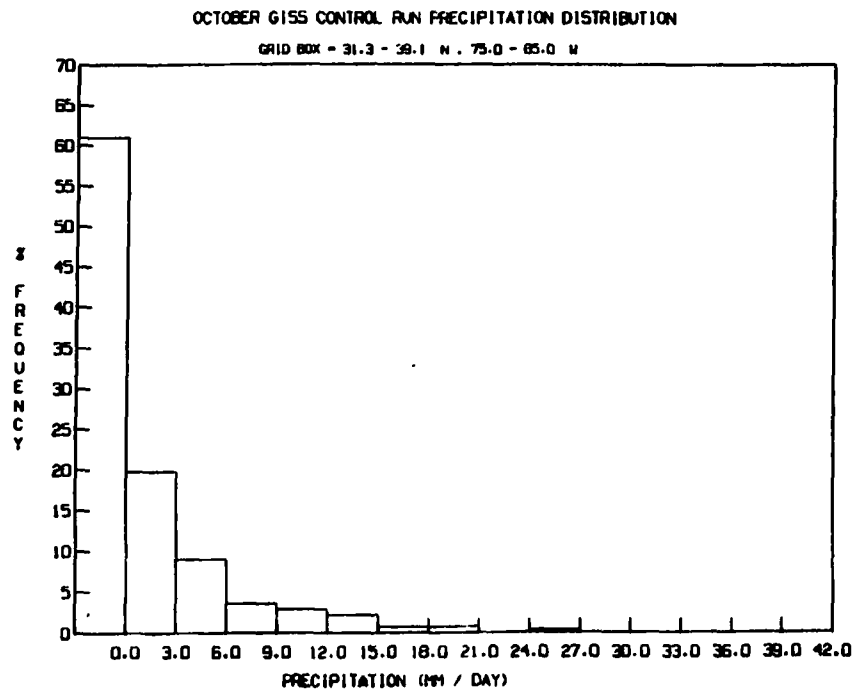
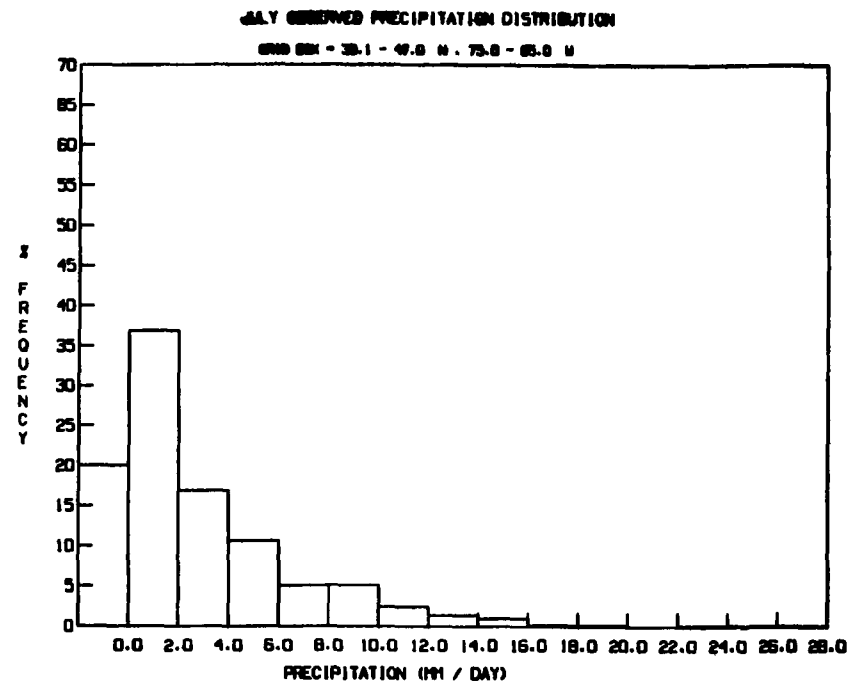
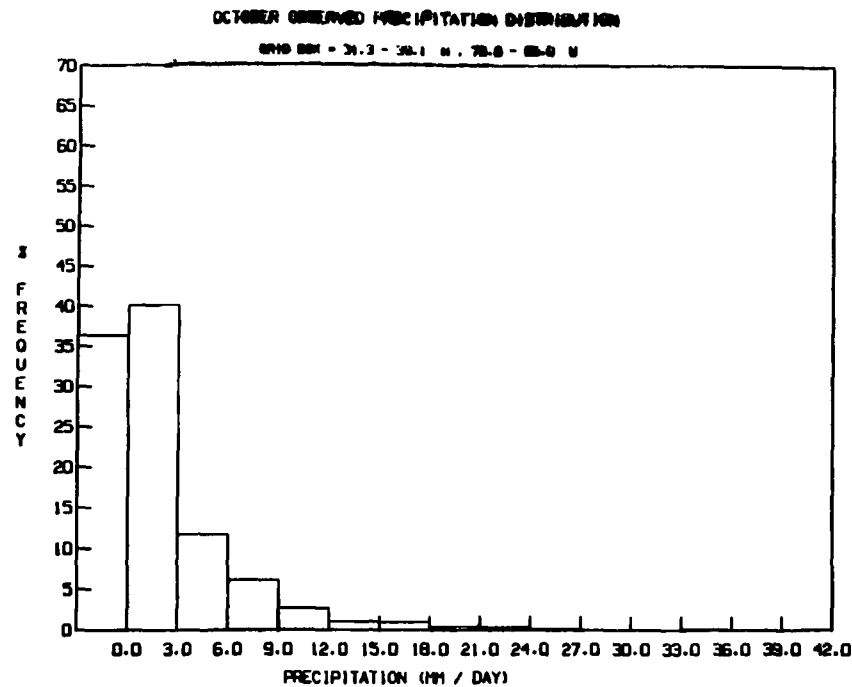


Figure 9. Observed (top) and model (bottom) daily precipitation intensities for the southeast in October (left) and the Great Lakes in July (right).

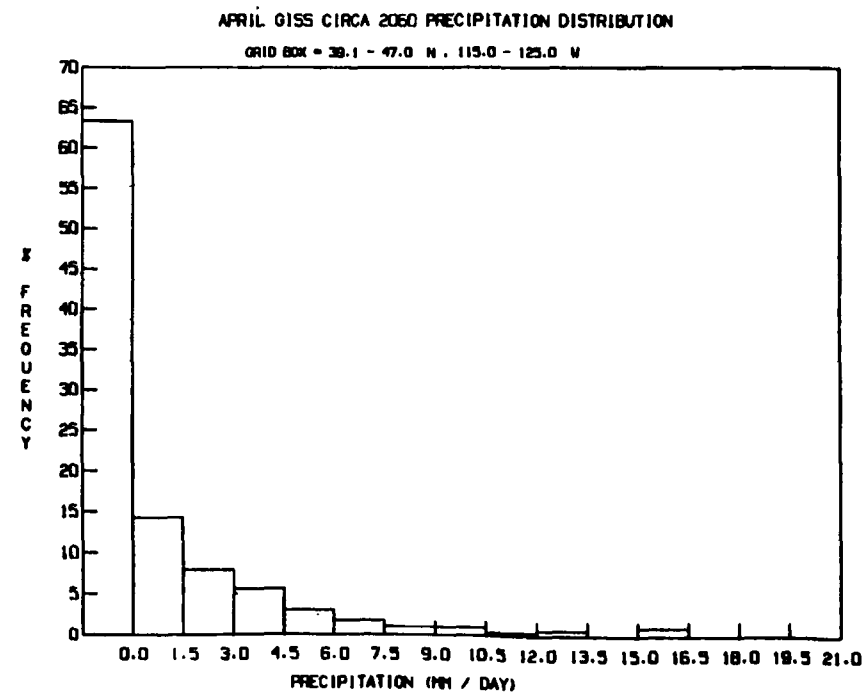
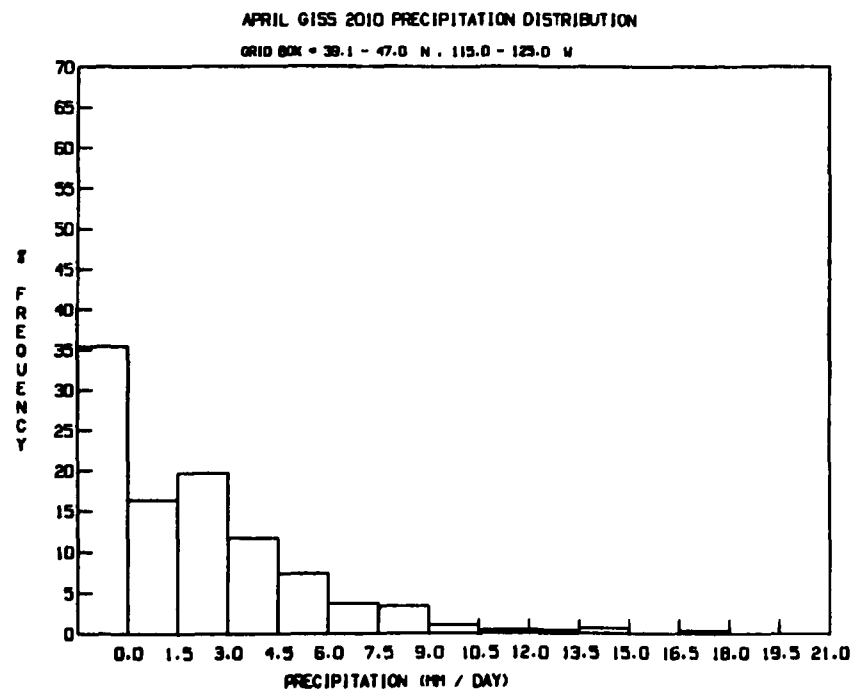
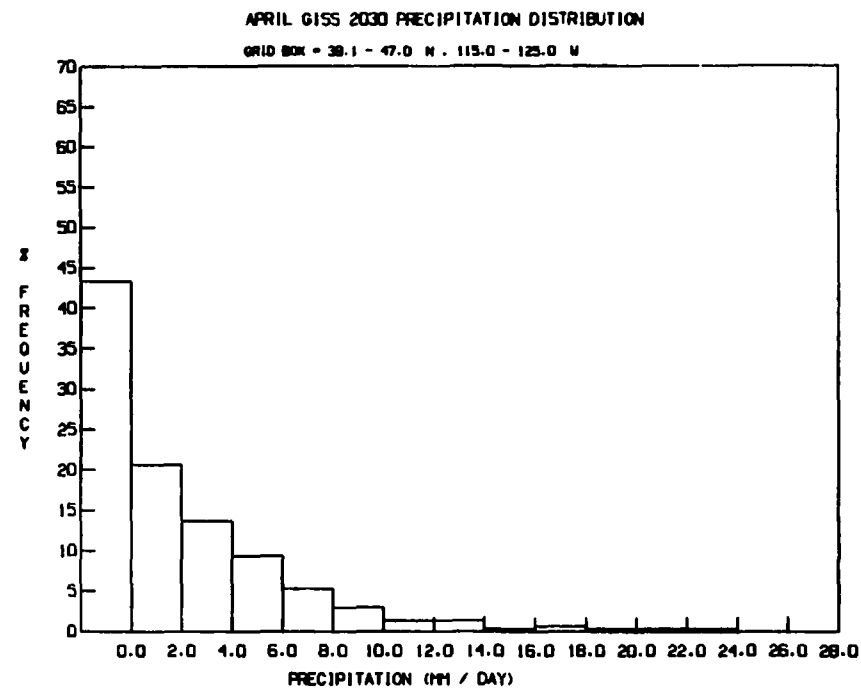
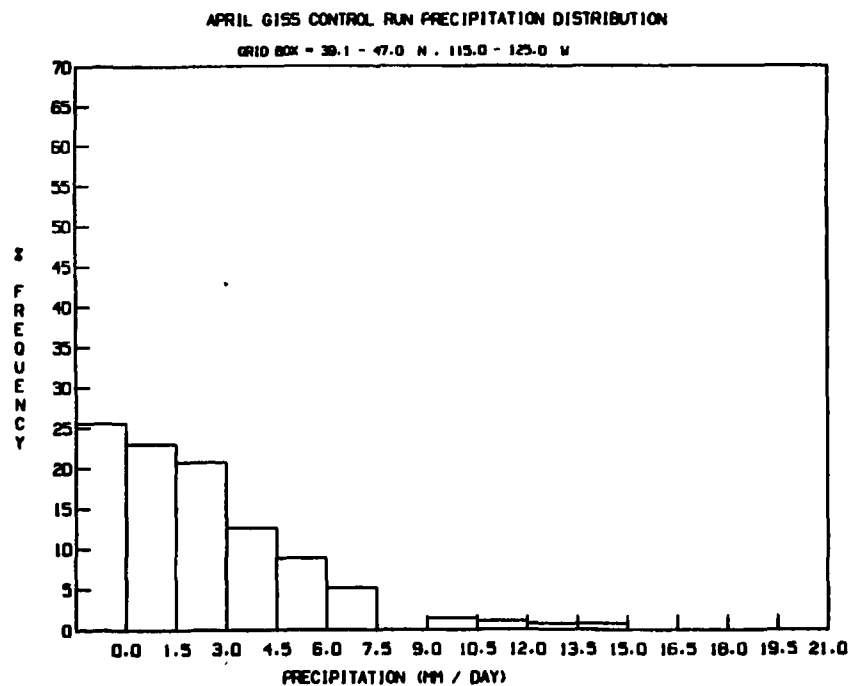


Figure 10. Daily precipitation intensities for the west coast grid box in April for the current climate (top left), and 2010s (bottom left), the 2030s (top right), and 2056-2065 (bottom right).

CHAPTER 6

VARIABILITY OF THE DIURNAL CYCLE

The GISS general circulation model includes a diurnal cycle, and for certain applications, especially those involving vegetation, variations in the amplitude of the diurnal temperature cycle as climate changed would be an important result. The expectation is that the amplitude should decrease, since additional CO₂ (and water vapor in the warmer climate) would act as greenhouse material in limiting radiative cooling at night, while leaving solar radiational heating during the day unaffected. Karl et al. (1984, 1986, 1987) have reported a decrease in the diurnal temperature range, especially during summer.

We first compare the model's diurnal cycle with the observed. Shown in Table 6 is a comparison of the model's annual average diurnal temperature range with observations (U.S. Air Force, 1979) calculated using the cities in Figure 1/Table 1 in each grid box (in some cases we had to use data which was available only for neighboring stations). In both cases the daily temperature maximum was compared with the daily temperature minimum to determine the diurnal range. The model values average very close to the observed, with a ratio of close to one (model/observed = $1.01 \pm .27$), although there is a tendency for model values to be higher in late summer, when the model ground dries out. The phasing also is appropriate, with temperature peaking during the mid-afternoon.

The change in the diurnal cycle amplitude for each month in the doubled CO₂ climate is shown in Table 6. The prevailing tendency is for the diurnal cycle amplitude to decrease in summer; out of the 12 records for the 3 months of June-August, decreases were recorded in 10 cases. The magnitudes of the decreases ranged from less than 1% to as much as 27%. There is no doubt about the reality of this effect; for the United States as a whole, during these 3 months 87% of the grid boxes showed decreases in the diurnal cycle amplitude. Given that the summer, when light winds occur, would be the season most likely to have its temperatures dominated by radiative effects, this result would appear to be in accordance with expectation. However, examination of the results indicates that other factors are operating as well. In the winter, spring, and fall seasons, the modeled doubled CO₂ climate features cloud cover decreases at night, which may offset radiative decreases due to different trace gas concentrations. In these seasons both increases and decreases in the diurnal cycle amplitude occur, with daytime temperature increases often exceeding those at night. In summer in the model there is little cloud cover change at night, which presumably allows the trace gas radiative effect to become apparent, and the warming is generally greater at night (thus reducing the diurnal temperature amplitude). This example illustrates how simple expectations can be altered by other aspects of the climate system.

Table 6. Diurnal Temperature Range (°C)

GRID BOX		JAN	FEB	MAR	APR	MAY	JUN	JUL	AUG	SEP	OCT	NOV	DEC
S.G. PLAINS	OBS	12.1	12.3	13.2	13.0	12.9	13.1	12.6	12.8	12.7	13.2	12.8	12.0
	CONT	10.5	11.2	12.5	15.4	10.4	10.1	9.7	11.2	21.8	19.2	13.6	10.9
	2CO2	10.2	12.3	13.5	16.0	10.2	9.9	10.6	10.9	17.5	19.6	14.0	11.3
SOUTHEAST	OBS	9.2	10.0	10.5	11.4	12.4	10.5	10.0	10.1	10.3	11.0	10.6	9.6
	CONT	9.1	10.1	11.1	13.6	9.1	8.7	9.3	10.9	13.6	13.2	11.0	9.3
	2CO2	9.3	9.5	12.4	12.8	8.5	7.9	7.3	8.0	13.6	13.3	10.5	9.7
WEST COAST	OBS	9.0	10.0	11.3	12.3	13.1	13.5	14.6	13.8	14.3	12.6	10.4	8.7
	CONT	6.6	6.9	8.7	12.1	10.0	10.7	13.1	17.1	19.0	14.8	10.1	7.1
	2CO2	6.5	7.5	8.6	13.2	9.5	10.1	11.5	17.0	20.3	14.4	9.0	8.2
GREAT LAKE	OBS	8.3	8.9	9.5	10.9	11.6	11.6	11.4	11.2	11.2	10.8	8.3	7.6
	CONT	7.4	7.3	8.4	11.4	8.9	9.7	10.5	12.7	14.3	10.1	7.7	6.7
	2CO2	7.0	7.2	9.4	12.7	9.1	9.4	10.2	12.8	15.0	11.9	8.9	7.2

CHAPTER 7

DISCUSSION

The results show that the year-to-year temperature variability and extremes in the daily temperature variability tended to decrease in the warmer climate during the winter and early spring. The precipitation variability on both time scales tended to increase, to the extent that the mean precipitation itself increased. The diurnal cycle amplitude tended to decrease in summer. In this section we discuss how likely these results are to be true, and briefly comment on their potential consequences.

The primary question that must be addressed is whether the model deficiencies for the current climate invalidate the results for future changes. This question is relevant when assessing the validity of predicted changes in the mean values as well as changes in variability. The comparison of modeled and observed temperatures and precipitation for the four grid boxes and four seasons has indicated the following deficiencies: 1) the model is too cool during summer and fall; 2) the model produces too much rain along the west coast and in the southern Great Plains; 3) the model generally overestimates temperature variability in summer, on both the interannual and daily time scales; 4) the model overestimates the interannual precipitation variability, and has too few days of light rain, as opposed to no rain, each month; and 5) the model persistence is too large, especially during summer and for precipitation. While these errors are not always large or significant, they are often of greater magnitude than the modeled climate change results. Can we believe the results under these circumstances?

A comparison was made of results from the $4^\circ \times 5^\circ$ version of the GISS climate model (when using doubled atmospheric CO_2 and the sea surface temperature changes produced in the equilibrium $8^\circ \times 10^\circ$ experiment, as discussed in Rind, 1987; 1988a,b), with those from the $8^\circ \times 10^\circ$. The finer resolution model control run produces less rain for the western United States (e.g., 1.4 mm d^{-1} in summer, compared with 2.6 mm d^{-1} in the coarse grid, Rind, 1988a) and smaller interannual variability (0.1 mm d^{-1} for the summer as a whole, compared with 0.5 mm d^{-1} with the coarser grid, Rind, 1988b), both of which are more realistic characteristics. In the doubled CO_2 simulations, there are smaller changes in the finer grid run for this region (Rind, 1988b), indicating that the climate change experiment mimics some of the characteristics of the control run. As the changes in precipitation variability are closely tied to the changes in mean precipitation, we might expect that the finer grid model would have reduced variability changes in that region. We could not use this model for the variability study, as it did not generate its own sea surface temperatures directly (nor were they allowed to vary from year to year), but the results do imply that model deficiencies can be expected to contaminate climate change estimates, both for mean changes and changes in variability.

What then can be gained from studies made with admittedly imperfect models? The current models can be used to explore potential physical interactions which they may be able to elucidate, albeit in an imperfect manner. As an example, the models have been used to estimate the global warming due to a doubling of atmospheric carbon dioxide. The magnitudes of warming produced may be inaccurate because of the strong positive feedback that is provided by the cloud cover response in the models, since cloud cover parameterizations are currently very crude. Nevertheless, the models have shown the potential strength of this physical process, and have highlighted the necessity to model clouds more accurately. By running model experiments we hope to learn what mechanisms are of first-order importance in climate change. This task requires models which allow for the multiplicity of interactions possible in the complicated, highly nonlinear physical system.

In the studies here, we are concerned with whether variability changes will occur along with the projected climate change. The physical processes that are being examined are 1) does the high latitude temperature change amplification produce significant reductions in interannual and daily temperature variability; 2) does the increased global rainfall produce increased precipitation variability; and 3) does the increased greenhouse capacity of the atmosphere reduce the diurnal temperature range. The results *in toto* verify these physical assumptions but with important caveats as to their generalizability. They thus give us a crude estimate as to the importance of the physical processes, and emphasize what must be done to improve our understanding. For

example, to get better estimates of precipitation variability, we must produce better representations of the mean value. While this could have been stated *a priori*, this study, which clearly indicates the relationship of changes in precipitation variability to the mean changes, helps to quantify the issue.

The reduction in the latitudinal temperature gradient during winter is approximately 10% in the GISS doubled CO₂ model, and the eddy energy decrease is about 5%. The model results indicate that these differences translate into average reductions in temperature variability of the order of 10% (Tables 3 and 5). The reliability of that conclusion is tempered by the tendency of this model to overestimate the variability for the current climate. Especially important in this regard is the need for a more realistic hydrology scheme which could limit late summer water loss and prevent unrealistic temperature changes. An additional uncertainty arises because of the lack of agreement among models as to what the reduction in the latitudinal temperature gradient will really be. The doubled CO₂ climate simulation done at the Geophysical Fluid Dynamics Laboratory produces a reduction in this temperature gradient that is two times as large. The results from this study imply that the decrease in temperature variability in their model might well exceed the values determined here. The use of several different models further serves to clarify areas requiring further research.

The diurnal cycle change is predominantly a radiative effect, and as noted, would be expected to be most apparent when winds are light, in summer. The model does reproduce this result. However, it also indicates the importance of competing effects, such as altered cloud cover, in occasionally reversing the sign of the change. While we cannot necessarily believe the individual results in this regard, owing to uncertainty in cloud and convection schemes, they do highlight the ability of models to provide interactions from other elements of the climate system which can cause the result to deviate from expectations. As models are developed which produce better representations of the current climate, and contain more sophisticated parameterizations for these processes, we should be able to increase our confidence in such projections.

Changes in variability may well be affected by processes that have been omitted in the standard climate change experiments. For example, significant interannual variability is associated with changes in ocean dynamics, such as the El Nino phenomenon. While the GISS model allows sea surface temperatures to change, it does not allow ocean dynamics to change. Were El Nino events to occur with an altered frequency, this would undoubtedly influence interannual variability, at least in specific regions. Ultimately, all variability studies, as well as model projections for mean climate changes, will have to be done with coupled ocean/atmosphere models.

The model does not include hurricanes, which occur on spatial scales (~100 km) too small to be resolved. Emanuel (1987) estimated that the CO₂ warming of the tropical oceans could increase hurricane intensity by 40-50%, an effect which would add to the future hydrologic variability.

If the results obtained here prove to be valid, what effects are likely as the result of the changes in variability? Decreased temperature variability would appear to be a positive factor in societal planning, limiting the variance around the mean with which we would have to deal. However the variability changes studied here will be superimposed upon a changing mean climate. The impact of changes in the interannual, daily, and diurnal cycle temperature variability on society will have to be compared with the potentially rapid rate of change of the mean temperature itself. All these factors will be folded in together in the climate that we experience, so even with reduced interannual temperature variability, the large decadal-scale warming might dominate the perception of temperature instability.

An increased variability of precipitation associated with an increase in mean precipitation might leave the relative variability unchanged. Nevertheless, society would likely alter its expectations of the mean conditions, and so increases in variability would still be likely to have a pronounced effect. Droughts, defined as lack of water availability relative to expectation or demand, might be expected to increase, as would floods. In conjunction with the likelihood of increased hurricane intensity, this would stress both ecosystems and civilization's structures. At the time of this writing (the late summer of 1988), we have had a graphic demonstration of such a world: the destructive power of hurricane Gilbert, the devastating floods of Bangladesh,

Rind

forest fires sweeping the western United States, and the impact of drought in the central Great Plains and the southeast, affecting everything from 30% of the nation's crops to the cooling water and hydroelectric capacity of power plants. Potential changes in precipitation variability need to be factored into the decision-making process.

CHAPTER 8

CONCLUSIONS

In this study we have looked at how variability on three time-scales, the inter-annual, daily, and diurnal cycle, may change in the future based on model projections. We concentrate on the areas of the southeast United States, the southern Great Plains, the west coast, and the Great Lakes. Extensive comparisons are made of observations and the model simulations of the current climate.

The primary results of this study are:

- 1) The interannual temperature and precipitation variability does not change significantly on the grid box level, but on a broader area, the sign of the change is significant, with temperature variability decreasing and precipitation variability increasing (as mean precipitation increases).
- 2) The daily variability in temperature is not significantly different, although there is a tendency for decreases. Precipitation variability on this time scale changes in the same manner as the mean precipitation.
- 3) The amplitude of the diurnal temperature range decreases in summer.

These results must be viewed in the context of the comparison between observations and the model's current climate, which shows the model is often too cool and wet, and somewhat too variable. The lack of significance of the changes in variability on the grid box level may well be related to an insufficient length of time of simulation, as the only variable whose variability changed significantly on this scale (daily precipitation) had the largest independent data set to work with. Alternatively, procedures should be developed to take advantage of the predominance of changes of a specific sign, which characterize these results. Finally, the impact of changes in variability on these time scales must be viewed in the context of the projected rapid change of the mean values themselves, to understand their potential consequences for society.

REFERENCES

- Angell, J. and Korshover, J.: 1978, 'Global Temperature Variation, Surface - 100 mb: An Update into 1977', Mon. Wea. Rev., **106**, 355-370.
- Barnett, T.: 1978, 'Estimating Variability of Surface Air Temperature in the Northern Hemisphere', Mon. Wea. Rev., **106**, 1353-1367.
- Chervin, R.M.: 1981, 'On the Comparison of Observed and GCM Simulated Climate Ensembles', J. Atmos. Sci., **38**, 885-901.
- Chin, E.H. and Miller, J.F.: 1980, 'On the Conditional Distribution of Daily Precipitation Amounts', Mon. Wea. Rev., **108**, 1462-1464.
- Diaz, H. and Quayle, R.: 1980, 'The Climate of the United States Since 1985: Spatial and Temporal Changes', Mon. Wea. Rev., **108**, 249-266.
- Emanuel, K.A.: 1987, 'The Dependence of Hurricane Intensity on Climate', Nature, **326**, 483-485.
- Hansen, J., and Lebedeff, S.: 1987, 'Global Trends of Measured Surface Air Temperature', J. Geophys. Res., **92**, 13,345-13,372.
- Hansen, J., Russell, G., Rind, D., Stone, P., Lacis, A., Lebedeff, S., Ruedy, R., and Travis, L.: 1983, 'Efficient Three-Dimensional Global Models for Climate Studies: Models I and II', Mon. Wea. Rev., **111**, 609-662.
- Hansen, J., Lacis, A., Rind, D., Russell, G., Stone, P., Fung, I., Ruedy, R., and Lerner, J.: 1984, 'Climate Sensitivity: Analysis of Feedback Mechanisms', in Climate Processes and Climate Sensitivity, eds. J. Hansen and T. Takahashi, American Geophysical Union, Washington, D.C., 130-163.
- Hansen, J., Lacis, A., Rind, D., Russell, G., Fung, I., and Lebedeff, S.: 1987, 'Evidence for Future Warming: How Large and When?', in The Greenhouse Effect, Climate Change, and U.S. Forests, eds. W. Shands and J. Hoffman, The Conservation Foundation, Washington, D.C., 57-76.
- Hansen, J., Fung, I., Lacis, A., Lebedeff, S., Rind, D., Ruedy, R., Russell, G., and Stone, P.: 1988, 'Global Climate Changes as Forecast by the GISS 3-d Model', J. Geophys. Res., **93**, 5385-5412.
- Karl, T.R., Kukla, G., and Gavin, J.: 1984, 'Decreasing Diurnal Temperature Range in the United States and Canada from 1941 through 1980', J. Clim. App. Meteor., **23**, 1489-1504.
- Karl, T.R., Kukla, G., and Gavin, J.: 1986, 'Relationship Between Decreased Temperature Range and Precipitation Trends in the United States and Canada, 1941-1980', J. Clim. App. Meteor., **25**, 1878-1886.
- Karl, T.R., Kukla, G., and Gavin, J.: 1987, 'Recent Temperature Changes During Overcast and Clear Skies in the United States', J. Clim. App. Meteor., **26**, 698-711.
- Katz, R.W.: 1984, Procedures for Determining the Statistical Significance of Changes in Variability Simulated by an Atmospheric General Circulation Model, Climate Research Institute Report No. 48, Oregon State University, Corvallis, Oregon.
- Knuth, D.C.: 1969, The Art of Computer Programming, Addison-Wesley, Reading, Mass., 624 pp.

- Panofsky, H. and Brier, G.: 1968, Some Applications of Statistics to Meteorology, The Pennsylvania State University, University Park, Pennsylvania, 224pp.
- Ratcliffe, R., Weller, J., and Collison, P.: 1978, 'Variability in the frequency of unusual weather over approximately the last century', Quart. J. Roy. Meteor. Soc., **104**, 243-256.
- Rind, D.: 1987, 'The Doubled CO₂ Climate: Impact of the Sea Surface Temperature Gradient', J. Atmos. Sci., **44**, 3235-3268.
- Rind, D.: 1988a, 'The Doubled CO₂ Climate and the Sensitivity of the Modeled Hydrologic Cycle', J. Geophys. Res., **93**, 5385-5412.
- Rind, D.: 1988b, 'Dependence of Warm and Cold Climate Depiction on Climate Model Resolution', J. of Climate, **1**, 965-997.
- Rind, D. and Lebedeff, S.: 1984, 'Potential Climatic Impacts of Increasing Atmospheric CO₂ with Emphasis on Water Availability and Hydrology in the United States', Rep. EPA 230-04-84-006, U.S. Environmental Protection Agency, Washington, D.C., 96pp.
- Schlesinger, M.E. and Mitchell, J.F.B.: 1987, Climate model simulations of the equilibrium climatic response to increased carbon dioxide, Rev. Geophys., **25**, 760-798.
- Solomon, A.M. and West, D.C.: 1985, 'Potential Responses of Forests to CO₂-Induced Climate Change, in Characterization of Information Requirements for Studies of CO₂ Effects: Water Resources, Agriculture, Fisheries, Forests, and Human Health, M.R. White (ed.), United States Department of Energy, DOE/ER-0236, 145-170.
- United States Air Force: 1979, 'AWS Climatic Briefs -- North America', USAFETAC/DS-79/088, USAF Environmental Technical Applications Center, Scott Air Force Base, Illinois 62225.
- United States Environmental Protection Agency : 1988, 'Report to Congress on the Effects of Global Climate Change', in preparation.
- Van Loon, H. and Williams, J.: 1978, 'The Association Between Mean Temperatures and Interannual Variability', Mon. Wea. Rev., **106**, 1012-1017.
- Wilson, C.A. and Mitchell, J.F.B.: 1987, 'Simulated Climate and CO₂-Induced Climate Change over Western Europe, Climatic Change, **10**, 11-42.